ISSN: 2687 - 4539

CHAOS

THEORY AND APPLICATIONS

IN APPLIED SCIENCES AND ENGINEERING

VOLUME 4, ISSUE 3, NOVEMBER 2022

AN INTERDISCIPLINARY JOURNAL OF NONLINEAR SCIENCE

ISSN: 2687 - 4539

CHAOS
THEORY AND APPLICATIONS
IN APPLIED SCIENCES AND ENGINEERING

Chaos Theory and Applications (CHTA)
Volume: 4– Issue No:3(November 2022)
https://dergipark.org.tr/en/pub/chaos/issue/73033

ISSN: 2687 - 4539

CHAOS THEORY AND APPLICATIONS

IN APPLIED SCIENCES AND ENGINEERING

Chaos Theory and Applications (CHTA)
Volume: 4 – Issue No: 3 (November 2022)
https://dergipark.org.tr/en/pub/chaos/issue/73033

Contents

CHAOS
Theory and Applications
in Applied Sciences and Engineering

e-ISSN: 2687-4539
EDITORIAL
Vol.4 / No.3 / 2022 / pp.111-118

Evolutionary Mathematical Science, Fractional Modeling and Artificial Intelligence of Nonlinear Dynamics in Complex Systems

Yeliz Karaca [*,1] **and Dumitru Baleanu** [γ,α,2]

[*]University of Massachusetts Chan Medical School (UMASS), 55 Lake Avenue North, Worcester, MA 01655, USA, [γ]Çankaya University, Balgat Campus, Çankaya 06530, Ankara, Türkiye, [α]Institute of Space Science (ISS), 409 Atomistilor Street, Magurele, Ilfov 077125, Romania.

ABSTRACT Complex problems in nonlinear dynamics foreground the critical support of artificial phenomena so that each domain of complex systems can generate applicable answers and solutions to the pressing challenges. This sort of view is capable of serving the needs of different aspects of complexity by minimizing the problems of complexity whose solutions are based on advanced mathematical foundations and analogous algorithmic models consisting of numerous applied aspects of complexity. Evolutionary processes, nonlinearity and all the other dimensions of complexity lie at the pedestal of time, reveal time and occur within time. In the ever-evolving landscape and variations, with causality breaking down, the idea of complexity can be stated to be a part of unifying and revolutionary scientific framework to expound complex systems whose behavior is perplexing to predict and control with the ultimate goal of attaining a global understanding related to many branches of possible states as well as high-dimensional manifolds, while at the same time keeping abreast with actuality along the evolutionary and historical path, which itself, has also been through different critical points on the manifold. In view of these, we put forth the features of complexity of varying phenomena, properties of evolution and adaptation, memory effects, nonlinear dynamic system qualities, the importance of chaos theory and applications of related aspects in this study. In addition, processes of fractional dynamics, differentiation and systems in complex systems as well as the dynamical processes and dynamical systems of fractional order with respect to natural and artificial phenomena are discussed in terms of their mathematical modeling. Fractional calculus and fractional-order calculus approach to provide novel models with fractional-order calculus as employed in machine learning algorithms to be able to attain optimized solutions are also set forth besides the justification of the need to develop analytical and numerical methods. Subsequently, algorithmic complexity and its goal towards ensuring a more effective handling of efficient algorithms in computational sciences is stated with regard to the classification of computational problems. We further point out the neural networks, as descriptive models, for providing the means to gather, store and use experiential knowledge as well as Artificial Neural Networks (ANNs) in relation to their employment for handling experimental data in different complex domains. Furthermore, the importance of generating applicable solutions to problems for various engineering areas, medicine, biology, mathematical science, applied disciplines and data science, among many others, is discussed in detail along with an emphasis on power of predictability, relying on mathematical sciences, with Artificial Intelligence (AI) and machine learning being at the pedestal and intersection with different fields which are characterized by complex, chaotic, nonlinear, dynamic and transient components to validate the significance of optimized approaches both in real systems and in related realms.

KEYWORDS
Complex systems
Chaos theory
Chaos-order and complexity
Computational complexity
Fractal operators
Fractional calculus
Fractional dynamics
Evolutionary models
Fractional-order algorithms
Complex-valued neural networks
Nonlinear systems
Data science
Mathematical biology and medicine
Prediction of changes
Fractional integro-differentiation
Artificial Intelligence.

INTRODUCTION

Having existed as a notion since antiquity, complexity is a concept and scientific term that entails the nexus of the origin of complex components accompanied not only by meticulous and detailed computations but also causal processes. A complex system, in that regard, is one with multiple interactions emerging and occurring among interacting components with adapting, synchronizing, noisy, reacting, self-ordering, self-steering, self-similar, irregular, non-periodic and unpredictable elements, feedback loops as well as evolving features, amidst many others. Complexity starts when causality breaks down and it reveals many deep layers considering the structure with variational principles and far-reaching conditions including spontaneous order, nonlinearity, feedback, robustness, lack of central control, numerosity, hierarchical organization and emergence.

The substantial number of independent interacting components and multiple pathways through which the complex system can evolve further point out a number of the reasons causality breaks down as complexity starts. Along these lines, causality is relative, prone to fundamental variations that depend on perception, the environment, external factors, space, time and so (Karaca 2022c). The inherent complexity of the varying phenomena in complex systems needs to exceed a reductionist outlook of traditional science; thus, complexity requires an understanding extending across a class of complex problems with myriad of intricate and subtle attributes based on innovative and novel ways of thinking as well as applicable laws. In view of these, evolution, order and complexity can more conspicuously reveal the relationship between natural and social worlds, which actually reflects a modern way of thinking that challenges the dichotomy of natural and social. Complex problems in nonlinear dynamics necessitate the critical support of artificial phenomena so that each domain of complex systems addresses research aspects and theories towards the solutions to the pressing challenges which almost exceed the possible limits of human comprehension. This view is capable of serving the needs of different aspects of complexity by minimizing the problems of complexity whose solutions are based on advanced mathematical foundations and corresponding algorithmic models that are made up of numerous applied aspects of complexity.

Evolutionary processes, nonlinearity and all the other dimensions of complexity rest on time, reveal time and occur within time. In the ever-changing landscape and variations, with causality breaking down, the idea of complexity can be stated to be a part of unifying and revolutionary scientific framework for the understanding of complex systems whose behavior is challenging to predict and control with the ultimate goal of attaining a global understanding pertaining to many branches of possible states as well as high-dimensional manifolds, while at the same time keeping up with actuality along the evolutionary and historical path, which itself, has also been through different critical points on the manifold. In this sense, evolution is dependent upon exploration, innovation and causal learning. Yet, changing or removing the causes does not necessarily mean to be capable of removing or altering the outcomes, and hence, modern scientific way of thinking is catered towards the development of models benefiting from theoretical insights, local computations and task-related manifolds in spaces with high dimensions instead of just route learning the rules or representations of the world (Karaca 2022c). Within this scope, the exploration of the way patterns evolves in time spans across turbulent flow of fluids, geological formations, microstructures of materials, spatial organization of microbes, germs, even the behavior of genes, covering quantitative biology, physics, evolution, materials science, ecology, chemistry, neurology, applied mathematics, nonequilibrium statistical mechanics, among many other ones. These aspects point to the observation that nature can produce complex structures even in simple situations, and can obey simple laws even in complex situations (Goldenfeld and Kadanoff 1999).

The nonlinear character and being out of equilibrium are the important qualities characterizing complex systems which have a substantial number of interacting variables or elements which can be simple elements that interact in a nonlinear, either locally or globally (Mateos 2009). In complex systems, the local interactions between the components of the system lead to regularities in the overall, global behavior of the system that appear to be impossible to be derived in a rigorous and analytic way based on the knowledge of the local interactions, which point to both an empirical fact and mathematical intuition (Waldrop 1993). Nonlinear dynamical systems, reflected as a complex library of plethora of different behaviors, overflow with models of varying phenomena in complex systems. Given that, nonlinearity signifies a relationship that cannot be explained or modeled through a linear algebraic or differential combination of input or state variables. Hence is the reason why it is often possible to characterize nonlinear dynamical systems by highly unpredictable and dynamic behaviors, which proves to be challenging for analysis as they occur across different temporal and spatial planes (Karaca 2022a; Kia *et al.* 2017). Across this strand of thought, nonlinear science serves to reveal the nonlinear descriptions of broadly different systems, with a fundamental impact on complex dynamics.

Complex and nonlinear dynamical systems are regarded as thriving as models of natural phenomena, usually characterized by unpredictable behavior whose analysis is challenging to be performed due to occurring like the incidents in chaotic systems. The essence of the problem is rooted in exactly understanding which sort of information, particularly concerned with their long-term evolution and memory properties, can be expected to be derived from those systems. Correspondingly, complexity, chaos, order and evolution all unearth the relationship between natural and social worlds, representing a modern process of thinking (Karaca 2022b). Complexities require a horizon that takes into account the subtleties making their own means of solutions and applicability necessary and applicable. Evolvability in this sense is concerned with the species owing their existence to the capability of their ancestors with respect to evolving and adapting besides the correlation between the complexity of model, design, visualization and optimality. These perspectives are of utmost importance in the future science of complexity as well (Karaca 2022b).

The properties of evolution and adaptation can shed light on the understanding of past to interpret the present in a holistic way and to design future plans and schemes in an appropriate, adaptive, systematic and timely way. If there is a situation of getting stuck in between two extremes of order and chaos under uncertain and unpredictable conditions, complexity thinking and theory can render the systems be adaptive, respond to the world and act spontaneously. Furthermore, being cognizant of complex systems ensures the analysis of the essence of the problem by understanding the way systems self-organize their structures and self-regulate their dynamics and nonlinearity. On theoretical aspect, the theory

Manuscript received: 12 October 2022,
Accepted: 14 October 2022.

[1] yeliz.karaca@ieee.org (**Corresponding author**)
[2] dumitru@cankaya.edu.tr

of complexity entails powerful evidence, providing elucidation to challenge mechanistic thinking to steer humanity toward the adaptation of an integrative way of thinking (Karaca 2022b).

Chaos theory, being an interdisciplinary theory, not only as a mathematical art but also as a means for practical engineering challenges, represents a set of techniques to analyze dynamical systems. As the founder of chaos theory, Edward Lorenz, put in summarized form: "*When the present determines the future, but the approximate present does not approximately determine the future*", which means that the systems are deterministic but a small change in initial conditions bring about evolution of a highly unpredictable behavior.

It should be noted that the deterministic behavior appears to be random and in that regard, chaos theory specifies the geometric patterns to be discerned in the seemingly random events of a complex system and introduces linear and nonlinear progressions. Initially originated from the simulation of dynamic systems in natural world, some practical applications of chaos include electronic circuit design, biological system analysis, information encryption, synchronization for communication and control, behavior prediction in complex systems, random number generators, modeling, parameter estimation of nonlinear systems, among others. The majority of the applications can benefit from the power of chaos theory in terms of modeling an irregular system with a deterministic equation which has high sensitivity to the initial condition.

Being able to utilize a chaotic system, which has sensitivity to initial condition, density of unstable periodic orbits in a chaotic attractor and topological transitivity, is treated as a library of different behaviors and patterns from which each behavior or pattern can be selected based on the related needs. These qualities pave the way to advances for understanding the physical world or design technology that interfaces with dynamical complex systems. As computation chaos was proposed, it was revealed that chaotic behavior exists not only in natural dynamic systems but also in the discretization process, including instances in which the original system manifests periodicity with its computational simulation being chaotic.

The investigation of the relationship between chaos theory and computational simulation shows that the precision of computer arithmetics has a remarkable impact on the final outcome of the simulation of a dynamic system where even a trivial change in arithmetic computation can modify the structure of orbits significantly. To put the defining idea of chaos differently, in chaotic systems, even minuscule uncertainties in measurements of initial position and momentum can lead to radical errors in the long-term predictions of the quantities. Yet, sensitive dependence upon initial conditions hints that even the tiniest errors in initial measurements in chaotic systems eventually produce critical errors in the prediction of the future motion of an object (Mitchell 2009).

In addition, a nonlinear dynamical system owns complex and flexible dynamics which combine different behaviors, and thus, it can be morphed for the implementation of different functions. Bifurcation parameters in a nonlinear dynamical system can be changed and the dynamics can be altered, namely qualitative behavior of the circuit. Hence, when a nonlinear system is in a chaotic regime, it is very sensitive to its initial conditions or state. Therefore, a change to its initial state can change the future state, and as a result, the type of function it builds. The number of these different functions that a nonlinear, complex system can implement exponentially increases by the evolution time (Kia *et al.* 2020).

In summary, this study puts forth the features of complexity of varying phenomena, properties of evolution and adaptation, memory effects, nonlinear dynamic system qualities, the importance of chaos theory and applications of related aspects. Processes of fractional dynamics, differentiation and systems in complex systems as well as the dynamical processes and dynamical systems of fractional order with respect to natural and artificial phenomena are discussed in terms of their modeling by ordinary or partial differential equations with integer order, ordinary and partial differential equations.

Fractional calculus and fractional-order calculus approach to provide novel models with fractional-order calculus as employed in machine learning algorithms to achieve optimized solutions is also discussed besides the justification of the need to develop analytical and numerical methods. Subsequently, algorithmic complexity and its goal to ensure a better handling of efficient algorithms in computational sciences is pointed out with regard to the classification of computational problems. Moreover, we set forth the importance of stochastic differential equations with respect to some of the real world problems for an effective and intensive addressing of real world problems which manifest randomness. Characteristics of and benefits derived from nonlinear science are elaborated on with a focus on their essential impact observed in complex dynamics, explores the implicit, latent and obscure dependence of schema, serving to reveal the nonlinear descriptions of widely different systems.

The study further points out the neural networks, as descriptive models, for providing the means to gather, store and use experiential knowledge as well as Artificial Neural Networks (ANNs) in relation to their employment for handling experimental data in differing domains. Furthermore, evolutionary computational models and their role in retrieving applicable answers to optimization problems for various engineering areas, medicine, biology, mathematical science, applied disciplines and data science, among many others, is discussed along with an emphasis on mathematical sciences, with Artificial Intelligence (AI) and machine learning being at the pedestal and intersection with different fields which are characterized by complex, chaotic, nonlinear, dynamic and transient components in order to demonstrate the significance of novel approaches in real systems and related realms.

PROCESSES OF FRACTIONAL DYNAMICS, DIFFERENTIATION AND SYSTEMS IN COMPLEX SYSTEMS

Dynamical processes and dynamical systems of fractional order with respect to natural and artificial phenomena are modeled by ordinary or partial differential equations with integer order, which can be described aptly by employing ordinary and partial differential equations. Fractional calculus approach, remarkably, provides novel models through the introduction of fractional-order calculus to optimization methods, and thus, is employed in machine learning algorithms since this scheme is geared towards attaining optimized solutions by maximizing the model accuracy and minimizing functions like the computational burden. Hence, mathematical-informed frameworks can be employed for enabling reliable and robust understanding of various complex processes that involve a variety of temporal and spatial scales. This complexity requires a holistic understanding of different processes through multi-stage integrative models capable of capturing the significant attributes on the respective scales.

Fractional-order differential and integral equations, fractals, fractional integro-differentiation (non-integer order integro-differentiation), nonlinear time-delay systems, linear and nonlinear fractional ordinaries, nonlinear differential equations, integral fractional differential equations, partial differential equations and stochastic integral problems, in those regards, can provide the generalization of traditional integral and differential equations through the extension of the conceptions.

Analytical and numerical methods have been developed to solve ordinary and partial differential equations whose classes have been investigated in depth. Despite being useful to model some of the real world problems with efficiency, some classes of such differential equations have failed to replicate the observed facts due to complexities of several real world problems. For instance, since some real world problems manifest randomness that cannot be captured by these differential equations, stochastic differential equations can be suggested and are employed intensively in an effective way. Furthermore, algorithmic complexity, as a way of comparing the efficiency of an algorithm, can ensure a better grasping and designing of efficient algorithms in computational sciences while enabling the classification of computational problems based on their algorithmic complexity, as defined according to how the resources are required for the solution of the problem, including the execution time and scale with the problem size (Karaca 2022a). These sorts of approaches through the application of fractional-order calculus to optimization methods and the experimental results reveal the benefit maximizing the model's accuracy and minimizing the cost functions like the computational burden, as mentioned above, pointing toward the applicability of the methods in different domains which are characterized by complex, chaotic, nonlinear, irregular, asymmetric, dynamic and transient components.

Fractional (non-integer order) calculus, as an interdisciplinary field, is able to build mathematical models that are concise enough to describe the dynamic events occurring in complex elements, which is important to understand the underlying multiscale processes that arise when there are electrical stimulation or mechanical stress. Fractional calculus attends to the co-evolving entities, actual state properties, observations and patterns of complex systems in a spot-on manner with respect to nonlinear dynamic systems, modeling of complexity evolution, order of fractional chaotic as well as complex systems.

Fractional differential equations, associated with non-local phenomena, benefit from both qualitatively and quantitatively different properties as compared to the classical ones since the nonlocality of fractional calculus turns it into a sound means to unearth new properties of non-local phenomena. Furthermore, when compared with classical integer-order models, the preliminary advantage of fractional models is their potential use in chaotic dynamics in engineering and applied fields. Besides these points, the dynamics of fractional order systems have captured prominence through the development of fractional-order algorithm (Sun *et al.* 2022).

The dynamics of many systems, whether they be biological, economic, medical, physical, mechanical, electrical, thermal, and so forth, can be described in terms of differential equations. Fractional derivatives are extensively employed to model realistic systems since these derivatives are capable of modeling memory and hereditary effects observed in physical systems owing to their nonlocal nature. Systems that involve fractional derivatives can exhibit chaos, and when below a certain threshold value of fractional order derivative, the systems can show regular behavior. Being a nonlocal operator, contrary to ordinary derivative, the fractional derivative is particularly useful for modeling the system's both memory and hereditary properties (Baleanu *et al.* 2015).

Fractional calculus is frequently opted for mathematical modeling to analyze the evolutionary systems which are known to have memory effect on dynamics. To extend ordinary calculus to fractional calculus, there are different ways, with the related common definitions, Riemann-Liouville fractional integral and derivative, the Grünwald-Letnikov fractional integral and derivative as well as the Caputo fractional derivative as being some of them (Karaca and Baleanu 2022b). Within this framework, Caputo definition is preferred to be used to solve differential equations, which is denoted as per Equation 1:

$$\mathrm{D}_{\alpha}^{m} f(t)=\frac{1}{\Gamma(m-\alpha)} \int_{0}^{t} \frac{\mathrm{f}^{(m)}(\tau)}{(\mathrm{t}-\varnothing)^{\alpha+1-m}} d\tau \tag{1}$$

The fundamental results on fractional integral and derivatives of the power function $(t-t0)\beta\ for\ \beta>-1$ are the case and for the Caputo's derivative, Equation 2 is employed in the following manner (see (Karaca and Baleanu 2022b) for further details):

$$D_{\mathrm{t}_0}^{\alpha}(t-\mathrm{t}_0)^{\beta}=\begin{cases} 0 & \beta\epsilon\{0,1,...,m-1\} \\ \frac{\Gamma(\beta+1)}{\Gamma(\beta-\alpha+1)}(\mathrm{t}-\mathrm{t}_0)^{\beta-\alpha} & \beta>m-1 \\ nonexisting & otherwise \end{cases} \tag{2}$$

Taken together, fractional calculus, equations with fractional derivatives, integrals and differences prove to be powerful tools for the description of local processes in time and space with different nonlocality types (Diethelm *et al.* 2022).

Nonlinear science, which has had a central impact on complex dynamics, explores the implicit, latent and obscure dependence of schema, serving to reveal the nonlinear descriptions of widely different systems (Karaca 2022a). As a substitution for fractional derivatives, the memory-dependent derivative reflects the memory effect distinctively, and as an application, representative processes are remodeled with it, considering the temporal-spatial evolution mechanisms of the related complex processes. Accordingly, the theory of fractional differentiation and applications constitutes a significant component of nonlinear analysis to be able to address highly diverse real-life problems. Analysis and control of fractional order nonlinear systems can appear to be another pressing challenge with the observation of unknown inputs and concepts used and derived analytically. Being a noteworthy attribute of complex systems, nonlinearity represents the various interactions between the variables in a nonlinear fashion.

Emergence, feedback, adaptiveness, irreducibility, chaos, operating between order and chaos, having multilayers of structure as well as self-organization seem to be among some of the other related attributes. Multiple nonlinear complex systems manifest phenomena in which oscillations enhance periodic behaviors and the system's synchronization. Accordingly, fractional-order control as a field of control theory employs the fractional-order integrator as part of the control system design compilation, through which well-established control methods and strategies can be generalized and improved (Monje *et al.* 2010). More complex physical problems, on the other hand, require advanced mathematical operators of differentiation.

The concept of non-local operators of differentiation some of which are power law, exponential decay law and generalized Mittag-Leffler law, has been employed by different engineering and medicine fields, applied sciences and technology owing to the fact that they have the capability of integrating more complex natural aspects into mathematical equations (Kober 1940; Baleanu and Karaca 2022). Thus, the extension of classical and modern control theories to integrative and novel perspectives ensures the development of algorithms applicable both in integer and non-integer order systems. Therefore, fractional and integral equations, fractional discrete calculus, fuzzy fractional calculus as well as fractional dynamics concern not only theoretical aspects but also the applications related to fractional differentiation extending broadly across other mathematical models within mathematical sciences and engineering mathematics (i.e.: entropy, fractals, wavelet, quantum, etc.) ranging along mathematical analysis, numerical analysis, chaos, image and/or signal analysis, bifurcation, data analysis, time series analysis, medicine, neurology, bioengineering, economics, finance, control systems, artificial intelligence, mathematical biology, biotechnology, genetics, nanotechnology, and so forth.

PROCESSES OF MATHEMATICAL SCIENCE, ARTIFICIAL INTELLIGENCE AND APPLICATIONS IN COMPLEX SYSTEMS

Complexity, as a highly correlated nonlinear phenomena evolving along an extensive array of timescales and length scales, poses challenges for technical analyses, theoretical modeling and numerical simulations in many domains. It becomes critical to control the underlying systems and processes across their spatio-temporal evolution. Thus, data, concerning biological, financial, physical or technological complex systems, can be rendered manageable through computer simulations that employ the effective nonlinear dynamic methods.

The attempt to understand a complex system with multiple interacting components, human body, for example, or weather patterns, financial market, living systems concern two factors, one of which is chaos and the other one being complexity. An important finding of modern chaos theory is that even though complex systems may be predictable in the short term, that would not be the case for the long term since there exists an element of uncertainty and unpredictability in all complex systems (Schueler 1996). In other words, complex interactions may make the prediction of long-term outcomes almost impossible; and complexity constitutes complex interacting systems with new emergent properties that make them more than the sum of their parts (Clegg 2020). A slight disturbance in the chaotic system could make one be unable to specify the future state with precision, meaning its evolution could not be predictable, which points to an intrinsic uncertainty situation (Sanjuán 2021). These significant findings of chaos theory have accordingly been transposed to other disciplines.

Chaos, which is a long-term aperiodic and random-like behavior, is exhibited by many nonlinear complex dynamic systems, which requires the revealing of accessible and applicable paths into abundance of complexity and the superfluity of experimental processes to generate novel, diverse and robust means. The use of predictive tools, Artificial Intelligence (AI) and machine learning techniques has made the number of applications possible, including the prediction of mechanisms ranging extensively from living organisms to other interactions across incredible spectra. These techniques combined with fractal analysis highlight the fractal dimension and measurement of lacunarity both on local and global scale as well as the entire volume of the samples being handled. Machine learning, as a subset of AI, signifies the methods which are capable of learning from experience, which enables the performance of designated tasks such as detection, recognition, iteration, diagnosis, optimization and prediction.

Machine learning is employed in different domains of complex systems within nonlinear dynamic processes, which involve the identification of the basic system structure, for instance network nodes and links, as well as the exploration of dynamic behavior of nonlinear systems like determining exponents, prediction of future evolution and inferring causality of interactions. Reservoir computing and long short-term memory which are machine learning processes are usually dynamical in nature, whose understanding of when, how and why to function well based on data can potentially be addressed by employing tools from dynamical systems theory (Tang *et al.* 2020).

Neural networks and physical systems have emergent collective computational abilities and their architecture is capable of producing an emergent associative memory. By providing an explicit physical interpretation, efficiency for practical applications and more manageable computational complexity, fractional mathematics and Artificial Intelligence (AI) can capture the history of dynamical effects existent in different natural and artificial phenomena, proving to be essential modes with their conceptions supporting a productive interplay in the exploration of the structure and functions with respect to complex system dynamics (Karaca 2022c). To be able to capture and observe the dynamic variations in complex systems, distributions can also be employed. For instance, heavy-tailed distributions, as found throughout many naturally occurring phenomena, are particularly preferable concerning their use in stochastic dynamical models for extreme events which display the presence of outliers and possibility of extreme values.

Machine learning and control theory, with high technological impacts, comprise gateways that are in proximity with each other in the complex landscape of the universe of mathematics. Involving the prompting of a dynamical system from an initial configuration to the final one over extended ranges of time and frequency through aptly designed and applicable controls, the notion of controllability allows the disclosing of the pathways between the disciplines. Hence, control theory can be stated to lie on the pillars of machine learning.

Machine learning and data science, as integrative domains, entail an optimized method to calculate mathematics and metamathematics derivatives in minimum timeframe with maximum efficiency; hence, evolutionary computation, in computer science, constitutes a cluster of algorithms for global optimization, which draws its inspiration from nature and biological evolutionary processes. Evolutionary computational models own a sophisticated searching technological foundation besides a mathematical problem optimization tool taking up less time and reducing complexity so that the precise and applicable answer to optimization problems for various engineering, mathematical and applied disciplines can be sought and found. Accordingly, AI and machine learning, situated at the core, can extend broadly across the related mathematical models within the framework of mathematical sciences and engineering mathematics as well as across the intersection of different fields.

Fractional-order calculus is concerned with the differentiation and integration of non-integer orders, and fractional calculus (FC), based on fractional-order thinking, is the quantitative analysis of functions using non-integer order integration and differentiation. Therein, the order can be a complex number, a real number of the function of a variable. Owing to these features, FC, entailed by complexity, can enhance the processing of complex signals, improve the control of complex systems extend the enabling of the potential for creativity, considering the fact that an observable phenomenon that is represented by a fractal function has integer-order derivatives which diverge. Hence, complex phenomena, no matter if they are natural or engineered, need to be described by fractional dynamics as such point of view is to be consulted for the characterization and regulation of complexity (West 2022). In view of these attributes, innovative approaches to machine learning with the introduction of fractional-order calculus have started to be extensively used as optimization methods used in machine learning algorithms. By performing the training of the models, making inferences and solving optimization problems, machine learning techniques are geared towards maximizing model's accuracy and minimizing cost functions. In short, these techniques provide flexible options for the analysis and prediction of changes that could occur in the dynamics of complex and chaotic systems.

Life, being the most complex physical system in the universe, at all scales, requires the understanding of the massive complexity encompassing its origin, structure, dynamics, adaptation and organization. The number of substructures and interacting pathways of each of the substructure along with the other ones as well as neurons determine the degree of complexity. Neural networks, as descriptive models provide the means to gather, store and use experiential knowledge; and are designed in such a way that they can emulate different operations of the human brain. A neuron is an imitation of the observations occurring in the human brain which is composed of interconnected neurons that transmit electrochemical elements, which forms the basis of all neural networks (Karaca and Baleanu 2022a).

A synapse is the connection between nodes, or neurons, in an artificial neural network (ANN); and in this configuration, the strength or amplitude controls this connection between the nodes, which is called the synaptic weight. There exists a complex structure with multiple connections as multiple synapses can connect with the same neurons, in which each synapse has a different level of trigger or impact on whether the neuron is fired and activates the next neuron. With relation to machine learning, a synapse is often referred to as a node in machine learning; yet, the artificial neurons, which output a value from a continuous function, do not fire, unlike biological neurons. To put differently, the main different point between a biological process and artificial process is concerned with the level of control imposed on the input values. Thus, the resulting output of the nodes is utilized as the input for the next layer of nodes, in an ongoing process, throughout the neural network brain until the final output layer is reached (Karaca and Baleanu 2022a) (see Figure 1).

One major ongoing challenge of integrating fractional calculus in cases of complexity is the effective use of empirical, numerical, experimental and analytical methods to be able to tackle complexity. In that regard, ANNs, including a family of nonlinear computational methods, can be employed to handle experimental data in various domains as a result of their capability of managing complex computations to direct their progressive application towards serving the applicable and timely solutions of practical problems.

The specific neural architectures are generated by AI, as instantiated in the brain, can provide applicable answers to the problems of cognition through the understanding of the way architectures implement cognitive processes. Thereby, if programmed properly and adjusted to the data at hand appropriately, AI enables availability at all times, providing more prompt decision-making processes, digital assistance, new inventions and rapid pattern analysis of large datasets while also reducing human error. To attain these goals, Bidirectional Encoder Representations from Transformers (BERT), as one of the applicable methods of Natural Language Processing (NLP) can be employed, with the related models which have the main stages like pre-training and fine-tuning. In the former one, the model is trained on unlabeled data over different pre-training tasks and in the latter stage, the BERT model is initialized with the pre-trained parameters (Karaca *et al.* 2022) (see Figure 2).

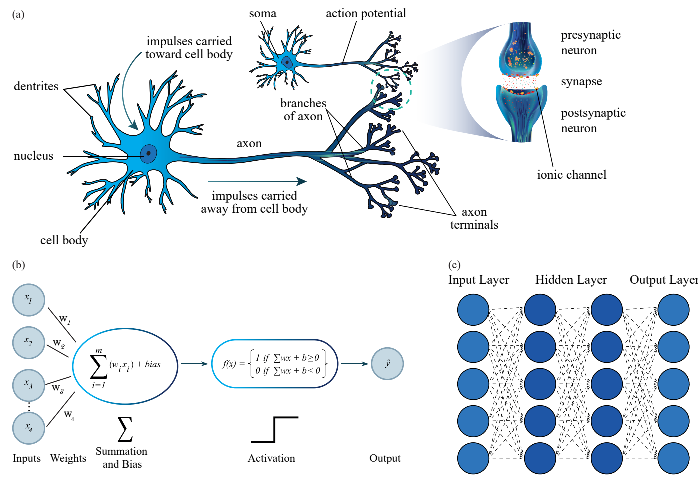

Figure 1 Biological versus artificial neuron interconnection from inputs at dendritic compartments to outputs at axon terminals: (a) the basic building blocks of biological neural processing with neurons and synapses. (b) artificial implementation of a neuron, as electrically excitable cell producing action potential. (c) synaptic interrelation among input layer, hidden layers and output layer (Karaca and Baleanu 2022a).

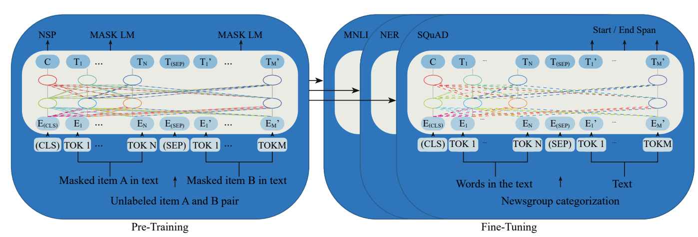

Figure 2 BERT model's pre-training and fine-tuning stages (Karaca *et al.* 2022).

All in all, the advanced theory and applications of computability enables one to distinguish complexity classes of problems, considering the order of corresponding functions that describe computational time pertaining to their algorithms or computational problems. This refers to the essential requirement of being concerned not only with the complexity of universal problem solving but also with the complexity of knowledge-based programs (Mainzer and Mainzer 1997). Through that perspective in conjunction with advanced mathematical modeling with AI support, it would be possible to generate applicable cumulative answers and customized solutions to real world problems in a novel, constructive, adaptive and flexible way on the ever-evolving global landscape.

CONCLUDING REMARKS AND FUTURE DIRECTIONS

The use of different predictive mathematical modeling, Artificial Intelligence (AI) and machine learning techniques has made the number of applications possible, including the prediction of mechanisms ranging extensively from life at simple level to other interactions getting gradually complex across incredible spectra. It is possible to observe that nature can produce complex structures even in simple situations, and can obey simple laws even in complex situations. Consequently, complex problems in nonlinear dynamics require the precarious support of artificial phenomena along with interpretability and predictability in order that each domain of complex systems can yield applicable answers and solutions to the pressing challenges of our current era. This view can help to cater the needs of different aspects of complexity by significantly diminishing the problems of complexity whose solutions are based on advanced mathematical foundations and corresponding algorithmic models that include numerous applied aspects of complexity.

Constituting the prompting of a dynamical system from an initial configuration to the final one over extended ranges of time and frequency through aptly designed and applicable controls, the notion of controllability allows the disclosing of the pathways across the related disciplines. Furthermore, processes of fractional dynamics, differentiation and systems in complex systems as well as the dynamical processes and dynamical systems of fractional order with relation to natural and artificial phenomena are important in terms of their modeling by ordinary or partial differential equations with integer order, ordinary and partial differential equations. Fractional calculus and fractional-order calculus approach to provide novel models with fractional-order calculus as employed in machine learning algorithms to achieve optimized solutions is also noteworthy considering the need to develop analytical and numerical methods.

Machine learning, a subset of AI, referring to the methods capable of learning from experience, enables the performance of designated tasks such as detection, recognition, iteration, diagnosis, optimization and prediction. It is employed in different domains of complex systems within nonlinear dynamic processes that involve the identification of the basic system structure, such as network nodes and links, as well as the exploration of dynamic behavior of nonlinear systems like determining exponents, prediction of future evolution and inferring causality of interactions. Besides conventional methods like approximation, estimation, convergence, stability analysis, and so forth, it is important to capture the latent aspects of complex nonlinear dynamic structures so that prediction can be made possible.

Accurate and prompt predictive processes can ensure foreseeing to be put in practice in order to cater the needs of our era with the landscape being transient and ever-evolving. These pressing challenges and needs point to the importance of yielding applicable solutions to problems for various engineering areas, medicine, biology, mathematical science, applied disciplines and data science, among many others. These points have been discussed in detail in this study along with an emphasis on power of predictability, relying on mathematical sciences and engineering mathematics with Artificial Intelligence (AI) and machine learning being at the pedestal and intersection with different fields characterized by complex, chaotic, nonlinear, dynamic and transient components to reveal the significance of optimized approaches in real systems and related realms. Significant developments based on these critical points and perspectives can pave the way for the future research towards optimized applicable solutions of unsolved problems arising as formidable challenges of our ever-evolving and fast-changing global landscape.

Conflicts of interest

The authors declare that there is no conflict of interest regarding the publication of this paper.

Availability of data and material

Not applicable.

LITERATURE CITED

Baleanu, D. and Y. Karaca, 2022 Mittag-leffler functions with heavy-tailed distributions' algorithm based on different biology datasets to be fit for optimum mathematical models' strategies. In *Multi-Chaos, Fractal and Multi-fractional Artificial Intelligence of Different Complex Systems*, pp. 117–132, Elsevier.

Baleanu, D., R. L. Magin, S. Bhalekar, and V. Daftardar-Gejji, 2015 Chaos in the fractional order nonlinear bloch equation with delay. Communications in Nonlinear Science and Numerical Simulation **25**: 41–49.

Clegg, B., 2020 *Everyday Chaos: The Mathematics of Unpredictability, from the Weather to the Stock Market*. MIT Press.

Diethelm, K., V. Kiryakova, Y. Luchko, J. Machado, and V. E. Tarasov, 2022 Trends, directions for further research, and some open problems of fractional calculus. Nonlinear Dynamics pp. 1–26.

Goldenfeld, N. and L. P. Kadanoff, 1999 Simple lessons from complexity. science **284**: 87–89.

Karaca, Y., 2022a Global attractivity, asymptotic stability and blow-up points for nonlinear functional-integral equations'solutions and applications in banach space BC(R+) with computational complexity. Fractals **30**: 2240188.

Karaca, Y., 2022b Multi-chaos, fractal and multi-fractional AI in different complex systems. In *Multi-Chaos, Fractal and Multi-fractional Artificial Intelligence of Different Complex Systems*, pp. 21–54, Elsevier.

Karaca, Y., 2022c Theory of complexity, origin and complex systems. In *Multi-Chaos, Fractal and Multi-fractional Artificial Intelligence of Different Complex Systems*, pp. 9–20, Elsevier.

Karaca, Y. and D. Baleanu, 2022a Artificial neural network modeling of systems biology datasets fit based on mittag-leffler functions with heavy-tailed distributions for diagnostic and predictive precision medicine. In *Multi-Chaos, Fractal and Multi-fractional Artificial Intelligence of Different Complex Systems*, pp. 133–148, Elsevier.

Karaca, Y. and D. Baleanu, 2022b Computational fractional-order calculus and classical calculus ai for comparative differentiability prediction analyses of complex-systems-grounded paradigm. In *Multi-Chaos, Fractal and Multi-fractional Artificial Intelligence of Different Complex Systems*, pp. 149–168, Elsevier.

Karaca, Y., Y.-D. Zhang, A. D. Dursun, and S.-H. Wang, 2022 Multifractal complexity analysis-based dynamic media text categorization models by natural language processing with bert. In *Multi-Chaos, Fractal and Multi-fractional Artificial Intelligence of Different Complex Systems*, pp. 95–115, Elsevier.

Kia, B., J. F. Lindner, and W. L. Ditto, 2017 Nonlinear dynamics as an engine of computation. Philosophical Transactions of the Royal Society A: Mathematical, Physical and Engineering Sciences **375**: 20160222.

Kia, B., A. Mendes, A. Parnami, R. George, K. Mobley, *et al.*, 2020 Nonlinear dynamics based machine learning: Utilizing dynamics-based flexibility of nonlinear circuits to implement different functions. Plos one **15**: e0228534.

Kober, H., 1940 On fractional integrals and derivatives. The quarterly journal of mathematics pp. 193–211.

Mainzer, K. and K. Mainzer, 1997 *Thinking in complexity: The complex dynamics of matter, mind, and mankind*, volume 3. Springer.

Mateos, J. L., 2009 Complex systems and non-linear dynamics. Fundamentals Of Physıcs-Volume I p. 356.

Mitchell, M., 2009 *Complexity: A guided tour*. Oxford university press.

Monje, C. A., Y. Chen, B. M. Vinagre, D. Xue, and V. Feliu-Batlle, 2010 *Fractional-order systems and controls: fundamentals and applications*. Springer Science & Business Media.

Sanjuán, M. A., 2021 Artificial intelligence, chaos, prediction and understanding in science. International Journal of Bifurcation and Chaos **31**: 2150173.

Schueler, G. J., 1996 The unpredictability of complex systems. Journal of the Washington Academy of Sciences pp. 3–12.

Sun, K., S. He, and H. Wang, 2022 Dynamics of fractional-order chaotic systems. In *Solution and Characteristic Analysis of Fractional-Order Chaotic Systems*, pp. 77–115, Springer.

Tang, Y., J. Kurths, W. Lin, E. Ott, and L. Kocarev, 2020 Introduction to focus issue: When machine learning meets complex systems: Networks, chaos, and nonlinear dynamics. Chaos: An Interdisciplinary Journal of Nonlinear Science **30**: 063151.

Waldrop, M. M., 1993 *Complexity: The emerging science at the edge of order and chaos*. Simon and Schuster.

West, B. J., 2022 Fractional calculus and the future of science.

How to cite this article: Karaca, Y., and Baleanu, D. Evolutionary Mathematical Science, Fractional Modeling and Artificial Intelligence of Nonlinear Dynamics in Complex Systems. *Chaos Theory and Applications*, 4(3), 111-118, 2022.

CHAOS
Theory and Applications
in Applied Sciences and Engineering

e-ISSN: 2687-4539
RESEARCH ARTICLE
Vol.4 / No.3 / 2022 / pp.119-127
https://doi.org/10.51537/chaos.1144123

Route to Chaos and Chimera States in a Network of Memristive Hindmarsh-Rose Neurons Model with External Excitation

Sishu Shankar Muni[*,1], **Zeric Tabekoueng Njitacke**[β,2], **Cyrille Feudjio**[α,3], **Theophile Fonzin Fozin**[§,4] **and Jan Awrejcewicz**[**,5]

[*]School of Mathematical and Computational Sciences, Massey University, Palmerston North, New Zealand, [β]Department of Electrical and Electronic Engineering, College of Technology (COT), University of Buea, P.O.Box 63, Buea (Cameroon), [α]Department of Electrical and Electronic Engineering, College of Technology (COT), University of Buea, P.O.Box 63, Buea (Cameroon), [§]Department of Electrical and Electronic Engineering, Faculty of Engineering and Technology (FET), University of Buea, P.O. Box 63, Buea, Cameroon, [**]Department of Automation, Biomechanics and Mechatronics, Lodz University of Technology, Lodz, Poland.

ABSTRACT In this paper we have introduced and investigated the collective behavior of a network of memristive Hindmarsh-Rose (HR) neurons. The proposed model was built considering the memristive autapse of the traditional 2D HR neuron. Using the one-parameter bifurcation diagram and its corresponding maximal Lyapunov exponent graph, we showed that the proposed model was able to exhibit a reverse period doubling route to chaos, phenomenon of interior and exterior crises. Three different configurations of the ring-star network of the memristive HR neuron model, including ring-star, ring, and star, have been considered. The study of those network configurations revealed incoherent, coherent , chimera and cluster state behaviors. Coherent behavior is characterized by synchronization of the neurons of the network, while incoherent behaviors are characterized by the absence of synchronization. Chimera states refer to a differet state where there is a coexistence of synchroniaed and asynchronized nodes of the network. One of the interesting result of the paper is the prevalence of double-well chimera states in both ring and ring-star network and has been first mentioned in the case of memrisitve HR neuron model.

KEYWORDS
2D Hindmarsh-Rose neuron
Memristive autapse
routes to chaos
Ring-star network
Chimera states
Double-well chimera state

INTRODUCTION

A brain, like a complex organ, is built from the interconnection of a very large number of neurons. These interconnected neurons are very important because they are the seat of the processing, calculation, storage, and transfer of information (Lin *et al.* 2021). These neurons are connected to each other using a synapse.As a result, a synapse is the part of the nervous system that allows a presynaptic neuron the transmission of electrical or chemical signals to the postsynaptic neuron. (Zhang *et al.* 2018). As a result, several mathematical models have been developed and studied in the literature to study some of the dynamical mechanisms of the brain. The Hopfield neural network model (Njitacke *et al.* 2021a; Tabekoueng Njitacke *et al.* 2020a; Doubla Isaac *et al.* 2020; Tabekoueng Njitacke *et al.* 2020b), the Hodgkin-Huxley neuron (Hodgkin and Huxley 1990), the 2-D Hindmarsh-Rose (HR), the 3D-HR neuron models (Hindmarsh and Rose 1982, 1984), the FitzHugh-Nagumo (FHN) neuron model (Izhikevich and FitzHugh 2006), the MorrisLecar neuron model (Tsumoto *et al.* 2006), the Chay neuron model (Chay 1985), the Izhikevich neuron model (Izhikevich 2003), and the Rulkov neuron model (Xu *et al.* 2021) are some examples. In the same vein, several artificial synapse models for presynaptic and postsynaptic neuron coupling have been developed in the literature. Some of them are hybrid synapse (Liu *et al.* 2019), Josephson junction synapse (Zhang *et al.* 2020b), memristive synapse (Li 2021), electrical synapse (Shaffer *et al.* 2016; Zhou *et al.* 2021a), and chemical

Manuscript received: 21 July 2022,
Revised: 13 September 2022,
Accepted: 4 October 2022.

[1] s.muni@massey.ac.nz
[2] zerictabekoueng@yahoo.fr (**Corresponding Author**)
[3] cyrille.feudjio@ubuea.cm
[4] fozintheo@gmail.com
[5] jan.awrejcewicz@p.lodz.pl

synapse (Burić *et al.* 2008). Following that, a large number of single neurons (Bao *et al.* 2018, 2019; Hou *et al.* 2021; Liu *et al.* 2020; Zhang *et al.* 2020a; Zhou *et al.* 2021b; Cai *et al.* 2021; Li *et al.* 2021a) and coupled neurons (Zhou *et al.* 2021b; Njitacke *et al.* 2022a, 2020, 2021b,c; Tabekoueng Njitacke *et al.* 2020c; Guo *et al.* 2020; Joshi 2021; Li *et al.* 2021b; Lin *et al.* 2020; Wu *et al.* 2020; Yao *et al.* 2021; Wouapi *et al.* 2020, 2021) models have been introduced and addressed in the literature using the quoted artificial synapses.

The authors of ref. (Qin *et al.* 2021) investigated the phenomenon of phase-amplitude coupling in nonlinearly coupled Stuart-Landau oscillators. Among the architectures used by the authors, it can be found the high-frequency neural oscillation driven by an external low-frequency input and two interacting local oscillations with distinct, locally generated frequencies. The problem of reconstructing the model equations for the network of 3rd order neuron-like oscillators from time series has been addressed in ref. (Sysoeva *et al.* 2021). The authors showed that by using phase-locked loop systems as nodes of the networks, dynamical regimes such as quasiharmonic oscillations, spiking, bursting, and chaotic behavior are based on different network typologies such as star, ring, chain, and random architectures. The dynamical and physiological effects of the presence of electric field on an improved version of FitzHugh-Nagumo model was investigated in (Takembo *et al.* 2022). Using the multiple scale expansion method on the system of N-differential equations, the authors obtained the angular frequency of the modulated impulse wave along the network. Finally, the formation of localized nonlinear wave patterns was confirmed in the proposed network.

The behavior of both single and a network of FHN neuron with memristors were investigated in ref. (Njitacke *et al.* 2022c). The investigation of the single neuron revealed the presence of hidden dynamics, which is an interesting feature in the qualitative theory of dynamical systems. The biophysical energy of that model was established using the famous the Helmholtz theorem. The authors found that variation of external current on the model had no effect on the energy. Interestingly, the autapse coupling strength affects the energy released by the neuron. A plethora of spiking and bursting patterns is observed in the model. Hysteretic dynamics due to the coexistence of different firing patterns was confirmed. To verify both the analytical, numerical results, an equivalent electronic circuit was constructed. It was found that the results obtained from the circuit are in good agreement with the numerical simulations. In the end, information pattern stability was explored statistically via modulational instability under memristive autapse strength using a chain network of 500 identical neurons. It was discovered that the new network enables localized information patterns with attributes of synchronization as a means of information coding when initial conditions are considered as slightly modulated plane waves. The improved information coding pattern and potential mode transition were also confirmed by stronger autaptic couplings caused by fixing the stimulation current.

After researchers have studied coupled pendulums and their dynamical behavior Willms *et al.* (2017), there has been a plethora of studies on network of oscillators. When the network elements have similar phases and frequencies the oscillators get synchronized. If the phases and frequencies are different they get desynchronized. Kuramoto found a new type of network state in which oscillators synchronize and desynchronize in a network of oscillators and these were termed as chimera states Kuramoto and Battogtokh (2002). There has been a lot of works on chimeras thereafter Schöll (2016); Majhi *et al.* (2019); Omel'chenko (2018); Panaggio and Abrams (2015), just to name a few. Scientists have even uncovered epilepsy and schizophernia as topological diseases that depend on the topology of the neurons interconnected in the brain Uhlhaas and Singer (2006). Neurons can also be considered as dynamical oscillators and in brain millions of neurons are interconnected in a complex fashion and neurons transmit nerve signals and sensory informations. This motivates to study the behavior of networks in neuron oscillators.

An autapse is a specific synapse developed from an auxiliary loop that enables it to connect the axon and the dendrite of the same neuron together. In this contribution, a memristor is introduced in a 2D Hindmarsh-Rose neuron model. Therefore, the memristive Hindmarsh-Rose neuron thus obtained is also called the 2D Hindmarsh-Rose neuron with a memristive autapse. The study of the network is based on the ring-star, ring, and star connection from the introduced model. So the outline of the paper is as follows: In Section 2, the mathematical model of the memristive Hindmarsh-Rose model is discussed. Its complex dynamical behavior is revealed through some numerical simulations. Its network topology is also presented. In Section 3, numerical simulations are used to explore the collective behavior of the various network topologies considered. Lastly, in Section 4, we conclude and present scope for further research work. All the simulations in the paper is carried out using MATLAB.

PRESENTATION OF THE NEURON MODEL

Framework of memristive autapse

When an axon is injured, such as by poisoning in ion channels or heterogeneity in a local area of the axon, signal transmission can be terminated or blocked during neuronal communication. As a result, neurons can develop new loops or secondary loops to help with signal transmission. This auxiliary loop is known as an autapse, which can be electrical autapse current, chemical autapse current, or memristive autapse current. Using memristor definition (Galinsky and Frank 2021) and applying Ohm's law, we get Eq.(1).The term $G(u)$ represents the memductance and i, u, v are state variables.

$$\begin{cases} i_m = G(u)\, v = \alpha \cos(u)\, v, \\ \frac{du}{dt} = g(u, v) = \sin(u) + ev. \end{cases} \tag{1}$$

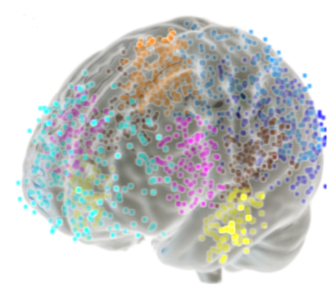

Figure 1 Complex interconnections of millions of neurons in the brain(Galinsky and Frank 2021)

The memristive nature of the autapse proposed in (1) is supported by the well-known fingerprint of the memristor, characterized by a pinched hysteresis loop at the origin of the current-voltage characteristic when applying an external stimulus in the form $v = A\sin(Ft)$. For the sake of brevity, that result is not provided. Recall that the memristive neuron model used for this investigation was previously introduced in (Njitacke *et al.* 2022b). In that work, the global dynamical behavior as well as the effect of the initial condition on the behavior of the neuronal model have been investigated. The authors discovered the considered neuron model with memristive autapse was able to exhibit a homogenous extreme multistability characterized by the coexistence of an infinite number of patterns of the same shape. Since the work was focused only on the dynamics of a single neuron, the investigation of the collective behavior of such a model with homogeneous extreme multistability has further supported the aim of this study.

Design of the coupled neurons

Neurons are the central organs of the brain since they enable computation, processing, and storage of information, just to name a few. As it can be seen in Fig.(1), the brain is made up of interconnections of a very large number of neurons. As a result, the investigation of a ring-star network of neurons composed of Hindmarsh-Rose neurons with memristive autapse will be addressed in this contribution. The mathematical model of the memristive HR neuron is given in (2).

$$\begin{cases} \dot{x} = y - ax^3 + bx^2 + \alpha \cos(u)\, x + i_s \\ \dot{y} = c - dx^2 - y \\ \dot{u} = \sin(u) + ex \end{cases} \tag{2}$$

In (2), x is the membrane potential of the HR neuron, y represents the retrieval variable related to a fast current of either Na^+ or K^+. The state variable u stands for the inner variable of the memristive autapse , variable $i_s = m \sin(2\pi f t)$ represents outward input current and α indicates the connection strength of the memristive autapse. For parameters $a = 1, b = 3, c = 1, d = 5, e = 0.5, m = 2, f = 0.5$ and α is tuneable. As it can be seen in Fig.(2). The single HR neuron with a memristive autapse is able to exhibit very rich and striking bifurcations. When decreasing the control parameter, phenomena such as reverse period doubling bifurcation, interior and exterior crises are observed.

These crises occur when a chaotic motion is suddenly destroyed and gives birth to periodic motion, or when a chaotic motion is suddenly created from a periodic one instead of being destroyed. As it can be seen in Fig.(3), four phase space trajectories have been computed to further support the phenomenon of the reverse period doubling bifurcation when the memristive autapse strength α is decreased. When decreasing α, it is observed that period-1 for $\alpha = 2$, period-2 for $\alpha = 1.5$, period-4 for $\alpha = 1.15$ and a chaotic attractor for $\alpha = 1$.

In addition, as the control parameter in the system is varied, alternating transitions of periodic and chaotic behavior is observed. When the control parameter α is tuned to 0.5, some two-dimensional and three-dimensional projections of the chaotic activity, generated by the memristive neuron of the network considered in this work, are provided in Fig.(4).

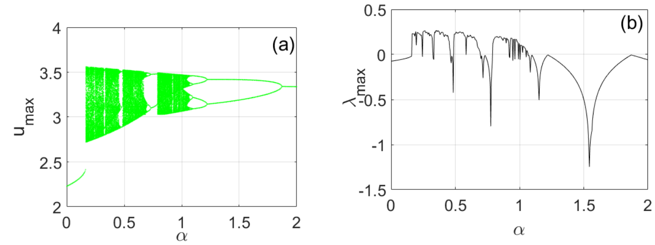

Figure 2 In (a), one-parameter bifurcation diagram of u vs α showing reverse period-doubling route to chaos as parameter α is increased. In (b), the corresponding Lyapunov exponent is estimated numerically. The parameters are set as $f = 0.5, m = 2$ with the initial condition $(0, 0, 1)$.

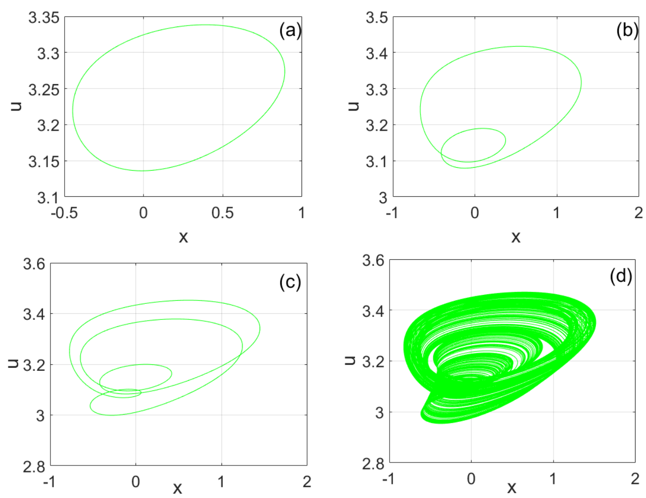

Figure 3 Phase space trajectories showing the phenomenon of the reverse period doubling bifurcation for some discrete values of the control parameter α

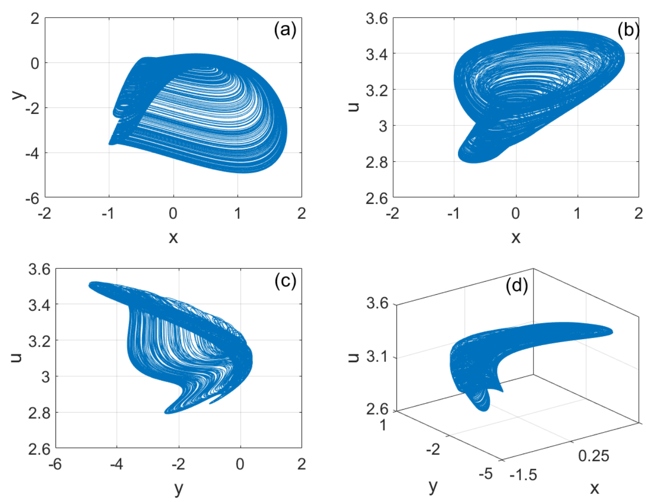

Figure 4 Phase space trajectories for a discrete value $\alpha = 0.5$ of model of the neuron memristive autapse displaying chaotic dynamics.

RING-STAR NETWORK OF MEMRISTIVE HINDMARSH-ROSE MODEL

After exploring the dynamical analysis of the memristive Hindmarsh-Rose neuron model in brief, we explore the collective behavior in a ring-star network of memristive Hindmarsh-Rose neuron model. An advantage of this mixed topological network is we get three different networks for free (ring-star, ring, and star network).

Ring and star networks find their applications in various real world systems (Roberts and Wessler 1970), gene regulatory networks (Shu *et al.* 2021), just to name a few. It is an important fundamental network to study first for a dynamical oscillator. A sketch of a ring-star network is illustrated in Fig. 5.

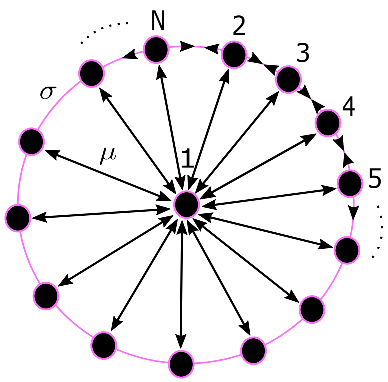

Figure 5 The memristive Hindmarsh-Rose neuron system connected in a ring-star network. Here we consider $N = 100$ memristive HR neurons where the central one is labeled $i = 1$ and the end nodes are labeled from $i = 2, \dots, N$. The ring and star coupling strengths are denoted by σ and μ respectively.

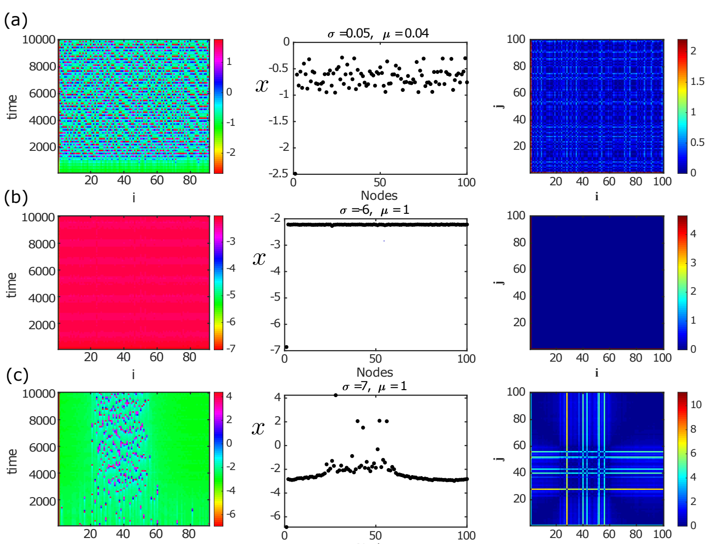

Figure 6 Ring-Star network of memristive Hindmarsh Rose neuron model with $\sigma \neq 0, \mu \neq 0$. Random initial conditions are set with the coupling range of $P = 70$. Number of nodes considered is $N = 100$. Asynchronous behavior in (a), synchronous behavior in (b), chimera state in (c) is shown.

The dynamical equations of the ring-star network are given by

$$\begin{aligned}
\dot{x}_i &= f_x + \mu(x_i - x_1) + \frac{\sigma}{2P}\sum_{n=i-P}^{n=i+P}(x_i - x_n), \\
\dot{y}_i &= f_y, \\
\dot{u}_i &= f_u, \\
\dot{w}_i &= f_w.
\end{aligned} \tag{3}$$

The central node ($i = 1$) is governed by the following system of differential equations:

$$\begin{aligned}
\dot{x}_1 &= f_x + \sum_{j=1}^{N}\mu(x_j - x_1), \\
\dot{y}_1 &= f_y, \\
\dot{u}_1 &= f_u, \\
\dot{w}_1 &= f_w.
\end{aligned} \tag{4}$$

where

$$\begin{aligned}
f_x &= y_i - ax_i^3 + bx_i^2 - \alpha x_i \cos(u_i) + m\sin(w_i), \\
f_y &= c - dx_i^2 - y_i, \\
f_u &= \sin(u_i) + ex_i, \\
f_w &= 2\pi f.
\end{aligned}$$

with periodic boundary conditions:

$$\begin{aligned}
x_{i+N}(t) &= x_i(t), \\
y_{i+N}(t) &= y_i(t), \\
u_{i+N}(t) &= u_i(t), \\
w_{i+N}(t) &= w_i(t)
\end{aligned}$$

for $i = 2, 3, \dots, N$. The parameters used throughout this study are: $a = 1, b = 3, c = 1, d = 5, e = 0.5, \alpha = 0.5, f = 0.5$. The size of the network is considered to be of 100 nodes with P nearest neighbors connected to each other. The network parameters such as the ring coupling strength σ, star coupling strength μ, and the coupling range P will be varied to explore different synchronization patterns arising in the ring-star network of memristive Hindmarsh-Rose neuron system.

Note that the ring-star network transforms to a ring network when $\mu = 0$ and it transforms to a star network when $\sigma = 0$. The mixed topological ring-star network prevails when $\sigma \neq 0$ and $\mu \neq 0$. We have divided our whole network analysis into three categories: category A: ring-star network, category B: ring network, category C: star network.

Characterization of chimera states

In order to characterize the spatiotemporal patterns obtained in the study, we use the measure of strength of incoherence (SI). SI was developed as a measure to characterize different spatiotemporal patterns exhibited by the network of neurons. Many studies have shown that SI is able to characterize different spatiotemporal states in a network of neurons.

Here we give a sketch of the method adapted by the Strength of Incoherence. The idea lies in transforming the original variables into new variables. Suppose $x_i, i = 1, \dots, N$ represents the original set of variables of the network system. Next, define new set of variables as $z_i = x_i - x_{i-1}, i = 1, \dots, N$. The average of z_i's is denoted by

$$\langle z \rangle = \frac{1}{N}\sum_{i=1}^{N} z_i.$$

We then evaluate the quantity

$$\chi(m) = \left\langle \sqrt{\sum_{j=n(m-1)+1}^{nm} (z_j - \langle z \rangle)^2 \rangle_t} \right\rangle.$$

We calculate $s_m = \Theta(\delta - \chi(m))$, where δ is a predetermined threshold based on which different characterizations of the network is carried out, and m denotes the number of bins the network is grouped, $m = N/n$. Strength of Incoherence (SI) is then defined as

$$\mathrm{SI} = 1 - \frac{\sum_{\mathrm{m}=1}^{\mathrm{M}} \mathrm{s_m}}{\mathrm{M}} \tag{5}$$

If SI ≈ 1, it denotes incoherent state, if SI $= 0$, it denotes a synchronized state, cluster state, and if $0 <$ SI < 1, it denotes chimera state.

Ring-star network

Here we consider the effect of both ring and star coupling strengths ($\sigma \neq 0, \mu \neq 0$) for our network and analyse the spatiotemporal patterns. When $\sigma = 0.05, \mu = 0.04$, the neuron nodes exhibit asynchronous patterns, see Fig. 6 (a) showing the nodes oscillating in an asynchronous fashion. The SI value is also 1, signifying incoherence. The leftmost plot shows the variation of the membrane potential (x) as time evolves. The right most plot illustrates the recurrence plot of the nodes of the network under study by considering the Euclidean norm of the x state values of different nodes. Each point (i, j) on the grid is color coded depending on the value of the $R_{ij} = ||x_i - x_j||$, where $1 \leq i, j \leq N$ and $||.||$ denotes the Euclidean norm.

Let us consider the figure on the left of Fig. 6 (a). The x-state variable is color coded according to its value. This gives us an idea as to how the oscillators are evolving with time, are they synchronized with their neighboring elements or not? This can be seen if the oscillators have same value or color. The leftmost plot illustrates the evolution of the network with time. The recurrence plot on the right, measures the Euclidean norm of the i th oscillator node versus the j th oscillator node. The color coding is done based on the Euclidean norm. If the norm between the i th and j th node is zero, then the nodes are synchronized. The shades represent the magnitude of the Euclidean norm of the ith oscillator versus the jth oscillator. When $i = j$, observe that the diagonal line is always blue denoting zero norm.

When the ring coupling strength σ is decreased to -6, the node gets synchronised. This is illustrated in Fig. 6 (b). Observe that the values of the x state variable are all arranged horizontally. The SI value here is 0 signifying synchronized state. This can also be confirmed from the spatiotemporal plot and the recurrence plot.

The ring-star network of memristive Hindmarsh-Rose neuron system shows chimera state when $\sigma = 7, \mu = 1$, see Fig. 6 (c). Observe that initial nodes and final nodes remain synchronised whereas nodes in the middle ($30 \leq$ Nodes ≤ 60) oscillate asynchronously. From such coexistence of synchronous and asynchronous states, it can confirmed as a chimera state. This can also be seen from the spatiotemporal plot on the left and the formation of the regular structures of colours other than blue in the recurrence plot. The SI value in this case is 0.7, confirming a chimera as $0 <$ SI < 1. Interestingly, double-well chimera state is found in this system. We refer the reader to the author's previous work in (Muni and Provata 2020), where double well chimera state were found in the ring-star network of Chua circuits. Double well chimera state is an important type of chimera state which traverses both

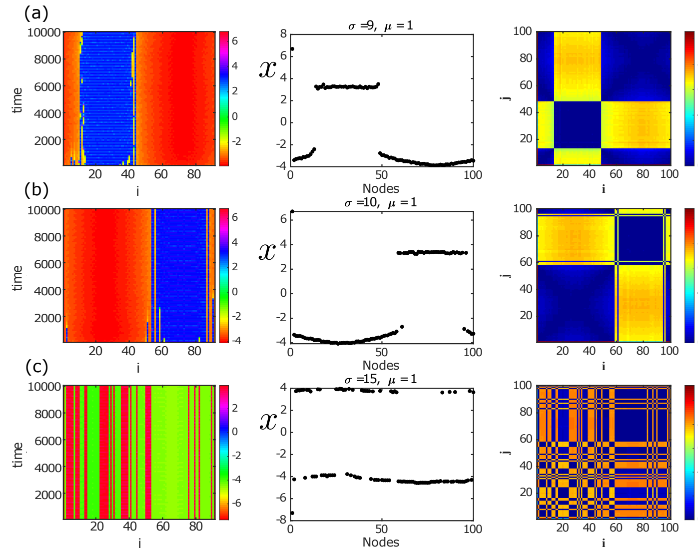

Figure 7 Ring-Star network of memristive Hindmarsh Rose neuron model with $\sigma \neq 0, \mu \neq 0$. Random initial conditions are set with the coupling range of $P = 70$. Number of nodes considered is $N = 100$. Double well chimera in (a), another double well chimera in (b), two synchronized cluster state in (c) is shown.

the positive and negative values of x state variable. It is interesting to observe in the case of memristive HR neuron system.

Such a double well chimera state is shown in Fig. 7 (a). Observe that in the middle plot, some nodes are in synchronous pattern in the positive range of x and some in the negative range of x. Notice that the spatiotemporal pattern on the left, has alternating strips of both red (in negative region) and blue (in positive regions). The regular structures in the recurrence plot on the right also confirms this as a double well chimera state.The SI value in this case is 0.68 and denotes a chimera. Another such double well chimera state is shown in Fig. 7 (b). The SI value is 0.68, denoting a chimera state.

The prevalence of the double-well chimera state was found to be robust with the variation of σ till $\sigma < 15$. When $\sigma = 15, \mu = 1$, the double well chimera state is destroyed and formation of the two clustered state takes place as shown in Fig. 7 (c). The SI value is around $0.02 \approx 0$, signifying a cluster state. The middle plot shows the two almost synchronized clusters traversing both positive and negative values of x. The right most plot shows very tiny square like regular structures indicating the presence of clusters and the recurrence plot differs topologically form other patterns such as synchronous, chimera states. In the next section, we discuss about the topological patterns shown by the ring network.

Ring network

In this section, we address various spatiotemporal patterns in the ring network of memristive Hindmarsh Rose neuron system by setting $\sigma \neq 0, \mu = 0$. In Fig. 8 (a), we showcase the asynchronous behavior of the end nodes of the ring network. This can be confirmed from the spatiotemporal plot and the recurrence plot. The SI value is 1 denoting an asynchronous state. In Fig. 8 (b), we showcase a double well chimera state. This can be confirmed by the regular structures in the recurrence plot on the right and the spatiotemporal plot on the left. The SI value is 0.44, signifying a chimera state.

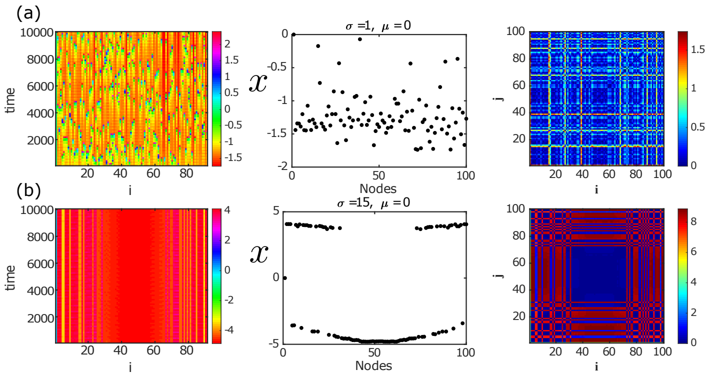

Figure 8 Ring network of memristive Hindmarsh Rose neuron model with $\sigma \neq 0, \mu = 0$. Random initial conditions are set with the coupling range of $P = 70$. Number of nodes considered is $N = 100$. Asynchronous behavior in (a), double well chimera state in (b) is shown.

Moreover, cluster states are also possible in ring network, see Fig. 9 (a). The SI value is 0.02, signifying synchronous state/ cluster state. This can be shown by the presence of small square structures in the recurrence plots. A single cluster synchronization state is shown in Fig. 9 (b).The SI value is 0, denoting a synchronized state.

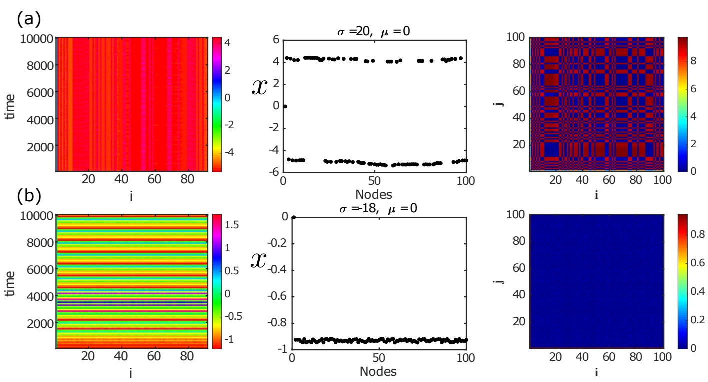

Figure 9 Ring network of memristive Hindmarsh Rose neuron model with $\sigma \neq 0, \mu = 0$. Random initial conditions are set with the coupling range of $P = 70$. Number of nodes considered is $N = 100$. Two cluster synchronized state behavior in (a), synchronized state in (b) is shown.

Star network

In this section, we explore the spatiotemporal patterns exhbited by the star network of memristive Hindmarsh Rose neuron model. Star networks is useful in many engineering systems, network hub system. Study on the synchronization aspect of star connected Chua oscillator were carried out in (Muni and Provata 2020). Unlike previous cases of ring-star and ring network, chimera state seems to be absent in the case of star networks.

The presence of sole central node drives more information to the end nodes of the network and hence chances of full synchronization is much more common in star networks. When $\mu = -0.5$, the star network enters the regime of asynchronization. The SI value is 1, signifying asynchronization. Increasing the star coupling strength μ to 1, we observe full synchronization in the system.The SI value is 0, signifying synchronization.

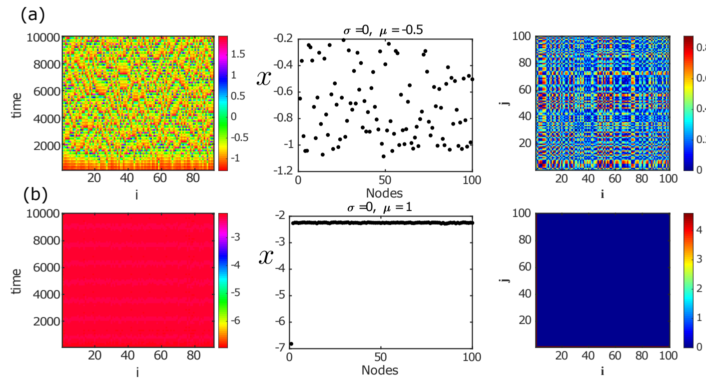

Figure 10 Star network of memristive Hindmarsh Rose neuron model with $\sigma = 0, \mu \neq 0$. Random initial conditions are set with the coupling range of $P = 70$. Number of nodes considered is $N = 100$. Asynchronous behavior in (a), synchronized state in (b) is shown.

Variation of the Strength of Incoherence with respect to coupling strength

Here we observe the variation of the strength of incoherence (SI) with respect to the ring coupling strength (σ), star coupling strength (μ). In Fig. 11 (a), (b), and (c), we have considered the variation of the strength of incoherence with the variation of the star coupling strength μ for three different values of coupling range $P = 30, 70,$ and 90. In Fig. 11 (a), with negative μ, the SI value is almost same and then increases as μ becomes positive and then follows an increasing trend as μ is increased.

The behavior is robust with the change in the coupling range P as evident from Fig. 11 (b), (c). In Fig. 11 (d), (e), (f), we have considered the variation of the strength of incoherence with the variation of ring coupling strength σ for three different values of coupling range $P = 30, 70,$ and 90. As can be seen in Fig. 11 (d), SI is 1 for negative values of σ and starts to decrease for positive σ and reaches to zero. So variation of σ from negative to positive value, we see a variation from asynchronous to synchronous state or cluster state. The behavior is robust for different other values of coupling ranges in Fig. 11 (e), and (f).

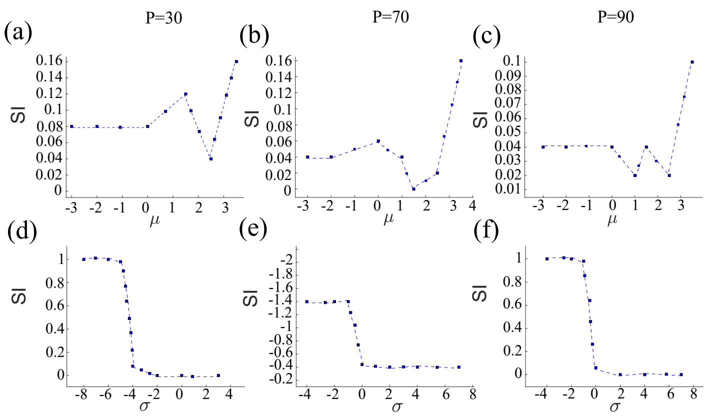

Figure 11 Variation of the strength of incoherence (SI) with respect to the star coupling strength (μ) in panels (a), (b), (c) for various coupling ranges $P = 30, 70$, and 90 respectively. Similarly, variation of the strength of incoherence (SI) with respect to the ring coupling strength σ for various values of coupling ranges $P = 30, 70$, and 90 respectively. The network size is $N = 100$.

CONCLUSION

In this manuscript, we have considered a memristive version of the Hindmarsh-Rose neuron model. We found the proposed model was able to exhibit a reverse period doubling route to chaos, as well as phenomena of interior and exterior crises. Three different networks (ring-star, ring, and star) networks of memristive Hindmarsh Rose neuron models were explored. Chimera states, including double well chimera states, were found in the ring-star and ring network, which shows that the memristive Hindmarsh-Rose neuron model is a promising neuron model to be explored further in the future. Many future directions emerge from this study. Study of lattice Shepelev *et al.* (2020a, 2021a), multilayer networks Shepelev *et al.* (2021c) of the neuron model can be explored. Emergence of spiral waves can be studied in the latter networks and a proper quantification can be carried similar to the methods used in Shepelev *et al.* (2020b).

The basin of attraction of double-well chimera state, synchronous and asynchronous state, can be explored in the future. Does the system exhibit anti-phase synchronization Shepelev *et al.* (2021b) is a topic that can be thought of. Does a discretized version of the proposed model in the present paper show extra qualitative dynamics is a future direction that can be looked upon in a similar spirit in Muni *et al.* (2022). Recently extreme multistability was found in memrisitve Hindmarsh-Rose model in Njitacke Tabekoueng *et al.* (2022), can this model also exhibit extreme multistability? A deep investigation of the global dynamics of the memristive Hindmarsh-Rose neuron proposed in this work will be carried out.

Acknowledgments

S.S.M acknowledges the School of Fundamental Sciences doctoral bursary funding during this research. This work is partially funded by the Polish National Science Center under the Grant OPUS 14$No.2017/27/B/ST8/01330$.

Conflicts of interest

The authors declare that there is no conflict of interest regarding the publication of this paper.

Availability of data and material

Not applicable.

LITERATURE CITED

Bao, B., A. Hu, Q. Xu, H. Bao, H. Wu, *et al.*, 2018 Ac-induced coexisting asymmetric bursters in the improved hindmarsh–rose model. Nonlinear Dynamics **92**: 1695–1706.

Bao, H., A. Hu, W. Liu, and B. Bao, 2019 Hidden bursting firings and bifurcation mechanisms in memristive neuron model with threshold electromagnetic induction. IEEE transactions on neural networks and learning systems **31**: 502–511.

Burić, N., K. Todorović, and N. Vasović, 2008 Synchronization of bursting neurons with delayed chemical synapses. Physical Review E **78**: 036211.

Cai, J., H. Bao, Q. Xu, Z. Hua, and B. Bao, 2021 Smooth nonlinear fitting scheme for analog multiplierless implementation of hindmarsh–rose neuron model. Nonlinear Dynamics **104**: 4379–4389.

Chay, T. R., 1985 Chaos in a three-variable model of an excitable cell. Physica D: Nonlinear Phenomena **16**: 233–242.

Doubla Isaac, S., Z. T. Njitacke, and J. Kengne, 2020 Effects of low and high neuron activation gradients on the dynamics of a simple 3d hopfield neural network. International Journal of Bifurcation and Chaos **30**: 2050159.

Galinsky, V. L. and L. R. Frank, 2021 Collective synchronous spiking in a brain network of coupled nonlinear oscillators. Physical review letters **126**: 158102.

Guo, Y., Z. Zhu, C. Wang, and G. Ren, 2020 Coupling synchronization between photoelectric neurons by using memristive synapse. Optik **218**: 164993.

Hindmarsh, J. and R. Rose, 1982 A model of the nerve impulse using two first-order differential equations. Nature **296**: 162–164.

Hindmarsh, J. L. and R. Rose, 1984 A model of neuronal bursting using three coupled first order differential equations. Proceedings of the Royal society of London. Series B. Biological sciences **221**: 87–102.

Hodgkin, A. and A. Huxley, 1990 A quantitative description of membrane current and its application to conduction and excitation in nerve. Bulletin of mathematical biology **52**: 25–71.

Hou, Z., J. Ma, X. Zhan, L. Yang, and Y. Jia, 2021 Estimate the electrical activity in a neuron under depolarization field. Chaos, Solitons & Fractals **142**: 110522.

Izhikevich, E. M., 2003 Simple model of spiking neurons. IEEE Transactions on neural networks **14**: 1569–1572.

Izhikevich, E. M. and R. FitzHugh, 2006 Fitzhugh-nagumo model. Scholarpedia **1**: 1349.

Joshi, S. K., 2021 Synchronization of coupled hindmarsh-rose neuronal dynamics: Analysis and experiments. IEEE Transactions on Circuits and Systems II: Express Briefs **69**: 1737–1741.

Kuramoto, Y. and D. Battogtokh, 2002 Coexistence of coherence and incoherence in nonlocally coupled phase oscillators. arXiv preprint cond-mat/0210694 .

Li, K., H. Bao, H. Li, J. Ma, Z. Hua, *et al.*, 2021a Memristive rulkov neuron model with magnetic induction effects. IEEE Transactions on Industrial Informatics **18**: 1726–1736.

Li, Y., 2021 Simulation of memristive synapses and neuromorphic computing on a quantum computer. Physical Review Research **3**: 023146.

Li, Z., H. Zhou, M. Wang, and M. Ma, 2021b Coexisting firing patterns and phase synchronization in locally active memristor coupled neurons with hr and fn models. Nonlinear Dynamics **104**: 1455–1473.

Lin, H., C. Wang, Q. Deng, C. Xu, Z. Deng, *et al.*, 2021 Review on chaotic dynamics of memristive neuron and neural network. Nonlinear Dynamics **106**: 959–973.

Lin, H., C. Wang, Y. Sun, and W. Yao, 2020 Firing multistability in a locally active memristive neuron model. Nonlinear Dynamics **100**: 3667–3683.

Liu, Y., W.-j. Xu, J. Ma, F. Alzahrani, and A. Hobiny, 2020 A new photosensitive neuron model and its dynamics. Frontiers of Information Technology & Electronic Engineering **21**: 1387–1396.

Liu, Z., C. Wang, G. Zhang, and Y. Zhang, 2019 Synchronization between neural circuits connected by hybrid synapse. International Journal of Modern Physics B **33**: 1950170.

Majhi, S., B. K. Bera, D. Ghosh, and M. Perc, 2019 Chimera states in neuronal networks: a review. Phys. Life Rev. **28**: 100–121.

Muni, S. S., H. O. Fatoyinbo, and I. Ghosh, 2022 Dynamical effects of electromagnetic flux on chialvo neuron map: nodal and network behaviors. arXiv preprint arXiv:2201.03219 .

Muni, S. S. and A. Provata, 2020 Chimera states in ring–star network of chua circuits. Nonlinear Dynamics **101**: 2509–2521.

Njitacke, Z. T., J. Awrejcewicz, B. Ramakrishnan, K. Rajagopal, and J. Kengne, 2022a Hamiltonian energy computation and complex behavior of a small heterogeneous network of three neurons: circuit implementation. Nonlinear Dynamics **107**: 2867–2886.

Njitacke, Z. T., I. S. Doubla, S. Mabekou, and J. Kengne, 2020 Hidden electrical activity of two neurons connected with an asymmetric electric coupling subject to electromagnetic induction: coexistence of patterns and its analog implementation. Chaos, Solitons & Fractals **137**: 109785.

Njitacke, Z. T., T. F. Fozin, S. S. Muni, J. Awrejcewicz, and J. Kengne, 2022b Energy computation, infinitely coexisting patterns and their control from a hindmarsh-rose neuron with memristive autapse: Circuit implementation. AEU-International Journal of Electronics and Communications p. 154361.

Njitacke, Z. T., S. D. Isaac, T. Nestor, and J. Kengne, 2021a Window of multistability and its control in a simple 3d hopfield neural network: application to biomedical image encryption. Neural Computing and Applications **33**: 6733–6752.

Njitacke, Z. T., B. N. Koumetio, B. Ramakrishnan, G. D. Leutcho, T. F. Fozin, *et al.*, 2021b Hamiltonian energy and coexistence of hidden firing patterns from bidirectional coupling between two different neurons. Cognitive Neurodynamics pp. 1–18.

Njitacke, Z. T., C. N. Takembo, J. Awrejcewicz, H. P. E. Fouda, and J. Kengne, 2022c Hamilton energy, complex dynamical analysis and information patterns of a new memristive fitzhugh-nagumo neural network. Chaos, Solitons & Fractals **160**: 112211.

Njitacke, Z. T., N. Tsafack, B. Ramakrishnan, K. Rajagopal, J. Kengne, *et al.*, 2021c Complex dynamics from heterogeneous coupling and electromagnetic effect on two neurons: Application in images encryption. Chaos, Solitons & Fractals **153**: 111577.

Njitacke Tabekoueng, Z., S. Shankar Muni, T. Fonzin Fozin, G. Dolvis Leutcho, and J. Awrejcewicz, 2022 Coexistence of infinitely many patterns and their control in heterogeneous coupled neurons through a multistable memristive synapse. Chaos: An Interdisciplinary Journal of Nonlinear Science **32**: 053114.

Omel'chenko, O. E., 2018 The mathematics behind chimera states. Nonlinearity **31**: R121.

Panaggio, M. J. and D. M. Abrams, 2015 Chimera states: coexistence of coherence and incoherence in networks of coupled oscillators. Nonlinearity **28**: R67.

Qin, Y., T. Menara, D. S. Bassett, and F. Pasqualetti, 2021 Phase-amplitude coupling in neuronal oscillator networks. Physical Review Research **3**: 023218.

Roberts, L. G. and B. D. Wessler, 1970 Computer network development to achieve resource sharing. In *Proceedings of the May 5-7, 1970, spring joint computer conference*, pp. 543–549.

Schöll, E., 2016 Synchronization patterns and chimera states in complex networks: Interplay of topology and dynamics. Eur. Phys. J. Spec. Top. **225**: 891–919.

Shaffer, A., A. L. Harris, R. Follmann, and E. Rosa Jr, 2016 Bifurcation transitions in gap-junction-coupled neurons. Physical Review E **94**: 042301.

Shepelev, I., A. Bukh, S. Muni, and V. Anishchenko, 2020a Role of solitary states in forming spatiotemporal patterns in a 2d lattice of van der pol oscillators. Chaos, Solitons & Fractals **135**: 109725.

Shepelev, I., S. Muni, and T. Vadivasova, 2021a Spatiotemporal patterns in a 2d lattice with linear repulsive and nonlinear attractive coupling. Chaos: An Interdisciplinary Journal of Nonlinear Science **31**: 043136.

Shepelev, I. A., A. V. Bukh, S. S. Muni, and V. S. Anishchenko, 2020b Quantifying the transition from spiral waves to spiral wave chimeras in a lattice of self-sustained oscillators. Regular and Chaotic Dynamics **25**: 597–615.

Shepelev, I. A., S. S. Muni, E. Schöll, and G. I. Strelkova, 2021b Repulsive inter-layer coupling induces anti-phase synchronization. Chaos: An Interdisciplinary Journal of Nonlinear Science **31**: 063116.

Shepelev, I. A., S. S. Muni, and T. E. Vadivasova, 2021c Synchronization of wave structures in a heterogeneous multiplex network of 2d lattices with attractive and repulsive intra-layer coupling. Chaos: An Interdisciplinary Journal of Nonlinear Science **31**: 021104.

Shu, H., J. Zhou, Q. Lian, H. Li, D. Zhao, *et al.*, 2021 Modeling gene regulatory networks using neural network architectures. Nature Computational Science **1**: 491–501.

Sysoeva, M. V., I. V. Sysoev, M. D. Prokhorov, V. I. Ponomarenko, and B. P. Bezruchko, 2021 Reconstruction of coupling structure in network of neuron-like oscillators based on a phase-locked loop. Chaos, Solitons & Fractals **142**: 110513.

Tabekoueng Njitacke, Z., J. Kengne, and H. B. Fotsin, 2020a Coexistence of multiple stable states and bursting oscillations in a 4d hopfield neural network. Circuits, Systems, and Signal Processing **39**: 3424–3444.

Tabekoueng Njitacke, Z., C. Laura Matze, M. Fouodji Tsotsop, and J. Kengne, 2020b Remerging feigenbaum trees, coexisting behaviors and bursting oscillations in a novel 3d generalized hopfield neural network. Neural Processing Letters **52**: 267–289.

Tabekoueng Njitacke, Z., I. Sami Doubla, J. Kengne, and A. Cheukem, 2020c Coexistence of firing patterns and its control in two neurons coupled through an asymmetric electrical synapse. Chaos: An Interdisciplinary Journal of Nonlinear Science **30**: 023101.

Takembo, C. N., H. P. E. Fouda, and T. C. Kofane, 2022 Modulational instability in chain diffusive neuronal networks under electric field. Indian Journal of Physics pp. 1–9.

Tsumoto, K., H. Kitajima, T. Yoshinaga, K. Aihara, and H. Kawakami, 2006 Bifurcations in morris–lecar neuron model. Neurocomputing **69**: 293–316.

Uhlhaas, P. J. and W. Singer, 2006 Neural synchrony in brain disorders: relevance for cognitive dysfunctions and pathophysiology. Neuron **52**: 155–168.

Willms, A. R., P. M. Kitanov, and W. F. Langford, 2017 Huygens' clocks revisited. R. Soc. Open Sci. **4**: 170777.

Wouapi, K., B. H. Fotsin, F. P. Louodop, K. F. Feudjio, Z. T. Njitacke, *et al.*, 2020 Various firing activities and finite-time synchronization of an improved hindmarsh–rose neuron model under electric field effect. Cognitive Neurodynamics **14**: 375–397.

Wouapi, M. K., B. H. Fotsin, E. B. M. Ngouonkadi, F. F. Kemwoue, and Z. T. Njitacke, 2021 Complex bifurcation analysis and synchronization optimal control for hindmarsh–rose neuron model under magnetic flow effect. Cognitive neurodynamics **15**: 315–347.

Wu, F., J. Ma, and G. Zhang, 2020 Energy estimation and coupling synchronization between biophysical neurons. Science China Technological Sciences **63**: 625–636.

Xu, Q., T. Liu, C.-T. Feng, H. Bao, H.-G. Wu, *et al.*, 2021 Continuous non-autonomous memristive rulkov model with extreme multistability. Chinese Physics B **30**: 128702.

Yao, Z., P. Zhou, Z. Zhu, and J. Ma, 2021 Phase synchronization between a light-dependent neuron and a thermosensitive neuron. Neurocomputing **423**: 518–534.

Zhang, G., D. Guo, F. Wu, and J. Ma, 2020a Memristive autapse involving magnetic coupling and excitatory autapse enhance firing. Neurocomputing **379**: 296–304.

Zhang, G., C. Wang, F. Alzahrani, F. Wu, and X. An, 2018 Investigation of dynamical behaviors of neurons driven by memristive synapse. Chaos, Solitons & Fractals **108**: 15–24.

Zhang, Y., C. Wang, J. Tang, J. Ma, and G. Ren, 2020b Phase coupling synchronization of fhn neurons connected by a josephson junction. Science China Technological Sciences **63**: 2328–2338.

Zhou, J.-F., E.-H. Jiang, B.-L. Xu, K. Xu, C. Zhou, *et al.*, 2021a Synaptic changes modulate spontaneous transitions between tonic and bursting neural activities in coupled hindmarsh-rose neurons. Physical Review E **104**: 054407.

Zhou, P., Z. Yao, J. Ma, and Z. Zhu, 2021b A piezoelectric sensing neuron and resonance synchronization between auditory neurons under stimulus. Chaos, Solitons & Fractals **145**: 110751.

How to cite this article: Muni, S. S., Njitacke, Z. T., Feudjio, C., Fozin, T. F., and Awrejcewicz, J. Route to Chaos and Chimera States in a Network of Memristive Hindmarsh-Rose Neurons Model with External Excitation. *Chaos Theory and Applications*, 4(3), 119-127, 2022.

CHAOS
Theory and Applications
in Applied Sciences and Engineering

e-ISSN: 2687-4539
RESEARCH ARTICLE
Vol.4 / No.3 / 2022 / pp.128-134
https://doi.org/10.51537/chaos.1164683

Dynamical Interpretation of Logistic Map using Euler's Algorithm

Sanjeev[*,1], **Anjali**[β,2], **Ashish**[α,3] **and A. K. Malik**[§,4]
[*]Department of Mathematics, Suraj Degree College, Mahendergarh, India, [β]Department of Mathematics, National Institute of Technology, Mizoram, India, [α]Department of Mathematics, Government College, Satnali-123024, India, [§]School of Mathematics, UP Rajarshi Tandon Open University, Prayagraj-211021, India.

ABSTRACT In the last two decades, the dynamics of difference and differential equations have found a celebrated place in science and engineering such as weather forecasting, secure communication, transportation problems, biology, the population of species, etc. In this article, we deal with the dynamical behavior of the logistic map using Euler's numerical algorithm. The dynamical properties of the Euler's type logistic system are derived analytically as well as experimentally using the bifurcation diagram. In the analytical section the dynamical properties such as fixed point, period-doubling, and irregularity are examined followed by a few theorems. Further, in the experimental section, the dynamical properties of the Euler's type logistic system are studied using the period-doubling bifurcation plot. Because the dynamics of the Euler's map depend on the Euler's control parameter h, therefore, the three major cases are discussed for $h = 0.1, 0.4$ and 0.7. The result shows that as the value of parameter h decreases from 1 to 0 the growth rate parameter r increases rapidly. Therefore, the improved chaotic regime in bifurcation plots may improve the chaos based applications in science and engineering such as secure communication.

KEYWORDS
Fixed point
Periodic orbit
Euler's Algorithm
Chaos

INTRODUCTION

In the last few decades, the term "Chaos" has become the subject matter of the study in mathematics which determines the fixed and periodic and irregularity in the nonlinear dynamical systems. This concept was described by Poincare (1899) when he examined the qualitative results in nonlinear systems and celestial mechanics. But in 1960's Lorenz (1963) again recalled it and examined it chaotic part which depends on the initial condition. Further, May (1976) and Lorenz (1963) researched much important arithmetic after that all the nonlinear dynamical system has been saturated with analytical and numerical results of difference and differential equations. The logistic map $rx(1-x)$, is the most researched difference map in the nonlinear dynamics which is also known as the model of population growth introduced by V. F. Verhulst. In 1978, Feigenbaum (1978) examined the generic dynamical properties of the logistic map using experimental and analytical simulations. Moreover, for a brief elementary analysis of about the nonlinear dynamical systems and their qualitative properties one may read the following published and unpublished research like Robinson (1995), Alligood *et al.* (1996), Ausloos *et al.* (2006), Devaney (1948), Holmgren (1994), and Ashish *et al.* (2019b).

Since 1930, the nonlinear dynamical systems have played a vital role in various applications of science and engineering such as cryptography, transportation problems, traffic signal control system, secure communication systems, neural network, switch technology, electronics and many other branches of science. In last two decades the discrete logistic map and its various generalized versions have been studied in the literature as a road map in the nonlinear dynamical systems. In 1996, Song *et al.* (1996) researched the dynamical behavior of logistic map using error valued feedback method for synchronization of the dynamics and Molina *et al.* (1996) examined the embedded dimension of various chaotic maps using time series methodology.

A communication system to develop irregular signals was developed using difference maps by Singh *et al.* (2010) in 2010. Further, in 2013 Radwan *et al.* (2013) introduced the various modulated

Manuscript received: 20 August 2022,
Revised: 29 September 2022,
Accepted: 28 October 2022.

[1] sanjeevrao.652@gmail.com
[2] anjaliyadav42877@gmail.com
[3] drashishkumar108@gmail.com (**Corresponding Author**)
[4] ajendermalik@gmail.com

discrete difference systems and described their dynamical properties such as fixed-point state, period-doubling interpretations and chaotic behavior. Parasad *et al.* (2014) described the stabilization in the fixed and periodic states of the logistic maps. In 2005, Rani *et al.* (2005) and Kumar*et al.* (2005), using the new technology examined the stabilization in the chaotic maps. They introduced a two-step feedback method, that is, Ishikawa iterates, that shows that the logistic map has fast convergence for the extra range of the control parameter r as compared to one-step feedback procedure and also presented a comparative study in Picard orbit in Agarwal and Rani Rani *et al.* (2009). In 1953, Mann (1953) introduced a novel three-step feedback procedure also known as Mann iterative method which give superior results in functional analysis and every branch of mathematics. Further, Chugh *et al.* (2012), in 2012 examined the stability and convergence of the logistic map using another four-step feedback procedure also known as Noor iterative method. Khamosh (2020) and Kumar (2020) studied the dynamics of the generalized logistic map in superior orbit (see also Renu *et al.* (2022)).

Recently, He *et al.* (2023) introduced an homotopy perturbation method which increases the effectiveness in nonlinear oscillator systems. It is also observed that the frequency accuracy may be improved the oscillators by increasing the iteration in the system. Ashish *et al.* (2019a) established the chaotic behavior of the logistic map using superior technique and examined the onset chaos properties like period-doubling to chaos, period-3 window a road map to chaos and maximum Lyapunov exponent. Later, they examined the dynamical properties using cobweb plot, time-series analysis and bifurcation plot in superior orbit Ashish *et al.* (2018).

In 2019, stabilization in fixed and periodic states was examined and its application in transportation system was examined Ashish *et al.* (2021a), Ashish *et al.* (2021b), and Ashish *et al.* (2021c). The article is divided into five major sections. Section 1 is introductory in nature and describes a brief literature review and Section 2 contains the basic definition of fixed point, periodic point and Picard feedback procedure. In Section 3, the analytical results are proved for the Euler's type logistic map and experimental analysis is carried out in section 4. Finally, the article is concluded in Section 5.

PRELIMINARIES

This section deals with the basic terminologies, notions and definition which are continuously used in the article.

Definition 1. . Let f be a one-dimensional map defined on non-empty sets X. Then the Picard orbit which is also known as orbit of function is the set of all iterates of an initial point x and defined as $x_{n+1} = f(x_n)$.

Definition 2. . Let f be a one-dimensional map defined on a set X, where X is a non-empty set. A point $x \in X$ is said to be periodic fixed point of period-p or cycle-p if it satisfies $f^p(x) = x$, where p is a positive integer.

Definition 3. . Let f be a one-dimensional map defined on a set X, where X is a non-empty set. A point $x \in X$ is said to be fixed if it satisfies the condition $f(x) = x$.

ANALYTICAL INTERPRETATION

This section deals with the analytical study of the logistic map $rz(1-z)$ where $r \in [0,4]$ and $z \in [0,1]$ using Euler's numerical algorithm. The Euler's numerical algorithm is given by

$$E_h(z,r) = z + hf_r(z). \tag{1}$$

This equation has two regular fixed points $z^* = 0$ and $z^* = 1$. Since the solutions for an initiator $z_0 \in [0,1]$ and $r > 0$, approaches to the regular fixed state $z^* = 1$ from the interval $[-z,z]$. But such type of system has not much importance in the dynamics of one-dimensional chaotic maps. Therefore, the given system (1) is modified in more simplified quadratic discrete system. For this let us consider the parameter $x = \frac{hr}{1+hr}z$, then the relation (1) is described by

$$E_h(x,r) = (1+hr)x(1-x) \tag{2}$$

where x belongs to the closed interval $[0,1]$ and the relation (2) is called as Euler's type novel logistic system. Now, let us determine the following result regarding fixed point, periodic point and the stability of this novel Euler's logistic map.

Theorem 1. *Let $f_r(x) = rx(1-x)$ be the one-dimensional logistic map defined on the closed interval $[0,1]$ and $r \in [0,4]$. Then, show that 0 and $\frac{hr}{1+hr}$ are the fixed points for the Euler's type logistic map.*

Proof. Since $f_r(x) = rx(1-x)$ and $E_h(x,r) = (1+hr)x(1-x)$, is the Euler's logistic system, then from the definition of the fixed point, we can say

$$\begin{aligned} E_h(x,r) &= x, \\ (1+hr)x(1-x) &= x, \\ (1+hr)x(1-x) - x &= 0, \\ x[(1+hr)(1-x) - 1] &= 0, \\ \text{thus,} \quad x = 0 \quad \text{and} \quad x &= \frac{hr}{1+hr}. \end{aligned}$$

Thus, the point $x = 0$ and $x = \frac{hr}{1+hr}$, where $h, r > 0$ is the Euler's fixed point for the Euler's Logistic map. This completes the proof of the theorem. While, Figure 1 shows the functional representation of the logistic map in Euler's numerical algorithm. Figure shows the fixed-point $x = 0$ and $x = \frac{hr}{1+hr}$ where the diagonal axis intersects the functional graph of the map. Similarly, the periodic fixed point of order two are also derived using the following theorem. □

Theorem 2. *Let $f_r(x) = rx(1-x)$ be the one-dimensional logistic map defined on the closed interval $[0,1]$ and $r \in [0,4]$. Then, show that $E_h^2(x,r)$ has four fixed points for the Euler's map.*

Proof. Since $f_r(x) = rx(1-x)$ and $E_h(x,r) = (1+hr)x(1-x)$, is the Euler's logistic system, then from the definition of fixed point, we can say

$$\begin{aligned} &E_h^2(x,r) = E_h(E_h(x,r),r) = x, \\ &(1+hr)2x(1-x)(1-((1+hr)x(1-x))) = x, \\ &(1+hr)2x(1-x)(1-((1+hr)x(1-x))) - x = 0. \end{aligned}$$

Then, solving the above relation, we obtain the following four roots:

$$x_1 = 0,$$
$$x_2 = \frac{hr}{1+hr},$$
$$x_3 = \frac{(1+hr) - \sqrt{(hr-2)(2+hr)}}{2(1+hr)},$$
$$x_4 = \frac{(1+hr) + \sqrt{(hr-2)(2+hr)}}{2(1+hr)}.$$

Thus, x_1, x_2, x_3, and x_4 are the four fixed points for the system $E_h^2(x,r)$. The fixed point x_1 and x_2 are the trivial point of order one as discussed in Theorem 1 and x_3 and x_4 are periodic point of order two for the given Euler's logistic system. But it is observed that the periodic roots are real if and only if $r > 2/h$. Further, the Figure 2 shows the graphical representation for the fixed points x_1, x_2, x_3, and x_4 which intersect the diagonal axis $y = x$ of the graph. Proceeding in this way the we can get the periodic points of higher orders, that is the periodic points of order 4, 8, 16, 32, and so on using the dynamical system $E_h^3(x,r)$, $E_h^4(x,r)$, $E_h^5(x,r)$, $E_h^6(x,r)$, and so on. But it is not so simple to solve the higher order equations using analytically. Therefore, they are determined using the numerical simulation in computational software Mathematica, and SPSS. □

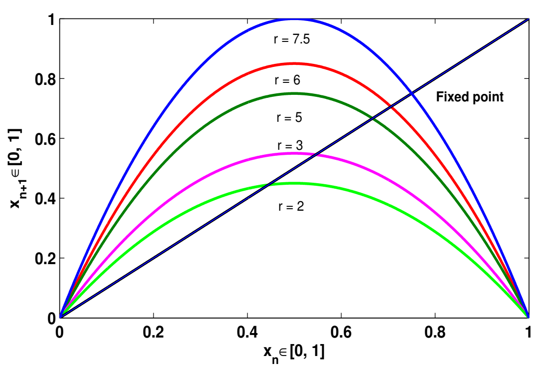

Figure 1 Functional plot for the Euler's Logistic Map $E_h(x,r)$ for a variety of r value at $h = 0.4$

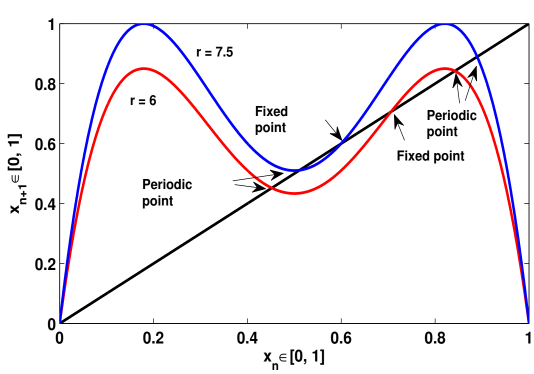

Figure 2 Functional plot for the Euler's Logistic Map $E_h^2(x,r)$ for $r = 7.5$ and 6 at $h = 0.4$

EXPERIMENTAL INTERPRETATION

This section deals with the experimental study of the one-dimensional logistic map $rx(1-x)$, where $r \in [0,4]$ and $x \in [0,1]$ using Euler's numerical algorithm. As studied in the above section the dynamics of the Euler's type logistic map depends on the two-control parameter, Euler's parameter h and the logistic parameter r. Therefore, the nature of the Euler's system $E_h(x,r)$ is examined for different parameter values of h and the regime and the dynamical behavior for the advanced range of parameter r is determined. Let us take the three cases for $h = 0.1, 0.4$ and 0.7 and examine the dynamical nature using bifurcation plot as follows:

Case-1: Dynamics for $E_h(x,r)$ at $h = 0.1$, and $0 \le r \le 30$

When $h = 0.1$, the Euler's map has stable fixed-point behavior up to value $r = 20$, after that the first bifurcation is seen at $r > 20$ at which the Euler's orbit is divided in to two period orbits x_3 and x_4 of order two as determined in above section and. The stability in the periodic fixed point of order 2 is then studied for $20 < r \le 24.899$ as shown in Figures 3 and 4. Further, for $r > 24.899$ the characteristics of the Euler's map is again noticed in which the periodicity of order two, that is, x_3 and x_4 are further divided in to the periodic fixed points of order four as shown in the Figure 4 for the range of parameter $24.899 < r \le 25.44$. But the parameter r increases through 24.899, the periodicity of order two becomes unstable and the periodic point of order four become stable for $24.899 < r \le 25.44$.

Proceeding in this way as the value of parameter r increases through 25.44 the Euler's orbit bifurcates in to higher order periodic fixed points, that is, in the order of $8, 16, 32, 64, \ldots$ and soon as shown in the Figure 4. But as the parameter r approaches to 25.6996 the dynamics of the Euler's logistic map tends to chaotic regime. The magnified Figure 4 shows the complete period-doubling regime, Figure 5 shows the magnified chaotic regime and Figure 6 represents the magnified period-3 window regime. Finally, the above analysis is summarized in the following proposition.

Proposition 1. *It is noticed that the dynamics of the Euler's type logistic system admits higher range of the control parameter r, that is, r lies between 0 and 30 at $h = 0.1$ as compared to the standard logistic system $rx(1-x)$, where r approaches from 0 to 4.*

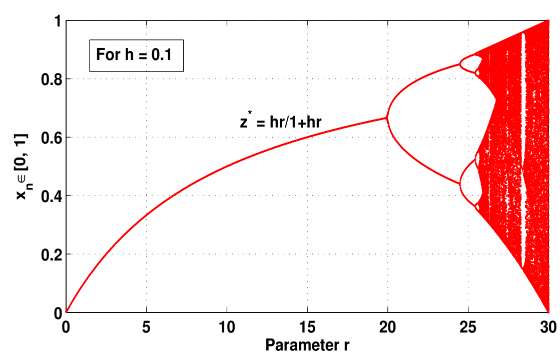

Figure 3 Bifurcation plot for the map $E_h(x,r)$ for $h = 0.1$ and $r \in [0,30]$

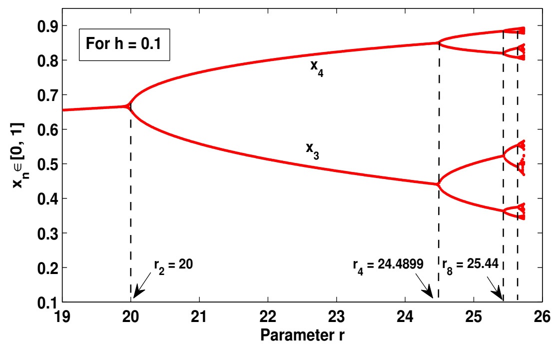

Figure 4 Magnified periodic regime for the map $E_h(x, r)$ for $h = 0.1$

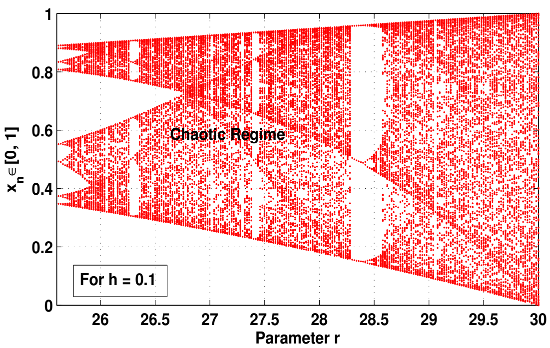

Figure 5 Magnified Chaotic regime for the map $E_h(x, r)$ for $h = 0.1$

Case-2: Dynamics for $E_h(x, r)$ at $h = 0.4$, and $0 \leq r \leq 7.5$

Further, as the range of parameter h is increased and is taken as $h = 0.4$, range the control parameter r decreases rapidly, that is, r approaches from 0 to 7.5 as shown in bifurcation plot Figure 4. While Figure 7 gives the complete dynamics of the Euler's logistic system which describes fixed-point state, periodic state and chaotic regime. At $h = 0.4$, the Euler's map has stable fixed-point behavior up to $r = 5$, after that the first bifurcation occurs at $r = 6.1255$ at which the Euler's orbit is divided in to two period orbits x_3 and x_4 of order two as determined in above the section. The stability in the periodic fixed points of order 2 is then studied for $6.1255 < r \leq 6.3573$ as shown in Figure 8. Further, for $r > 6.3573$ the orbit of the Euler's logistic map is again noticed in which the periodicity of order two, that is, x_3 and x_4 are further divided in to the periodic fixed points of order four as shown in the Figure 8 for the range of parameter $6.1255 < r \leq 6.3573$. But the parameter r increases through 6.1255, the periodicity of order two becomes unstable and the periodic point of order four become stable for $6.1255 < r \leq 6.3573$.

Proceeding in this way as the value of parameter r increases through 6.4299 the Euler's orbit bifurcates in to higher order periodic fixed points, that is, in the order of $8, 16, 32, 64, \ldots$ and soon as shown in the Figure 8. But as the parameter r approaches to 6.4299 the dynamics of the Euler's logistic map tends to chaotic regime as shown in the magnified Figure 9. The magnified Figure 8 shows the complete period-doubling regime while the magnified Figure 10 represent the complete chaotic regime with period-3 window.

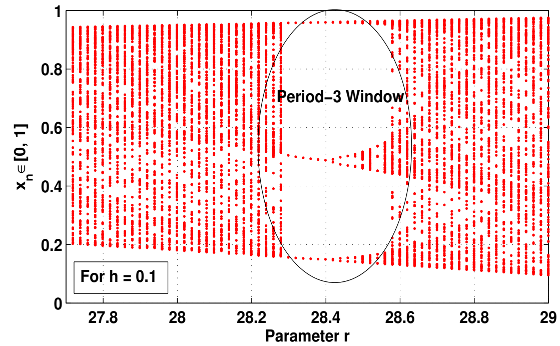

Figure 6 Magnified period-3 window for the map $E_h(x, r)$ for $h = 0.1$

Proposition 2. *It is noticed that the dynamics of the Euler's type logistic system again admits higher range of the control parameter r, that is, r lies between 0 and 7.5 at $h = 0.4$ as compared to the standard logistic system $rx(1 - x)$, where r approaches from 0 to 4.*

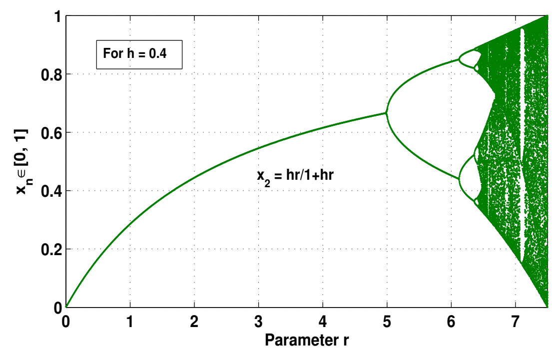

Figure 7 Bifurcation plot for the map $E_h(x, r)$ for $h = 0.4$ and $r \in [0, 7.5]$

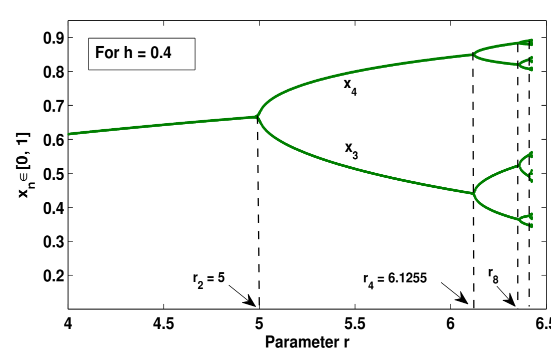

Figure 8 Magnified periodic regime for the map $E_h(x, r)$ for $h = 0.4$

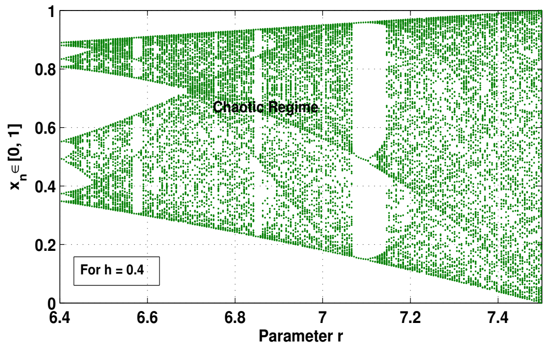

Figure 9 Magnified Chaotic regime for the map $E_h(x, r)$ for $h = 0.4$

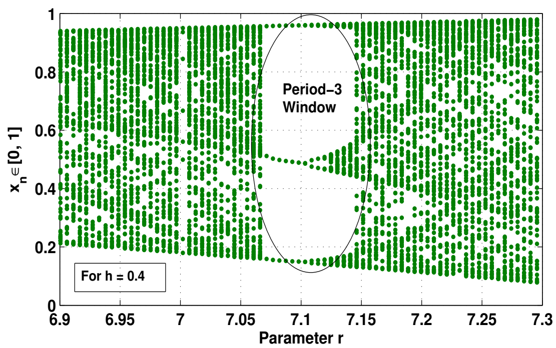

Figure 10 Magnified period-3 window regime for the map $E_h(x, r)$ for $h = 0.4$

Case-3: Dynamics for $E_h(x, r)$ at $h = 0.7$, and $0 \le r \le 4.25$

Further, as the range of parameter h is increased and is taken as $h = 0.4$, range the control parameter r decreases rapidly, that is, r approaches from 0 to 4.25 as shown in bifurcation plot Figure 11. While Figure 11 gives the complete dynamics of the Euler's logistic system which describes fixed-point state, periodic state and chaotic regime. At $h = 0.7$, the Euler's map has stable fixed-point behavior up to $r = 2.8339$, after that the first bifurcation occurs at $r = 3.4953$ at which the Euler's orbit is divided in to two period orbits x_3 and x_4 of order two as determined in above section and.

Proceeding in this way as the value of parameter r increases through 3.4953 the Euler's orbit bifurcates in to higher order periodic fixed points, that is, in the order of $8, 16, 32, 64, \ldots$ and soon as shown in the Figure 12. But as the parameter r approaches to 3.6696 the dynamics of the Euler's logistic map tends to chaotic regime. The magnified Figure 12 shows the complete period-doubling regime while the magnified Figure 13 represent the complete chaotic regime with period-3 window. While Figure 14 shows a comparative representation of the bifurcation plots for the parameter value $h = 0.1, 0.4$ and 0.7. Thus, we summarize the case 3 as follows:

Proposition 3. *It is observed that as the Euler's parameter range of the h is increased the range of the growth rate parameter r are decreases simultaneously. But for the lower range of Euler's parameter h the growth rate parameter range is higher than the standard logistic system.*

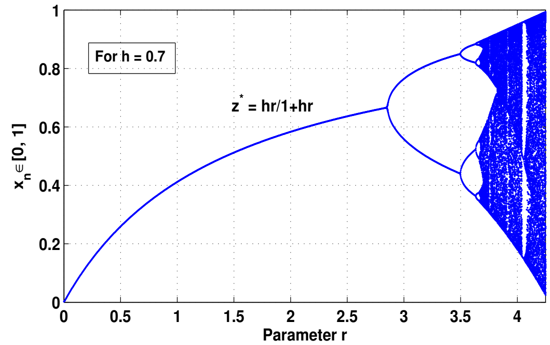

Figure 11 Bifurcation plot for the map $E_h(x, r)$ for $h = 0.7$ and $r \in [0, 4.25]$

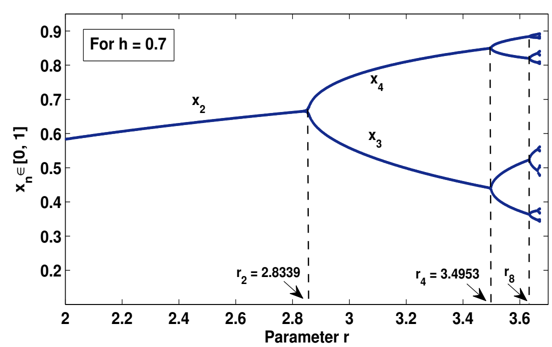

Figure 12 Magnified periodic regime for the map $E_h(x, r)$ for $h = 0.7$

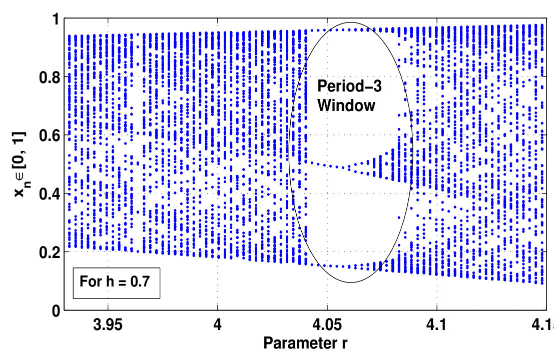

Figure 13 Magnified period-3 window region for the map $E_h(x, r)$ for $h = 0.7$

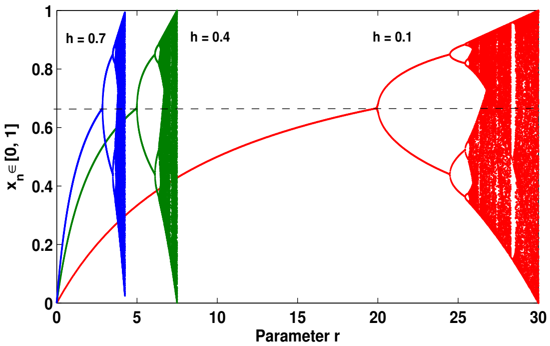

Figure 14 Comparative representation of bifurcation plots for $h = 0.1, 0.4$ and 0.7

CONCLUSION

In this article using some computational work on conventional logistic map in Euler's numerical algorithm is studied. The whole dynamics depends on the two control parameters h and r. Therefore, the following results are concluded from the main section:

- The dynamical properties of the Euler's type logistic map are determined analytically as well as experimentally.
- In the analytical section the Euler's logistic type map is derived and the fixed and periodic points are calculated followed by the Theorem 1 and Theorem 2.
- Further, in experimental section the dynamical properties of the Euler's logistic map are studied using period-doubling bifurcation plot. Because the dynamics of the Euler's map depends on the Euler's control parameter h, three cases are discussed for all the dynamical properties for $h = 0.1, 0.4$ and 0.7.
- It is also observed that the map exhibits its dynamical properties for a large range of parameter r, as compared to the existing methods. It is also observed that as compared to Picard iteration method which has growth rate $r \in [0, 4]$ and Mann iteration $r \in [0, 4.22]$, in this technique the growth rate parameter r approaches to 30. Hence it may improve the chaos-based application in engineering and science such as secure communication and cryptography.

Acknowledgments

The authors would like to express their sincere gratitude to all editors and anonymous reviewers for their valuable comments that helped to improve the article.

Conflicts of interest

The authors declare that there is no conflict of interest regarding the publication of this paper.

Availability of data and material

Not applicable.

LITERATURE CITED

Alligood, K. T., Sauer, T. D. and Yorke, J. A., 1996 Chaos : An Introduction to Dynamical Systems, Springer Verlag, New York Inc.

Ashish, Cao, J. and Chugh, R., 2018 Chaotic behavior of logistic map in superior orbit and an improved chaos-based traffic control model, Nonlinear Dynamics **94**: 959-975.

Ashish and Cao, J., 2019a A novel fixed point feedback approach studying the dynamcial behaviour of standard logistic map, International Journal of Bifurcation and Chaos **29**: 1950010-16, 16 pages.

Ashish, Cao, J., Alsaadi, F. and Malik, A. K., 2021a Discrete Superior Hyperbolicity in Chaotic Maps, Chaos Theory and Applications **03**: 34-42

Ashish, Cao, J. and Chugh, R., 2021b Discrete chaotification in modulated logistic system, International Journal of Bifurcation and Chaos **31**: 2150065, 14 Pages.

Ashish, Cao, J. and Chugh, R., 2019b Controlling chaos using superior feedback technique with applications in discrete traffic models, International Journal of Fuzzy System **21**: 1467-1479.

Ashish, Cao, J. and Alsaadi, F., 2021c Chaotic evolution of difference equations in Mann orbit, J. Appl. Anal. Comput. **11**: 1-20.

Ausloos, M. and Dirickx M., 2006 The Logistic Map and the Route to Chaos : from the Beginnings to Modern Applications, Springer Verlag, New York Inc.

Chugh, R., Rani, M. and Ashish, 2012 Logistic map in Noor orbit, Chaos and Complexity Letter **6**, 167-175.

Devaney, R. L., 1948 An Introduction to Chaotic Dynamical Systems, 2nd Edition (Addison-Wesley).

Feigenbaum, M. J., 1978 Quantitative universality for a class of nonlinear transformations, J. Stat. Phys. **19**: 25-52.

He, J. H., Jiao, M. L., Gepreel, K. A. and Khan, Y., 2023 Homotopy perturbation method for strongly nonlinear oscillators, Mathematics and Computers in Simulation **204**: 243-258.

Holmgren, R. A., 1994 A First Course in Discrete Dynamical Systems, Springer Verlag, New York Inc.

Khamosh, Kumar, V. and Ashish, 2020 A novel feedback control system to study the stability in stationary states, Journal of Mathematical and Computational Science **10**: 2094-2109.

Kumar, M. and Rani, M., 2005 An experiment with summability methods in the dynamics of logistic model, Indian J Math **47**: 77-89.

Kumar, V., Khamosh and Ashish, 2020 An empirical approach to study the stability og generalized logistic map in superior orbit, Advances In Mathematics: Scientific Journal **10**: 2094-2109.

Lorenz, E. N., 1963 Deterministic nonperiodic flows, J. Atoms. Sci. **20**: 130-141.

Mann, W. R., 1953 Mean value methods in iteration, Proceedings of American Mathematical Society **04**: 506-510.

May, R., 1976 Simple mathematical models with very complicated dynamics, Nature **261**, 459-475.

Molina, C., Sampson N., Fitzgerald W. J. and Niranjan M., 1996 Geometrical techniques for finding the embedding dimension of time series, Proc. IEEE Signal Processing Society Workshop, 161-169.

Parasad, B. and Katiyar, K., 2014 A stability analysis of logistic model, Int. J. Non-Lin Sci. **17**: 71-79.

Poincare H., 1899 Les Methods Nouvells de la Mecanique Leleste, Gauthier Villars, Paris.

Rani, M. and Kumar, V., 2005 A new experimental approach to study the stability of logistic maps, J. Indian Acad. Math. **27**: 143-156.

Rani, M. and Agarwal, R., 2009 A new experiment approach to study the stability of logistic map, Chaos Solitions Fractals **04**: 2062-2066.

Radwan, A. G., 2013 On Some Generalized Discrete Logistic Map, J. Adv. Research **04**: 163-171.

Renu, Ashish, and Chugh, R., 2022 On the dynamics of a discrete difference map in mann orbit, Computational and Applied Mathematics **41**: 1-19.

Robinson, C., 1995 Dynamical Systems: Stabilily, Symbolic Dynamics, and Chaos, CRC Press.

Singh, N. and Sinha, A., 2010 Chaos based secure communication system using logistic map, Optics and Lasers in Engineering **48**: 398-404.

Song, N. and Meng, J., 1996 Research on Logistic mapping and Synchronization, Proc. IEEE Intell. Contr. Autom. **01**: 987-991.

How to cite this article: Sanjeev, Anajli, Ashish, and Malik, A. K. Dynamical Interpretation of Logistic Map using Euler's Algorithm. *Chaos Theory and Applications*, 4(3), 128-134, 2022.

CHAOS Theory and Applications
in Applied Sciences and Engineering

e-ISSN: 2687-4539
RESEARCH ARTICLE
Vol.4 / **No.**3 / 2022 / **pp.**135-143
https://doi.org/10.51537/chaos.1131966

Modeling Love with 4D Dynamical System

Kadir Can Erbaş *,1
*Department of Biomedical Engineering, Faculty of Engineering, Başkent University, Ankara, Türkiye.

ABSTRACT Dynamic modeling of romantic relationships explains the development of love/hate feelings between two people over time with a system of differential equations. Rather than postulating an individual's emotions as a one-component feeling of love, this study assumed two-component feelings of intimacy and passion. As a result of this assumption, relationship dynamics are represented by a four-dimensional system of equations. The possible outcomes of this new 4D model were compared with the results of the classical 2D model and it was seen that they could give very different outputs. In addition, situations that cannot be explained by classical models such as the end of passion in long-term relationships, relationships that turn from friendship to love, and the reunion of couples after separation are interpreted.

KEYWORDS
Dynamics of love
Fixed points
Human behaviour
Linear systems
Mathematical sociology

INTRODUCTION

The dynamic systems approach has been used for many years in applied mathematics and physics to model the behavior of many physical systems, such as the motion of planets (position and velocity), mass-spring systems, oscillators, and electrical circuits. Afterward, it expanded its field of use in the field of engineering and gained a respectable place. An example of this is the solution of flow models, which are in the form of partial differential equations, by converting them to systems of ordinary differential equations (Shah *et al.* 2022) (Shahzad *et al.* 2023) (Bilal *et al.* 2021) (Qureshi *et al.* 2022). In the last few decades, its use has become widespread in disciplines such as biology, economics, and psychology (Richardson *et al.* 2014). This study primarily scanned the dynamic modeling efforts of the study of romantic relationships in the literature, which are included in the field of psychology, and aimed to make psychological theories and dynamical approaches consistent with each other.

Psychologists have developed various theories to explain love. According to Rubin, liking and loving are separate emotions. He defines liking with feelings such as being appreciated, admired, enjoying, spending time, and wanting to be with the partner. He defines love as a more intense emotion with strong desires for physical contact and intimacy (Rubin 1970). The color wheel model was developed by Lee in 1973 and according to Lee, there are three main styles of love. These are EROS with physical and emotional passion, LUDUS with playful style, and STORGE, which combines family love with friendship (Lee *et al.* 1988). In 1987, Hazan and Shaver put forward the attachment theory, three styles of adult attachment; she described them as "anxious-indecisive" who fears that her partner does not love her, "avoidant" who has difficulty developing trust, and "safe" who has no fear of abandonment (Hazan and Shaver 2017). According to Hatfield, there are two basic types of love, compassionate and passionate. While mutual trust and respect are at the forefront of tender love, deep feelings and sexual attraction are at the forefront of passionate love (Hatfield *et al.* 1988).

One of the most popular love theories is the triangular love theory developed by Sternberg in 1986. Three basic components of love in this theory are named intimacy, passion, and commitment. Intimacy encompasses the emotions that lead to the experience of warmth in a loving relationship. Passion represents emotions that lead to sexual attraction and romance. Finally, the commitment component describes the determination to maintain the relationship for a long time (Sternberg 1986).

There are also psychological studies on the relationship between intimacy and passion. Baumeister and Bratslavsky reported that passion is a function of the change in intimacy, hence the time derivative of intimacy, and that there may be a positive or negative correlation between passion and intimacy within the same relationship(Baumeister and Bratslavsky 1999). In addition, Aykutoğlu and Uysal state that they found evidence for the existence of a relationship between intimacy and passion, and that physical attraction is effective on this relationship (Aykutoğlu 2015) (Aykutoğlu and Uysal 2017).

Manuscript received: 16 June 2022,
Revised: 23 October 2022,
Accepted: 9 November 2022.

[1] kcerbas@gmail.com (**Corresponding Author**)

Table 1 **Several models expressing the love dynamics between couples or love-triangle among triples.**

1	$\dot{x}_1 = a_1 x_1(t) + b_1 x_2(t)$, $\dot{x}_2 = b_2 x_1(t) + a_2 x_2(t)$.	(Sprott 2004), (Erbaş 2022) and (Sunday *et al.* 2012)
2	$\dot{x}_1 = -\alpha_1 x_1(t) + \beta_1 x_2(t) + \gamma_1 A_2$, $\dot{x}_2 = -\alpha_2 x_2(t) + \beta_2 x_1(t) + \gamma_2 A_1$.	(Rinaldi 1998b) and (Bielczyk *et al.* 2012)
3	$\dot{x}_1 = -\alpha_{10} x_1(t) + \beta_{10} x_2(t) + F_{10}(t)$, $\dot{x}_2 = -\alpha_{20} x_2(t) + \beta_{20} x_1(t) + F_{20}(t)$.	(Wauer *et al.* 2007) and (Chen *et al.* 2016)
4	$\dot{R}_J = aR_J + b(J-G)$, $\dot{J} = cR_J + dJ$, $\dot{R}_G = aR_G + b(G-J)$, $\dot{G} = eR_G + fG$.	(Sprott 2004)
5	$\dot{R} = aR + bJ(1-\lvert J\rvert)$, $\dot{J} = cR(1-\lvert R\rvert) + dJ$.	(Sprott 2004)
6	$\dot{R} = aR + bJ(1-\lvert J\rvert) + y(t)$, $\dot{J} = cR(1-\lvert R\rvert) + dJ + f(t)$.	(Huang and Bae 2018a)
7	$\dot{x} = R^L(y(t)) + R^A(A)(1 + B(x(t))) - \alpha x(t)$	(Rinaldi and Della Rossa 2020)
8	$\dot{x}_1 = ax_1 + bx_2(1-\varepsilon x_2^2)$, $\dot{x}_2 = dx_2 + cx_1(1-\varepsilon x_1^2)$.	(Barley and Cherif 2011)
9	$\dot{x}_1 = -\alpha_{10} x_1 + \beta_{10} \frac{x_2}{1+\varepsilon_0\lvert x_2\rvert} + F_{10}$, $\dot{x}_2 = -\alpha_{20} x_2 + \beta_{20} \frac{x_1}{1+\varepsilon_0\lvert x_1\rvert} + F_{20}$.	(Wauer *et al.* 2007)
10	$\dot{x}_1 = -\alpha_1 x_1(t) + \rho_1 A_2 + R_1(x_2)$, $\dot{x}_2 = -\alpha_2 x_2(t) + \rho_2 A_1 + R_2(x_1)$.	(Rinaldi *et al.* 2013a), (Rinaldi *et al.* 2010), (Rinaldi *et al.* 2013b), (Liao and Ran 2007), (**?**)
11	$\dot{L} = -\alpha_1 L + \beta_1 \left[P(1-(P/\gamma)^2) + A_P\right]$ $\dot{P} = -\alpha_2 P + \beta_2 \left[L + \frac{A_L}{1+\delta Z}\right]$ $\dot{Z} = -\alpha_3 Z + \beta_3 P$	(Rinaldi 1998a)
12	$\dot{R}_J = aR_J + b(J-G)\left(1-(J-G)^2\right)$, $\dot{J} = cR_J\left(1-R_J^2\right) + dJ - mJG$, $\dot{R}_G = aR_G + b(G-J)\left(1-(G-J)^2\right)$, $\dot{G} = eR_G(1-R_G^2) + fG - nJG$.	(Liu and Chen 2015)

■ **Table 2 continuation of Table 1**

13	$\dot{R}_J = aR_J + b(J-G)(1-\|J-G\|),$ $\dot{J} = cR_J(1-\|R_J\|) + dJ,$ $\dot{R}_G = aR_G + b(G-J)(1-\|G-J\|),$ $\dot{G} = eR_G(1-\|R_G\|) + fG.$	(Ahmad and El-Khazali 2007)
14	$D_t^{\alpha} u(t) = -\rho_1 u(t) + \sigma_1 v(t)\left(1-\epsilon v^2(t)\right) + \varphi_1$ $D_t^{\alpha} v(t) = -\rho_2 v(t) + \sigma_2 u(t)\left(1-\epsilon u^2(t)\right) + \varphi_2$	(Owolabi 2019), (Goyal *et al.* 2019) and (Ozalp and Koca 2012)
15	$d^{\alpha}R/dt^{\alpha} = aR + bJ(1-J) + 5\sin(\pi t)$ $d^{\beta}J/dt^{\beta} = cR(1-R) + dJ$	(Huang and Bae 2018b)
16	$d^{\alpha}R_J/dt^{\alpha} = aR_J + b\, sgn(J-G),$ $d^{\beta}J/dt^{\beta} = c\, sgn(R_J) + dJ,$ $d^{\gamma}R_G/dt^{\gamma} = aR_G + b\, sgn(G-J),$ $d^{\eta}G/dt^{\eta} = e\, sgn(R_G) + fG.$	(Ahmad and El-Khazali 2007)
17	$D^{2\alpha}x_1(t) = -\alpha_1 x_1(t) + \beta_1(x_2-x_3)\left(1-\varepsilon(x_2-x_3)^2\right) + \gamma_1$ $D^{2\alpha}x_2(t) = -\alpha_2 x_2(t) + \beta_2 x_4\left(1-\varepsilon x_1^2\right) + \gamma_2$ $D^{2\alpha}x_2(t) = -\alpha_2 x_3(t) + \beta_3 x_4\left(1-\varepsilon x_4^2\right) + \gamma_3$ $D^{2\alpha}x_4(t) = -\alpha_1 x_4(t) + \beta_1(x_3-x_2)\left(1-\varepsilon(x_3-x_2)^2\right) + \gamma_4$	(Koca and Ozalp 2014)
18	${}^{C}D_t^{\Theta,\rho} M_r(t) = \beta_a + L_r^2 - L_i^2 + \beta_c M_r,$ ${}^{C}D_t^{\Theta,\rho} M_i(t) = 2L_r L_i + \beta_c M_i,$ ${}^{C}D_t^{\Theta,\rho} L_r(t) = \beta_b + M_r^2 - M_i^2 + \beta_d L_r,$ ${}^{C}D_t^{\Theta,\rho} L_i(t) = 2M_r M_i + \beta_d L_i.$	(Kumar *et al.* 2021) and (Jafari *et al.* 2016)

Dynamical modeling of romantic relationships has led researchers in physics, mathematics, and engineering to the idea of explaining the evolution of romantic relationships with a system of differential equations. There is a consensus that the first attempt at this was a short article published by Strogatz. Strogatz suggested the following system of equations in the study of Romeo and Juliet in which he tried to predict the love relationship (Strogatz 1988):

$$\frac{dR}{dt} = -aJ \text{ and } \frac{dJ}{dt} = bR \tag{1}$$

In Equation 1, R(t) represents the quantity of Romeo's love/hate for Juliet and, J(t) represents the quantity of Juliet's love/hate for Romeo at time t. Here, a and b are the positive parameters that characterize their romantic styles of the couple. After Strogatz, researchers proposed more complex models to obtain the love/hate evolution of individuals in a romantic relationship as a function of time. In general, the models in the literature can be generalized by Equation 2 (Erbaş 2022).

$$\frac{dx}{dt} = f(x,y,t) \text{ and } \frac{dy}{dt} = g(x,y,t) \tag{2}$$

In this equation, the left-hand sides of the equation are the derivatives with respect to time and the right-hand sides are functions (f_1 and f_2) that explain the rate of change in their feelings with instantaneous feelings and time. The models proposed by various authors in their studies are summarized in Table 1. Same equations are combined in the table so notations of the authors may be different from their original papers. The reader who wants to reach detailed information about these studies can refer to the references in the last column.

The first five rows in Table 1 are examples of homogeneous or in homogeneous first-order systems of linear equation. Rows 5-10 are nonlinear first order systems with two unknowns, rows 14 and 18 are systems of fractional order equations. In the literature, systems of equations with more than two unknown functions have also been used. The system of equations seen in row 11 deals with the relationship of Laura and Petrarch. $L(t)$ indicates Laura's feelings towards *Petrarch*, $P(t)$ indicates Petrarch's feelings toward *Laura*, and $Z(t)$ indicates *Petrarch's poetic inspiration*.

The four-dimensional models in rows 4, 12, 13 and 16-18 model three-person romantic relationships, called love triangles. In the love triangle model, Sprott assumes that Romeo has a mistress named Guinevere and that she and Juliet do not know each other. In this case, Romeo has two different affections or interests (R_J and R_G), while Juliet and Guinevere only have feelings for Romeo (J and G).

While systems of fractional differential equations are used between lines 14-18, the feelings of individuals are modeled with complex numbers in the last line. In line 18, Jafari and Sprott represent feelings with complex numbers, while their fractional derivatives are assigned as nonlinear functions of feelings (Jafari *et al.* 2016). In studies of the dynamic analysis of love, the individual's feeling for his partner is called love for positive values and hate for negative values. In models that express emotions with complex numbers, Jafari and Sprott consider the individual's feelings as a state of indecision in which love and hate coexist (Jafari *et al.* 2016). But even this is far from the fact that the individual has two-dimensional emotions that affect each other.

The triangular theory of love, which has a wide research area in psychology, sees emotions in a romantic relationship as two components (intimacy and passion) that affect each other. Although this distinction has been accepted in the school of psychology, there is, to our knowledge, no work in the school of mathematics where dynamic calculations are made. To fill this gap in the literature and to help interdisciplinary reconciliation between psychology and mathematics, in this study, the dynamics of the relationship between individuals with two-dimensional feelings were modeled with a four-dimensional differential equation system. This study, which is a first in this respect, aimed to construct and test the simplest linear model. If this model is developed;

- Relationships that minimal models cannot explain can be explained more comprehensively,

- Relationships evolving from friendship to love can be predicted,

- The situations of couples who come together after a long separation are predictable.

MATHEMATICAL MODEL

In the studies on the dynamic modeling of love, the emotions of the individual were handled as one-dimensional in the love/hate range. This study aims to linearly model how individuals' romantic relationships evolve in a two-dimensional emotional state. For this reason, a two-component emotional state, which is the intimacy of the individual to his/her partner and the deeper passions he feels, has been determined as a function of time. The intimacy and passion of x to his/her partner y are shown with $x_i(t)$ and $x_p(t)$ respectively. For example, if the individual is in the emotional state of $(x_i,x_p) = (2,-1)$, she has sincere feelings towards her partner and wants to spend time with him, but has no passions and desires with him. That is, she does not feel romantic or sexual desire.

Throughout the study, the emotions denoted by x and y will represent the emotions of the fictional couples named Xena and Yorgo. x_i and x_p will show Xena's intimacy and passion for Yorgo, and y_i and y_p will show Yorgo's intimacy and passion for Xena. Since an individual's state of emotion is handled in two components, four qualitative combinations can occur. These combinations can be interpreted as follows according to the signs of the components.

$(x_i,x_p) = (+,+)$: Xena feels warm, close, and passionate toward Yorgo. She enjoys spending time and being with him and desires romance/sexuality with him.

$(x_i,x_p) = (+,-)$: Xena has a good time with Yorgo and likes him friendly. But they have no romantic or sexual desires toward him.

$(x_i,x_p) = (-,+)$: Xena does not find Yorgo close or sincere, and even finds him boring. But she is fascinated by Yorgo's charm and desires him.

$(x_i,x_p) = (-,-)$: Xena does not feel intimacy or passion towards Yorgo. He does not enjoy spending time with her and does not desire romance or sex with her.

In the two-component feeling of love modeling, it is clear that a romantic relationship can be expressed with a total of four functions. The simplest dynamic modeling of these four functions is the linear differential equation system. In Equation 3, the intimacy and passion of individuals x and y and their relationship with the rate of change of these feelings are shown.

$$\frac{d}{dt}\begin{pmatrix} x_i \\ y_i \\ x_p \\ y_p \end{pmatrix} = \begin{pmatrix} a_{xx} & a_{xy} & b_{xx} & b_{xy} \\ a_{yx} & a_{yy} & b_{yx} & b_{yy} \\ c_{xx} & c_{xy} & d_{xx} & d_{xy} \\ c_{yx} & c_{yy} & d_{yx} & d_{yy} \end{pmatrix}\begin{pmatrix} x_i \\ y_i \\ x_p \\ y_p \end{pmatrix} \tag{3}$$

In this equation, the parameters that make up the coefficients matrix was defined in Table 3. After these parameters and initial feelings of the couple are determined, readers can use the MATLAB script in the Appendix to visualize the future of the relation. How to comment on the visualizations is expressed in the Results section.

RESULTS AND DISCUSSION

Results of some possible scenarios

To set an example for the model described above, a scenario was prepared considering the characteristics of Xena and Yorgo when they met. According to this scenario, the romantic styles of Xena and Yorgo are shown in Table 3. The explanations of the parameters in the tables are given. In the first interview, it was assumed that both of them started with neutral emotions and the initial condition was chosen as (0,0,0,0). The development of the relationship starting from this condition over time is shown in Figure 1a. As can be seen from this figure, as Xena's sense of intimacy increases, her passions decrease over time. On the contrary, Yorgo's passion for her increases as he gets colder from Xena.

One of the interesting features in this scenario is the influence of individuals' impressions on each other. When a small change is made in the values shown in Table 3, the course of the relationship changes. If Yorgo had found Xena sympathetic, that is, if f_{yx} was one instead of zero, the development of the relationship would have been as in Figure 1b. In Figure 1b, while Yorgo's intimacy and passions increase over time.

Table 3 Romantic styles of Xena and Yorgo.

$a_{xx} = -0.2$	Forgetting coefficient of the intimacy of Xena to Yorgo.
$a_{xy} = -0.4$	If Yorgo's intimacy increases, Xena's will decrease, and if it decreases, it will increase. If Xena's partner shows closeness/interest to her, Xena gradually loses her sense of intimacy.
$b_{xx} = +0.5$	If Xena's passion increases, her sense of intimacy increases, and if it decreases, it decreases. She is intimate with someone she is passionate about. She might just want to fall in love.
$b_{xy} = -0.2$	As Yorgo's passion for Xena increase, Xena's closeness to Yorgo decreases. When she realizes that Yorgo is not in love, Xena increases her intimacy. Maybe she doesn't want someone in love with her.
$c_{xx} = +0.3$	Her passion increase when Xena feels close. Men with whom she does not feel close are not attractive, but men with whom she feels sincere can be attractive.
$c_{xy} = +0.7$	Intimate men are very attractive to Xena. Her passion for men who do not behave closely is significantly reduced.
$d_{xx} = -0.1$	Forgetting coefficient of the passion of Xena for Yorgo.
$d_{xy} = +0.4$	As Yorgo's passion grows, so does Xena's. A man who acts romantic may attract her.
$f_{xy} = +1.0$	Xena's impression of intimacy or friendship with Yorgo. Xena finds Yorgo intimate and friendly. She enjoys being friends and spending time with him.
$g_{xy} = -1.0$	Xena's impression of glamorousness or attractiveness about Yorgo. Xena does not find Yorgo romantically or sexually attractive.
$a_{yy} = -0.2$	Forgetting coefficient of the intimacy of Yorgo to Xena.
$a_{yx} = +0.6$	If Yorgo's intimacy increases, Xena's will decrease, if it decreases, it will increase. If Yorgo's partner shows intimacy/interest to him, Yorgo increases his sense of intimacy.
$b_{yy} = -0.5$	If Yorgo's passion increases, his sense of intimacy decreases, and if it decreases, it increases. He is intimate with someone he is not passionate about. He might just want not to fall in love.
$b_{yx} = +0.6$	As Xena's passion for Yorgo increases, Yorgo's intimacy with Xena increases. When he realizes that Xena is not in love, Yorgo decreases his intimacy. Maybe he wants someone in love with her.
$c_{yy} = -0.3$	His passion decreases when Yorgo feels close. Women with whom he does not feel close are attractive, but women with whom he feels intimacy are not attractive.
$c_{yx} = -0.1$	Intimate women are not attractive to Yorgo. His passion for women who are close to him weakens a little.
$d_{yy} = -0.1$	Forgetting coefficient of the passion of Yorgo to Xena.
$d_{yx} = -0.4$	As Xena's passion increases, Yorgo's decreases. A romantic woman does not attract him.
$f_{yx} = +0.0$	Yorgo's impression of intimacy or friendship with Xena. Yorgo found Xena neither sympathetic nor antisympathetic.
$g_{yx} = +1.0$	Yorgo's impression of glamorousness or attractiveness about Xena. Yorgo finds Xena attractive. He desires her romantically and sexually.

Xena's emotions show a similar development. However, as Xena's intimacy decreases initially and then increases, her passion initially increases and then decreases. But they still enter into an ideal relationship together. While the relationship shown in the first case goes to the incompatible regions (2^{nd} and 3^{rd} quadrants) in every sense, in the second case it goes to the best region. In Figure 1a, while Zeyna wants to remain friends and not have emotional relations, Yorgo wants an emotional relationship and refuses to meet. In Figure 1b, they both enter into a friendly and passionate relationship. What makes such a big difference is that Yorgo doesn't find Xena sympathetic. It can be said that the impressions of individuals on each other affect the relationship very sensitively.

In another scenario, the romantic styles of our fictional characters Xena and Yorgo are parameterized as in Table 4. In the relationship that started according to these parameters, it can be understood from Figure 2a that Xena wants friendship without a romantic relationship and Yorgo seeks love, not intimacy. As an example of Yorgo's strategy for obtaining Xena, when the a_{yx} parameter is increased to -3, the relationship evolves as in figure 2b. So if Yorgo exaggerates his avoidance of friendship, it may cause Xena to desire him because a friendly man is not attractive to Xena, but a man who avoids intimacy with her is attractive ($c_{xy} = -1$).

Suppose that individuals with romantic styles in Table 3 meet again after a long separation, but during this time their impressions of each other, not their characteristics, have changed. Now both of them have neutralized the impression of being close to each other ($f_{xy} = f_{yx} = 0$), but their attraction has become $g_{xy} = 0.5$ and $g_{yx} = 0.7$. How such an encounter would progress is shown in Figure 3a. We can see that their feelings of intimacy are gradually developing, but Yorgo's passion first increases and then decreases, while Xena's passion increases steadily. In other words, ex-lovers reconcile and become friends, but it can be said that while Xena wants to try again, Yorgo does not take kindly to this.

When the matrix in Equation 3 is grouped and divided into four sub-matrices, 2x2 matrices A, B, C, and D in Eqs.4 and 5 are obtained. Matrices A and D respectively model the effect of intimacies on intimacies, while matrix D represents the effect of passions on passions. The B matrix represents the influence of passions on intimacy, and the C matrix represents the influence of intimacy on passions. Situations, where there is no reciprocal cross-effect on intimacies and passions, can be expressed by Equations 4 and 5. In general, the studies seen in the literature are 2-dimensional. The two-dimensional work done by ignoring the cross-interactions and the four-dimensional study with the cross-interaction introduced in this study are visualized with the data in Table 2, and the results are compared in Figure 3b. According to Figure 3b, intimacy and passion follow a very different course when cross interactions come into play.

$$\begin{bmatrix} \overrightarrow{I'}_{2x1} \\ \overrightarrow{P'}_{2x1} \end{bmatrix} = \begin{bmatrix} \hat{A}_{2x2} & \hat{B}_{2x2} \\ \hat{C}_{2x2} & \hat{D}_{2x2} \end{bmatrix} \begin{bmatrix} \overrightarrow{I}_{2x1} \\ \overrightarrow{P}_{2x1} \end{bmatrix} + \begin{bmatrix} \overrightarrow{f}_{2x1} \\ \overrightarrow{g}_{2x1} \end{bmatrix} \tag{4}$$

If B_{2x2}=C_{2x2}=0, then

$$\begin{aligned} \overrightarrow{I'}_{2x1} &= \hat{A}_{2x2}\overrightarrow{I}_{2x1} + \overrightarrow{f}_{2x1}, \\ \overrightarrow{P'}_{2x1} &= \hat{D}_{2x2}\overrightarrow{P}_{2x1} + \overrightarrow{g}_{2x1}. \end{aligned} \tag{5}$$

Discussion

When the results obtained here are discussed, perhaps the first issue that comes to mind is how to determine the parameters that determine romantic styles. The parameters explained in Table 2 can be obtained by surveys to be applied to individuals, by observation, or by examining the past relationships of individuals. But as this would be a thorny work in psychology, it is not covered here. The signs of these parameters will give the romantic style of the individual, but the question of how much is quite difficult to answer.

Another issue that needs to be discussed is that the relationship dynamics are linear. One might argue that a complex subject such as human behavior cannot be modeled with linear systems. Suggesting more complicated non-linear equations will of course give results closer to reality, but the fact that a four-dimensional structure is tried for the first time and measurement difficulties in human emotions made it necessary to start with the simplest model, the linear model. Moreover, the approximation of nonlinear systems by linearizing them around fixed points is a commonly used approximation technique. The model described here can be said to be a model that approximately explains the evolution of a short-term relationship around neutral emotions. It would be appropriate to interpret the evolution of the relationship for the first few days or a week or two. Otherwise, in long-term developments, the model will deviate too much from reality.

To model the chaotic nature of love, it is necessary to construct two-dimensional nonlinear and non-homogeneous or at least three-dimensional nonlinear dynamic systems (Sprott 2010). Although nonlinear studies have been tried in the studies in the literature, it does not seem possible for a system with two unknowns to create a chaotic system by itself. However, it has been determined that chaos occurs when non-homogeneous terms are added.

In addition, since the love triangle models are expressed with a system of equations with four unknowns, it has been observed that four-dimensional nonlinear models can produce chaos (Kacar *et al.* 2018; Wang *et al.* 2022). However, when the individual's feelings for his partner are divided into two intimacy and passion, a nonlinear four-dimensional system alone can produce chaos. There is no need for two-dimensional homogeneous systems as Huang and Bae have pointed out (Huang and Bae 2018a) or for the four-dimensional nonlinear love triangle dynamics as Liu and Chen (Liu and Chen 2015). Even the simplest love affair can be chaotic, with no outside human influence or involvement of a third party.

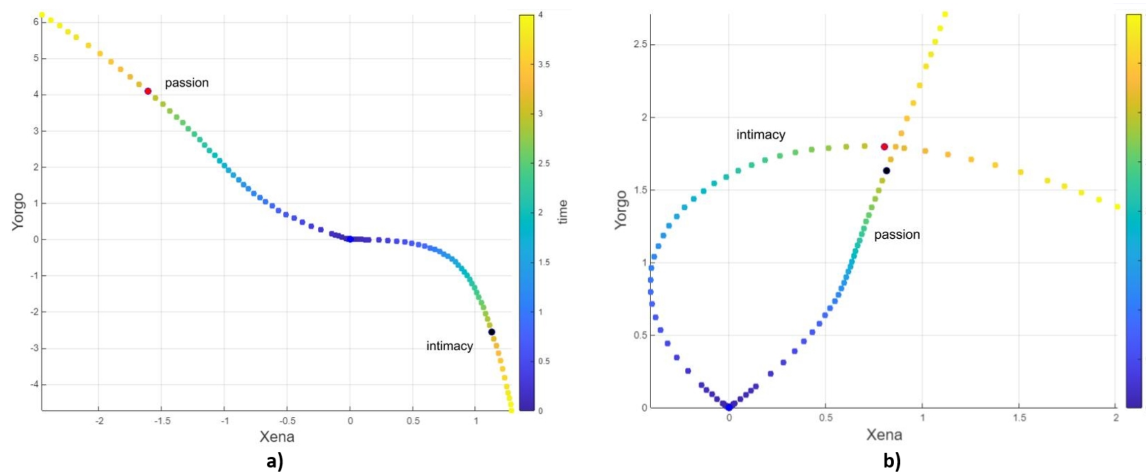

Figure 1 Evolution of the intimacy (black dot) and passion (red dot) between Xena and Yorgo according to the parameter in Table 3 with **a)** $f_{yx} = 0$ and **b)** $f_{yx} = +1.0$.

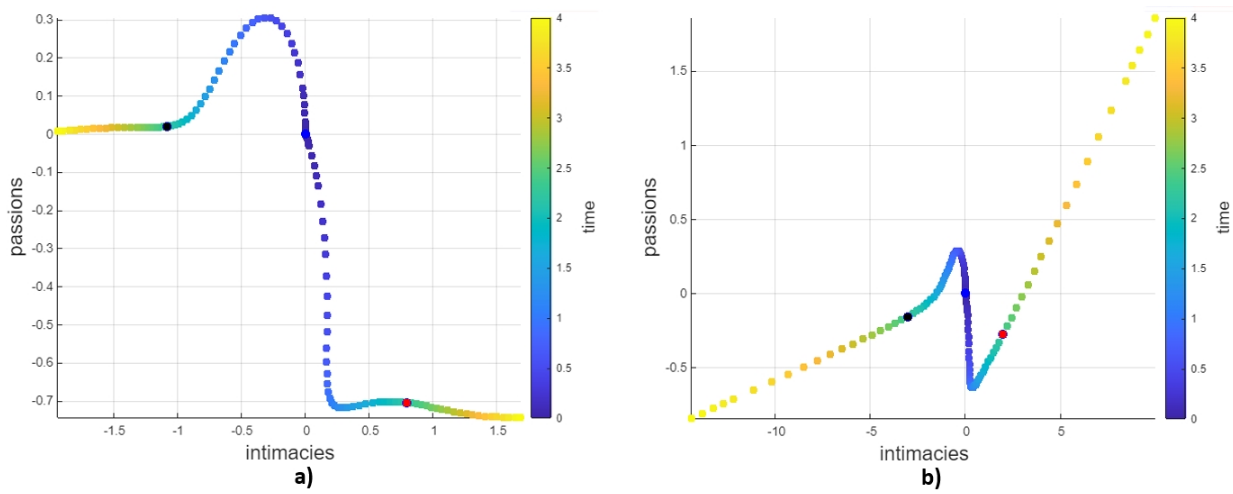

Figure 2 Evolution of the intimacy (black dot) and passion (red dot) between Xena and Yorgo according to the parameter in Table 4 with **a)** $a_{yx} = -1.0$ and **b)** $a_{yx} = -3.0$.

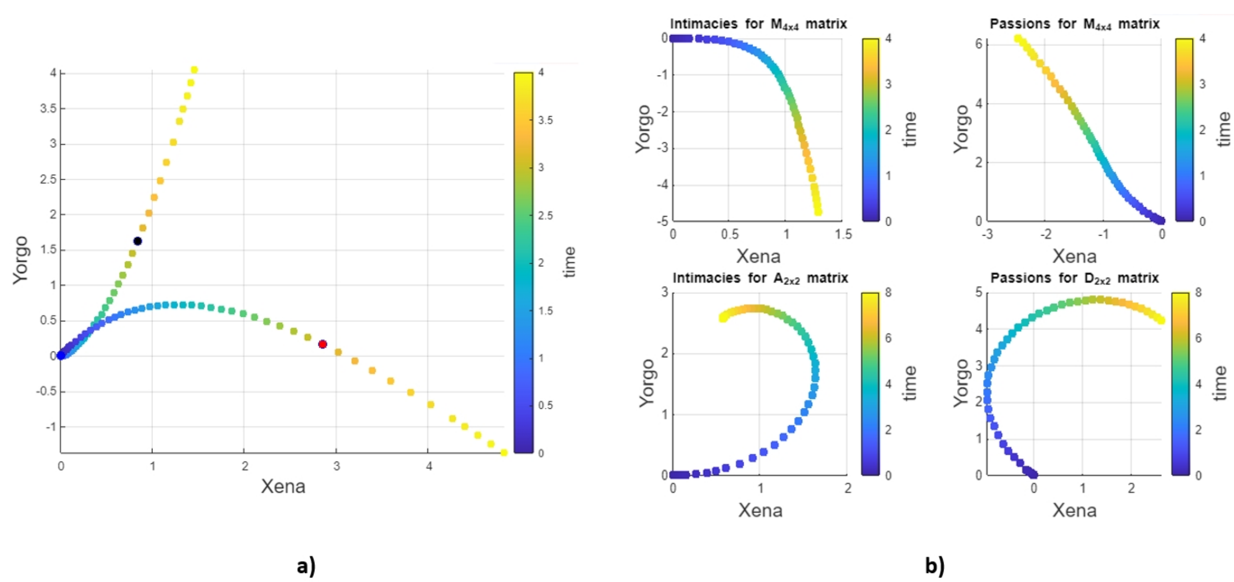

Figure 3 a) Intimacy (black dot) and passion (red dot) after a long separation ($f_{xy} = f_{yx} = 0$, $g_{xy} = 0.5$, $g_{yx} = 0.7$), **b)** Grouping the matrix according to Eqs.4 and 5.

Table 4 Romantic Styles for Scenario 2

Xena	a_{xx}=-1	a_{xy}=-1	b_{xx}=+1	b_{xy}=-2	c_{xx}=-1	c_{xy}=-1	d_{xx}=-1	dxy=-1	fxy=+1	gxy=-1
Yorgo	ayy=-1	**ayx=-1**	byy=-1	byx=+1	cyy=+1	cyx=+1	dyy=-1	dyx=+1	fyx=0	gyx=+1

CONCLUSION

As a result, in this study, emotions in a romantic relationship are discussed in two dimensions, intimacy, and passion, which are predicted by the triangular love theory. In cases where an individual's sense of intimacy influences his passion, results appear very different from those predicted by classical one-dimensional emotion models. In addition, it has been seen that the parameters that determine the romantic styles of individuals and their impressions of each other can affect the future of the relationship quite sensitively. Finally, it can be said that romantic relationships, which are seen as fragile in one-dimensional emotion models, are more fragile in two-dimensional models.

APPENDIX

```
clear all; clc; close all;
% Input the parameters and initial conditions
axx= -0.2; axy= -0.4; bxx= +0.5; bxy= -0.2; cxx= +0.3; cxy= +0.7;
dxx= -0.1; dxy= +0.4; fxy=0; gxy=0.5;
ayy= -0.2; ayx= +0.6; byy= -0.5; byx= +0.6; cyy= -0.3; cyx= -0.1;
dyy= -0.1; dyx= -0.4; fyx=0; gyx=0.7;
xi0=-0.0; yi0=-0.0; xp0=+0.0; yp0=+0.0;
% Matrix and calculations. Do not type anything below
A=[axx axy bxx bxy;ayx ayy byx byy;cxx cxy dxx dxy;cyx cyy dyx dyy]; B=[fxy;fyx;gxy;gyx];
f = @(t,x) A*[x(1);x(2);x(3);x(4)]+B;
[t,xa] = ode45(f,[0 4],[xi0 yi0 xp0 yp0]);
% Xena vs Yorgo. Black dot:intimacy, Red dot:passion
subplot(2,2,1)
%figure(1);
s1=scatter(xa(:,1),xa(:,2),40,t,'filled'); grid on; ax = gca;ax.XDir = 'normal';view(-31,14); xlabel('Xena','FontSize',16); ylabel('Yorgo','FontSize',16);
cb = colorbar;cb.Label.String = 'time'; cb.Label.FontSize = 14;hold on;
s2=scatter(xa(:,3),xa(:,4),40,t,'filled'); grid on; ax = gca;ax.XDir = 'normal';view(-31,14);
cb = colorbar;cb.Label.String = 'time'; cb.Label.FontSize = 14;
hold on;L1 = plot(xa(50,1),xa(50,2), 'ob', 'MarkerSize',7, 'MarkerFaceColor','black'); axis tight;
hold on;L2 = plot(xa(50,3),xa(50,4), 'ob', 'MarkerSize',7, 'MarkerFaceColor','red'); axis tight;
hold on; L3 = plot(xa(1,1),xa(1,2), 'ob', 'MarkerSize',7, 'MarkerFaceColor','blue');
hold on; L4 = plot(xa(1,3),xa(1,4), 'ob', 'MarkerSize',7, 'MarkerFaceColor','blue'); view(2);
% Intimacy vs Passion. Black dot:Yorgo, Red dot:Xena
subplot(2,2,2)
%figure(2);
s3=scatter(xa(:,1),xa(:,3),40,t,'filled'); grid on;
ax = gca;ax.XDir = 'normal';view(-31,14); xlabel('intimacies','FontSize',16); ylabel('passions','FontSize',16);
cb = colorbar;cb.Label.String = 'time'; cb.Label.FontSize = 14;hold on;
s4=scatter(xa(:,2),xa(:,4),40,t,'filled'); grid on;
ax = gca;ax.XDir = 'normal';view(-31,14);
cb = colorbar;cb.Label.String = 'time'; cb.Label.FontSize = 14;
hold on;L1 = plot(xa(50,1),xa(50,3), 'ob', 'MarkerSize',7, 'MarkerFaceColor','r'); axis tight;
hold on;L2 = plot(xa(50,2),xa(50,4), 'ob', 'MarkerSize',7, 'MarkerFaceColor','black'); axis tight;
hold on; L3 = plot(xa(1,2),xa(1,4), 'ob', 'MarkerSize',7, 'MarkerFaceColor','blue');
hold on; L4 = plot(xa(1,1),xa(1,3), 'ob', 'MarkerSize',7, 'MarkerFaceColor','blue'); view(2);
% Intimacy of Xena vs intimacy of Yorgo vs passion of Xena.
subplot(2,2,3)
%figure(3);
s5=scatter3(xa(:,1),xa(:,2),xa(:,3),40,t,'filled'); grid on;
ax = gca;ax.XDir = 'normal';view(-31,14); xlabel('intimacy of Xena','FontSize',16); ylabel('passion of Xena','FontSize',16); zlabel('passion of Xena','FontSize',16);
cb = colorbar;cb.Label.String = 'time'; cb.Label.FontSize = 14;hold on;
% Intimacy of Xena vs intimacy of Yorgo vs passion of Yorgo.
subplot(2,2,4)
%figure(4);
s6=scatter3(xa(:,1),xa(:,2),xa(:,4),40,t,'filled'); grid on;
ax = gca;ax.XDir = 'normal';view(-31,14); xlabel('intimacy of Xena','FontSize',16); ylabel('passion of Yorgo','FontSize',16); zlabel('passion of Yorgo','FontSize',16);
cb = colorbar;cb.Label.String = 'time'; cb.Label.FontSize = 14;
```

Conflicts of interest

The author declares that there is no conflict of interest regarding the publication of this paper.

Availability of data and material

Not applicable.

LITERATURE CITED

Ahmad, W. M. and R. El-Khazali, 2007 Fractional-order dynamical models of love. Chaos, Solitons & Fractals **33**: 1367–1375.

Aykutoğlu, B., 2015 *The Relationship between intimacy and passion: gender, relationship length, physical attractiveness as moderators*. Master's thesis, Middle East Technical University.

Aykutoğlu, B. and A. Uysal, 2017 The relationship between intimacy change and passion: A dyadic diary study. Frontiers in psychology **8**: 2257.

Barley, K. and A. Cherif, 2011 Stochastic nonlinear dynamics of interpersonal and romantic relationships. Applied Mathematics and Computation **217**: 6273–6281.

Baumeister, R. F. and E. Bratslavsky, 1999 Passion, intimacy, and time: Passionate love as a function of change in intimacy. Personality and social psychology review **3**: 49–67.

Bielczyk, N., M. Bodnar, and U. Foryś, 2012 Delay can stabilize: Love affairs dynamics. Applied Mathematics and Computation **219**: 3923–3937.

Bilal, S., M. Rehman, S. Noeiaghdam, H. Ahmad, and A. Akgül, 2021 Numerical analysis of natural convection driven flow of a non-newtonian power-law fluid in a trapezoidal enclosure with a u-shaped constructal. Energies **14**: 5355.

Chen, K., W. Liu, and J. Park, 2016 Modified models for love and their dynamical properties. Miskolc Mathematical Notes **17**: 119–132.

Erbaş, K. C., 2022 Determination of romantic relationship categories and investigatıon of their dynamical properties. Chaos Theory and Applications **4**: 37–44.

Goyal, M., A. Prakash, and S. Gupta, 2019 Numerical simulation for time-fractional nonlinear coupled dynamical model of romantic and interpersonal relationships. Pramana **92**: 1–12.

Hatfield, E., R. J. Sternberg, and M. L. Barnes, 1988 Passionate and companionate love. the psychology of love. Sternberg RJ & Barnes MSL .

Hazan, C. and P. Shaver, 2017 Romantic love conceptualized as an attachment process. In *Interpersonal Development*, pp. 283–296, Routledge.

Huang, L. and Y. Bae, 2018a Analysis of chaotic behavior in a novel extended love model considering positive and negative external environment. Entropy **20**: 365.

Huang, L. and Y. Bae, 2018b Chaotic dynamics of the fractional-love model with an external environment. Entropy **20**: 53.

Jafari, S., J. C. Sprott, and S. Golpayegani, 2016 Layla and majnun: a complex love story. Nonlinear Dynamics **83**: 615–622.

Kacar, S., Z. Wei, A. Akgul, and B. Aricioglu, 2018 A novel 4d chaotic system based on two degrees of freedom nonlinear mechanical system. Zeitschrift für Naturforschung A **73**: 595–607.

Koca, I. and N. Ozalp, 2014 On a fractional order nonlinear dynamic model of a triadic relationship. Journal: Journal of Advances in Mathematics **5**.

Kumar, P., V. S. Erturk, and M. Murillo-Arcila, 2021 A complex fractional mathematical modeling for the love story of layla and majnun. Chaos, Solitons & Fractals **150**: 111091.

Lee, J. A. *et al.*, 1988 Love-styles. The psychology of love pp. 38–67.

Liao, X. and J. Ran, 2007 Hopf bifurcation in love dynamical models with nonlinear couples and time delays. Chaos, Solitons & Fractals **31**: 853–865.

Liu, W. and K. Chen, 2015 Chaotic behavior in a new fractional-order love triangle system with competition. J. Appl. Anal. Comput **5**: 103–113.

Owolabi, K. M., 2019 Mathematical modelling and analysis of love dynamics: A fractional approach. Physica A: Statistical Mechanics and its Applications **525**: 849–865.

Ozalp, N. and I. Koca, 2012 A fractional order nonlinear dynamical model of interpersonal relationships. Advances in Difference Equations **2012**: 1–7.

Qureshi, Z. A., S. Bilal, U. Khan, A. Akgül, M. Sultana, *et al.*, 2022 Mathematical analysis about influence of lorentz force and interfacial nano layers on nanofluids flow through orthogonal porous surfaces with injection of swcnts. Alexandria Engineering Journal **61**: 12925–12941.

Richardson, M. J., R. Dale, and K. L. Marsh, 2014 Complex dynamical systems in social and personality psychology: Theory, modeling, and analysis. .

Rinaldi, S., 1998a Laura and petrarch: An intriguing case of cyclical love dynamics. SIAM Journal on Applied Mathematics **58**: 1205–1221.

Rinaldi, S., 1998b Love dynamics: The case of linear couples. Applied Mathematics and Computation **95**: 181–192.

Rinaldi, S. and F. Della Rossa, 2020 From individual traits to couple behavior. International Journal of Bifurcation and Chaos **30**: 2050219.

Rinaldi, S., F. Della Rossa, and P. Landi, 2013a A mathematical model of “gone with the wind”. Physica A: Statistical Mechanics and its Applications **392**: 3231–3239.

Rinaldi, S., P. Landi, and F. D. ROSSA, 2013b Small discoveries can have great consequences in love affairs: the case of beauty and the beast. International Journal of Bifurcation and Chaos **23**: 1330038.

Rinaldi, S., F. D. Rossa, and F. Dercole, 2010 Love and appeal in standard couples. International Journal of Bifurcation and Chaos **20**: 2443–2451.

Rubin, Z., 1970 Measurement of romantic love. Journal of personality and social psychology **16**: 265.

Shah, I. A., S. Bilal, A. Akgül, M. T. Tekin, T. Botmart, *et al.*, 2022 On analysis of magnetized viscous fluid flow in permeable channel with single wall carbon nano tubes dispersion by executing nano-layer approach. Alexandria Engineering Journal **61**: 11737–11751.

Shahzad, A., M. Imran, M. Tahir, S. A. Khan, A. Akgül, *et al.*, 2023 Brownian motion and thermophoretic diffusion impact on darcy-forchheimer flow of bioconvective micropolar nanofluid between double disks with cattaneo-christov heat flux. Alexandria Engineering Journal **62**: 1–15.

Sprott, J., 2004 Dynamical models of love. Nonlinear dynamics, psychology, and life sciences **8**: 303–314.

Sprott, J. C., 2010 *Elegant chaos: algebraically simple chaotic flows*. World Scientific.

Sternberg, R. J., 1986 A triangular theory of love. Psychological review **93**: 119.

Strogatz, S. H., 1988 Love affairs and differential equations. Mathematics Magazine **61**: 35–35.

Sunday, J., D. Zirra, and M. Mijinyawa, 2012 A computational approach to dynamical love model: The romeo and juliet scenario. International Journal of Pure and Applied Sciences and Technology **11**: 10.

Wang, X., Y. Feng, and Y. Chen, 2022 A new four-dimensional chaotic system and its circuit implementation. Frontiers in Physics p. 376.

Wauer, J., D. Schwarzer, G. Cai, and Y. Lin, 2007 Dynamical models of love with time-varying fluctuations. Applied Mathematics and Computation **188**: 1535–1548.

How to cite this article: Erbaş, K.C. Modeling Love with 4D Dynamical System. *Chaos Theory and Applications*, 4(3), 135-143, 2022.

e-ISSN: 2687-4539
RESEARCH ARTICLE
Vol.4 / **No.**3 / 2022 / **pp.**144-151
https://doi.org/10.51537/chaos.1183113

Dynamics of a Prey-Predator System with Harvesting Effect on Prey

Özlem Ak Gümüş *,1
*Adıyaman University, Faculty of Arts and Sciences, Department of Mathematics, 02040, Adıyaman, Türkiye.

ABSTRACT This article is about the dynamic nature of a prey-predator model exposed to the harvesting effect on prey. Firstly, the model's fixed points' existence and stability are determined, and then, the presence and direction of a Neimark-Sacker bifurcation are examined. By using the bifurcation theory, we show that the system experiences Neimark-Sacker bifurcation. The hybrid control strategy is handled to control the chaos caused by the Neimark-Sacker bifurcation. Additionally, some numerical simulations are given to validate the theoretical outcomes obtained.

KEYWORDS
Prey-Predator model
Fixed point
Stability
Harvesting
Bifurcation
Chaos control

INTRODUCTION

Basic models based on biological assumptions are used to better understand the behavior of populations. Lotka and Volterra (Lotka 1925; Volterra 1978) are pioneers in proposing a mathematical prey-predator model. In the interaction of the prey and the predator, both the prey and the predator develop various strategies to survive and adapt to their environment. The balance of nature is maintained by the continuity of the life of the species. Models are used as tools to learn about future numbers of species. Here, the analysis conducted by including the factors affecting the population in the model allows us to reach more realistic results. It is possible to have information about the dynamics of the population with model analysis depending on these factors.

The analysis of prey-predator models with the harvesting effect has an important place in dynamic systems. Since there is great interest in the use of bioeconomic models (Clark 1985; Clark and Clark 1990), the dynamic behaviors of harvesting populations are examined in many studies. At the same time, this factor is effective in controlling populations (Liu *et al.* 2008; Paul *et al.* 2021). In most cases, the goal is not only population control; but also getting a significant harvest gain from the population. If the harvest pushes the population to extinction, this process should be stopped for a certain period. It is possible to reach qualified conclusions about the dynamics of these models with stability, bifurcation analysis, presence of chaotic behaviors and chaos control (Elaydi 1996; Gümüş and Feckan 2021; Kuznetsov *et al.* 1998; Liu *et al.* 2008; Madhusudanan *et al.* 2014; Murray 2002; Peng *et al.* 2009; Robinson 1998).

In the literature, many continuous-time prey-predator models have been introduced to explain the complex relationships between species. However, in ecology, populations evolve in discrete time steps, as there is no overlap between successive generations. It is therefore benefical to use difference equations (Ak Gümüş 2014; Gümüş and Kose 2012; Gümüş *et al.* 2022b,c; Merdan and Gümüş 2012; Merdan *et al.* 2018) or discrete-time systems involving prey-predator models (Danca *et al.* 2019; Elsadany *et al.* 2012; Gümüş 2020; Liu and Xiao 2007; Rana 2015), host-parasitoid models (Gümüş 2015; Gümüş and Kangalgil 2015; Gümüs *et al.* 2020), epidemic models (Gümüş *et al.* 2022a, 2019), and also fractional models (Selvam *et al.* 2020; Singh *et al.* 2019).

In prey-predator population models, one can say that the prey population has a limiting influence on the population dynamics since the size of the predator population depends on the size of the prey population. The size of predator populations that do not catch sufficient numbers of prey decreases. Therefore, small numerical changes in the prey population can cause large changes in the dynamics of such models. To maintain a balanced life in prey-predator populations, the prey population must have an appropriate growth rate. The harvesting factor on the prey will affect the growth rate of the prey population. In this study, our aim is to investigate prey-predator dynamics by examining the effect of the harvest factor on the internal growth rate of the prey population. For this purpose, the prey population's growth rate is taken as the bifurcation parameter, and results are obtained about the long-term behavior of the population.

Manuscript received: 1 October 2022,
Revised: 16 November 2022,
Accepted: 17 November 2022.

[1] akgumus@adiyaman.edu.tr (**Corresponding Author**)

This paper examines a discrete-time prey-predator system that depicts interactions between two populations of non-overlapping generations that are affected by the harvesting effect.

$$\begin{aligned} x_{n+1} &= ax_n(1-x_n) - bx_ny_n - hx_n \\ y_{n+1} &= dx_ny_n \end{aligned} \tag{1}$$

where x_n and y_n denote the numbers of prey and predator in year (generation) n, respectively, and the parameters a, b, h, and d are all positive parameters. In this model, bx_n indicates the number of prey individuals ingested per unit area and per unit time by an individual predator, and dx_ny_n is the predator reaction. Here, a is the growth rate of the prey population which has a logistic growth rate, d is the growth rate of the predator population limited by the number of prey, and h is the harvesting rate, where $0 < h < 1$.

In a previous study (Danca *et al.* 2019), the dynamics of discrete-time prey-predator model (1) are presented without the harvesting effect. We explore the stability and bifurcation of the system (1) by incorporating the harvesting effect and observe the dynamics of the system. We refer to studies (Elaydi 1996; Liu and Xiao 2007; Din 2013) for some basic concepts that we have used throughout our paper.

The paper is arranged as follows: In Section 2, we present the existence and local asymptotic stability of fixed points of the system (1) in $\mathbb{R}^2_+$ with plots showing system behavior. In Section 3, the dynamics of system (1) which undergoes a Neimark-Sacker bifurcation are investigated by choosing a as a bifurcation parameter. The chaos emerging with the Neimark-Sacker bifurcation is controlled by a hybrid method. The dynamical characteristics of the system (1) are displayed via numerical simulations in the form of trajectories, bifurcation diagrams, and phase portraits. The last section provides a summary of the results.

THE EXISTENCE AND STABILITY OF FIXED POINTS OF SYSTEM (1)

The analyses of the system (1)'s fixed points' existence and local stability are presented in this section. First, let us examine the existence of all available fixed points of system (1). System (1) has a trivial (extinction) fixed point $E_0 = (0,0)$ for all positive parameters. If $a > h+1$, then, system (1) has an exclusion fixed point $E_1 = (\frac{a-h-1}{a}, 0)$.

If $a > \frac{d(h+1)}{d-1}$ such that $d > 1$, then $E^* = (\frac{1}{d}, \frac{ad-a-d-dh}{bd})$ is a unique coexistence fixed point of system (1).

Remark 1 *When $a < h+1$, the fixed point E_0 is locally asymptotically stable, and when $1 < d$ and $h+1 < a < \min(3-h, \frac{d(h+1)}{d-1})$, the fixed point E_1 is locally asymptotically stable. The magnitude of the eigenvalues of the Jacobian matrix determines the local stability conditions of the fixed points of discrete-time systems.*

- **The Local Stability of the Coexistence Fixed Point**

Let us investigate the locally asymptotic stability of the coexistence fixed point as follows:

$$E^* = (x^*, y^*) = (\frac{1}{d}, \frac{ad-a-d-dh}{bd}). \tag{2}$$

where $a > \frac{d(h+1)}{d-1}$, $d > 1$. The Jacobian matrix of system (1) assessed at E^* is

$$J_{E^*} = \begin{pmatrix} 1-\frac{a}{d} & \frac{-b}{d} \\ \frac{-a-d+ad-dh}{b} & 1 \end{pmatrix}$$

and the characteristic polynomial of the Jacobian matrix is

$$F(\lambda) = \lambda^2 + [-2 + \frac{a}{d}]\lambda + a - \frac{2a}{d} - h.$$

So, we have the following Lemma.

Lemma 2 *Suppose that $a > \frac{d+dh+d^2h}{d-1}$, $d > 3$. Then the coexistence fixed point E^* is respectively locally asymptotically stable and unstable, if the following cases are provided:*

(i) *If $a < \frac{d(h+1)}{d-2}$, $h < \frac{1}{d^2-2d-1}$, then E^* is a sink point.*

(ii) *If $a > \frac{d(h+1)}{d-2}$, $h < \frac{1}{d^2-2d-1}$, then E^* is a source point.*

We can give examples to confirm the results obtained in Lemma 2. The trajectories and phase portrait of the prey-predator densities are exhibited in Figure 1 and Figure 2 with the parameter values $b = 0.2$, and $d = 3.5$ which are taken from a previous study (Danca *et al.* 2019).

Example 3 *Let us take into account the following population model to expose the appearance of the trajectories and phase portrait of system (1) for the parameter values $a = 2.33$, $b = 0.2$, $d = 3.5$, and $h = 0.002$:*

$$\begin{aligned} x_{n+1} &= 2.33x_n(1-x_n) - 0.2x_ny_n - 0.002x_n, \\ y_{n+1} &= 3.5x_ny_n \end{aligned} \tag{3}$$

where the initial conditions are $x_0 = 0.5$ and $y_0 = 2.5$.

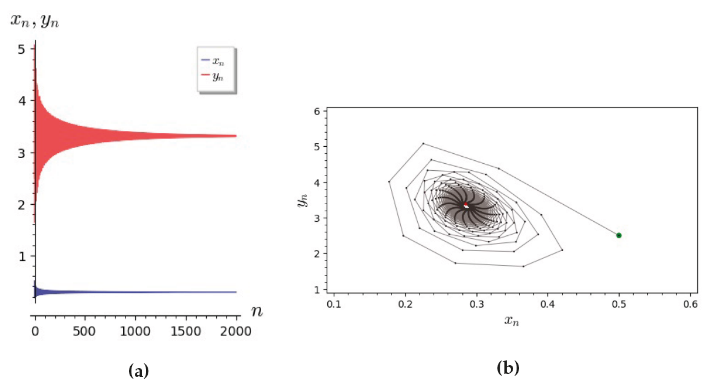

Figure 1 **(a)** *The trajectories of the prey and predator densities in system (3) when $a = 2.33, b = 0.2, h = 0.002$, and $d = 3.5$.* **(b)** *The phase portrait of system (3) when $a = 2.33$, $b = 0.2$, $h = 0.002$ and $d = 3.5$.*

In this example, it is seen that the fixed point $(0.285714, 3.31143)$ is locally asymptotically stable (see Lemma 2-(i)).

Example 4 *Let us take into account the following population model to expose the appearance of the trajectories and phase portrait of system (1) for $a = 2.34$, $b = 0.2$, $h = 0.002$ and $d = 3.5$:*

$$\begin{aligned} x_{n+1} &= 2.34x_n(1-x_n) - 0.2x_ny_n - 0.002x_n, \\ y_{n+1} &= 3.5x_ny_n \end{aligned} \tag{4}$$

where the initial conditions are $x_0 = 0.5$ and $y_0 = 2.5$.

The fixed point $(0.285714, 3.34714)$ of system (4) with the selected values is unstable (see the Lemma 2-(ii)).

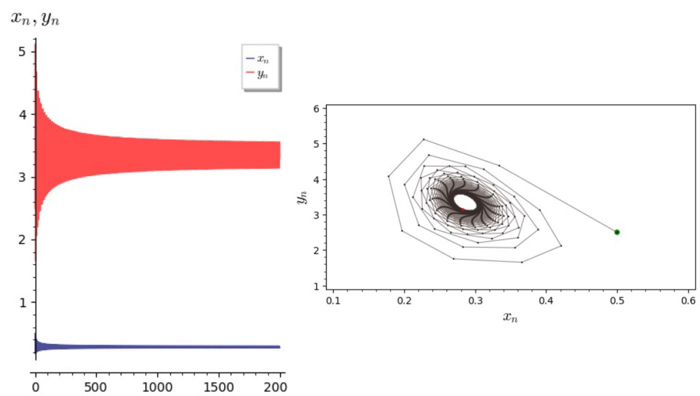

(a) **(b)**

Figure 2 **(a)** *The trajectories of the prey and predator densities in system (4) when* $a = 2.34$, $b = 0.2$, $h = 0.002$, *and* $d = 3.5$. **(b)** *The phase portrait of system (4) when* $a = 2.34$, $b = 0.2$, $h = 0.002$ *and* $d = 3.5$.

NEIMARK-SACKER BIFURCATION ANALYSIS AND CHAOS CONTROL

- **Neimark-Sacker Bifurcation**

In this section, we discuss whether system (1) experiences a Neimark-Sacker bifurcation by using the bifurcation theory (Kuznetsov *et al.* 1998; Wiggins 2003).As the prey population's growth rate changes, we see that system (1) has a Neimark-Sacker bifurcation. In other words, a is taken as a bifurcation parameter to get the conditions of Neimark–Sacker bifurcations. The direction of the Neimark–Sacker bifurcation is also obtained for system (1). If system (1) ensures the eigenvalue assignment, transversality and nonresonance conditions, then the Neimark–Sacker bifurcation emerges at a bifurcation point a_{NS}. The conditions that cause the bifurcation to occur at the coexistence fixed point E^* are determined as

$$NSB_{E^*} = \{a, b, h, d \in \mathbb{R}_+ : d > 3,\ a_1 < a < a_2 \text{ and } a = a_{NS}\}$$

where

$$a_1 = -2\sqrt{d^4 - 2d^3 - d^2h} + 2(-d + d^2),$$

$$a_2 = +2\sqrt{d^4 - 2d^3 - d^2h} + 2(-d + d^2),$$

$$h < -2\sqrt{\frac{(-1+d)^2 d[-1 + (-2+d)d^2]}{(1+d)^4}} + \frac{-1 + d[1 + 2(-2+d)d]}{(1+d)^2},$$

and

$$a_{NS} = \frac{d(1+h)}{d-2}.$$

By using the transformation $u = x - \frac{1}{d}$, $v = y - \frac{ad-a-d-dh}{bd}$, the fixed point E^* is shifted to the origin. So, we obtain

$$\begin{pmatrix} u \\ v \end{pmatrix} \to J_{E^*} \begin{pmatrix} u \\ v \end{pmatrix} + \begin{pmatrix} F_1(u,v) \\ F_2(u,v) \end{pmatrix}. \tag{5}$$

where

$$F_1(u,v) = -au^2 - buv + O(\|U\|^3) \tag{6}$$

$$F_2(u,v) = duv + O(\|U\|^3) \tag{7}$$

such that $U = (u,v)^T$. From here, system (1) becomes

$$(U_{n+1}) \to J_{E^*}(U_n) + \frac{1}{2}B(u_n, u_n) + \frac{1}{6}C(u_n, u_n, u_n) + O(\|U_n\|^4), \tag{8}$$

with the multilinear vector functions of $u, v, w \in \mathbb{R}^2$:

$$B(u,v) = \begin{pmatrix} B_1(u,v) \\ B_2(u,v) \end{pmatrix}$$

and

$$C(u,v,w) = \begin{pmatrix} C_1(u,v,w) \\ C_2(u,v,w) \end{pmatrix}.$$

These vectors are stated by

$$B_1(u,v) = \sum_{j,k=1}^{2} \frac{\partial^2 F_1}{\partial\xi_j \partial\xi_k}\Big|_{\xi=0} u_j v_k = -2au_1v_1 - b(u_2v_1 + u_1v_2)$$

$$B_2(u,v) = \sum_{j,k=1}^{2} \frac{\partial^2 F_2}{\partial\xi_j \partial\xi_k}\Big|_{\xi=0} u_j v_k = d(u_2v_1 + u_1v_2)$$

$$C_1(u,v,w) = \sum_{j,k=1}^{2} \frac{\partial^3 F_1}{\partial\xi_j \partial\xi_k \xi_l}\Big|_{\xi=0} u_j v_k w_l = 0$$

$$C_2(u,v,w) = \sum_{j,k=1}^{2} \frac{\partial^3 F_2}{\partial\xi_j \partial\xi_k \xi_l}\Big|_{\xi=0} u_j v_k w_l = 0.$$

For $a = a_{NS}$, the eigenvalues of the matrix J_{E^*} associated with the linearization in map (5) are conjugate complex numbers. These eigenvaues are

$$\lambda, \overline{\lambda}\,\Big|_{a=a_{NS}} = \frac{-5 + 2d - h \pm i\sqrt{(1+h)(-9+4d-h)}}{2(d-2)}$$

such that

$$|\lambda(a_{NS})| = 1.$$

For $a \in NSB_{E^*}$, we get

$$\frac{\partial\,|\lambda_i(a)|}{\partial a}\Big|_{a=a_{NS}} \neq 0\ ,\ i = 1, 2. \tag{9}$$

Moreover, if

$$trJ(a)\,\Big|_{a=a_{NS}} \neq 0, -1, \tag{10}$$

then, we reach

$$\lambda^k(a_{NS}) \neq 1\ ,\ k = 1, 2, 3, 4. \tag{11}$$

Let $q, p \in \mathbb{C}^2$ be the eigenvectors which correspond to the eigenvalues λ of $J(NSB_{E^*})$ and the eigenvalues $\overline{\lambda}$ of $J(NSB_{E^*})^T$, respectively. If these eigenvectors are computed with the Mathematica program, then we get

$$q \sim \left(\frac{-b(h+1) + ib\sqrt{(-9+4d-h)(h+1)}}{2d(h+1)}, 1\right)^T$$

and

$$p \sim \left(\frac{d(h+1) - id\sqrt{(-9+4d-h)(h+1)}}{2b(d-2)}, 1 \right)^T.$$

By using the inner product in $\mathbb{C}^2 : < p, q >= \overline{p_1}q_1 + \overline{p_2}q_2$, we get the following vector to normalize p in accordance with q

$$p \sim \left(\frac{d^2(1+h)}{bdi\sqrt{(-9+4d-h)(h+1)}}, \frac{2(d-2)}{-9+4d-h+i\sqrt{(-9+4d-h)(h+1)}} \right)^T$$

where $< p, q >= 1$. $\forall\, U \in \mathbb{R}^2$ can be uniquely represented for some z as

$$U = zq + \overline{zq} \tag{12}$$

Here, $\bar{z}$ denotes the conjugate of the complex number z, and $z =< p, U >$. For all sufficiently small $|a|$ about a_{NS}, we can convert system (1) as follows:

$$z \to \lambda(a)z + g(z, \bar{z}, a), \tag{13}$$

where $\lambda(a) = (1 + \omega(a))e^{i\theta(a)}$ for $\omega(a_{NS}) = 0$, and $g(z, \bar{z}, a)$ is a smooth function of z and $\bar{z}$. The Taylor expression of g with respect to $g(z, \bar{z})$ is

$$g(z, \bar{z}, a) = \sum_{k+l \geq 2} \frac{1}{k!l!} g_{kl}(a) z^k \bar{z}^l, \tag{14}$$

and the Taylor coefficients g_{kl} calculated through multilinear vector functions are expressed by the formulae

$$g_{20}(a_{NS}) =< p, B(q, q) >$$
$$g_{11}(a_{NS}) =< p, B(q, \bar{q}) >$$
$$g_{02}(a_{NS}) =< p, B(\bar{q}, \bar{q}) >$$
$$g_{21}(a_{NS}) =< p, C(q, q, \bar{q}) > .$$

For system (5) which exhibits the Neimark-Sacker bifurcation, the coefficient $\varphi(a_{NS})$ determining the direction of the appearance of the invariant curve can be calculated as:

$$\varphi(a_{NS}) = Re\left(\frac{e^{-i\theta(a_{NS})} g_{21}}{2}\right) - Re\left(\frac{(1 - 2e^{i\theta(a_{NS})})e^{-2i\theta(a_{NS})}}{2(1 - e^{i\theta(a_{NS})})} g_{20} g_{11} \right) \tag{15}$$
$$-\frac{1}{2}|g_{11}|^2 - \frac{1}{4}|g_{02}|^2$$

where $e^{i\theta(a_{NS})} = \lambda(a_{NS})$. As a result, we get the following theorem regarding the Neimark-Sacker bifurcation:

Theorem 5 *If (10) holds, $\varphi(a_{NS}) \neq 0$ and the parameter a changes in the small vicinity of NSB_{E^*}, then system (1) experiences a Neimark-Sacker bifurcation at the only fixed point E^*. Moreover there is a unique attracting ($\varphi(a_{NS}) < 0$) or repelling (($\varphi(a_{NS}) > 0$)) invariant closed curve that bifurcates from E^*.*

Example 6 *Let us take into account the following system for the parameter values $b = 0.2$, $d = 3.5$, and $h = 0.002$,*

$$\begin{aligned} x_{n+1} &= 2.338x_n(1 - x_n) - 0.2x_n y_n - 0.002x_n, \\ y_{t+1} &= 3.5x_n y_n \end{aligned} \tag{16}$$

where $a_{NS} = 2.338$ is the Neimark-Sacker bifurcation point. The computation yields $(x^*, y^*) = (0.285714, 3.34)$, and the Jacobian matrix assessed at (x^*, y^*) is

$$J_{(x^*, y^*)} = \begin{pmatrix} 0.332 & -0.0571429 \\ 11.69 & 1 \end{pmatrix}.$$

The eigenvalues are $\lambda_{1,2} = 0.666 \pm 0.745952i$ such that $|\lambda_{1,2}| = 1$. Let $q, p \in \mathbb{C}^2$ be the complex eigenvectors corresponding to $\lambda_{1,2}$, respectively, $q \sim (-0.0285714 + 0.0638111i, 1)^T$ and $p \sim (5.845 - 13.0542i, 1)^T$. We get the vector $p \sim (-7.83563i, 0.5 - 0.223875i)^T$ by normalizing p according to q, such that $< p, q >= 1$. So, we obtain

$$\begin{aligned} g_{20}(a_{NS}) &= 2.338 + 1.31495i \\ g_{11}(a_{NS}) &= 2.238 + 1.09161i \\ g_{02}(a_{NS}) &= -2.538 + 0.868276i \\ g_{21}(a_{NS}) &= 0 \end{aligned}$$

where

$$\begin{aligned} F_1(u, v) &= -au^2 - buv + O(\|U\|^3) \\ F_2(u, v) &= duv + O(\|U\|^3) \end{aligned}$$

$$B(q, q) = \begin{pmatrix} 0.145029 - 0.323905i \\ -0.2 + 0.446678i \end{pmatrix}$$

$$C(q, q, q) = \begin{pmatrix} 0 \\ 0 \end{pmatrix}$$

$$C(q, q, \bar{q}) = \begin{pmatrix} 0 \\ 0 \end{pmatrix}$$

$$\begin{aligned} B_1(u, v) &= -4.676u_1v_1 - 0.2(u_2v_1 + u_1v_2) \\ B_2(u, v) &= 3.5(u_2v_1 + u_1v_2) \end{aligned}$$

$$\begin{aligned} C_1(u, v, w) &= 0 \\ C_2(u, v, w) &= 0. \end{aligned}$$

From (15), we get $\varphi(a_{NS}) = -3.57837 < 0$. Consequently, the Neimark-Sacker bifurcation emerges at $a_{NS} = 2.338$. The Figure 3 gives the bifurcation and phase portraits of system (16) with the initial conditions $x_0 = 0.5$ and $y_0 = 2.5$. Figure 3.(a) shows Neimark-Sacker bifurcation diagram of the system (16). The phase portraits of system (16) are presented in Figure 3.(b)-(d).

- **Chaos control**

For many researchers, the focus point is the control of chaos in dynamic systems. It is possible to avoid chaos with some chaos strategies applied to systems (Danca *et al.* 2019; Din *et al.* 2017; Gümüş and Feckan 2021; Gümüş *et al.* 2022b; Liu *et al.* 2008; Yuan and Yang 2015). We apply a controlling strategy based on the hybrid control feedback methodology to control the chaos in system (1).

As system (1) undergoes a Neimark-Sacker bifurcation at the fixed point (x^*, y^*), the corresponding controlled system can be handled as follows:

$$\begin{aligned} x_{n+1} &= \beta[ax_n(1 - x_n) - bx_n y_n - hx_n] + (1 - \beta)x_n \\ y_{n+1} &= \beta d x_n y_n + (1 - \beta)y_n \end{aligned} \tag{17}$$

where β is the control parameter for $0 < \beta < 1$. The Jacobian matrix of the controlled system (17) is provided by

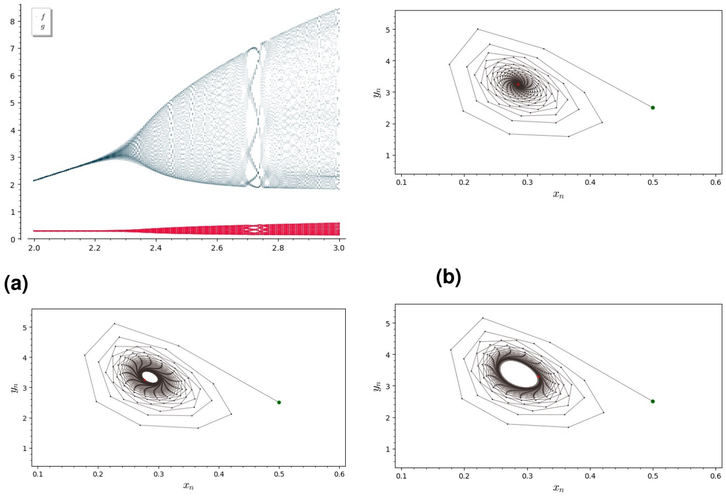

(a) **(b)** **(c)** **(d)**

Figure 3
(a) *Bifurcation diagram of the prey-predator system (16) with the parameter values* $a \in (2,3)$, $b = 0.2$, $d = 3.5$, and $h = 0,002$. **(b)** *The phase portrait of system (16) when* $a = 2.31, b = 0.2, d = 3.5$, and $h = 0,002$. **(c)** *The phase portrait of system (16) when* $a = 2.338, b = 0.2$, $d = 3.5$, and $h = 0,002$. ***(d)*** *The phase portrait of system (16) when* $a = 2.35, b = 0.2, d = 3.5$, and $h = 0,002$.

$$\begin{bmatrix} 1-\beta+(-h+a(1-x^*)-ax^*-by^*)\beta & -bx^*\beta \\ dy^*\beta & 1-\beta+dx^*\beta \end{bmatrix}.$$

If

$$\left|\frac{a\beta}{d}-2\right| < 1 + \frac{-a\beta(1+\beta)+d(1+(-1+a-h)\beta^2)}{d} < 2$$

is provided, then the positive fixed point (x^*, y^*) of the controlled system (17) is locally asymptotically stable.

Example 7 *We consider the parameters* $b = 0.2$, $d = 3.5$, $h = 0.002$, *and* $a = 2.35$ *for the initial conditions* $x_0 = 0.5$ *and* $y_0 = 2.5$. *For these parametric values, the controlled system is*

$$\begin{aligned} x_{n+1} &= \beta[2.35x_n(1-x_n)-0.2x_ny_n-hx_n]+(1-\beta)x_n \quad (18)\\ y_{n+1} &= 3.5\beta x_ny_n+(1-\beta)y_n \end{aligned}$$

and system (18) has a unique coexistence fixed point $(x^*, y^*) = (0.285714, 3.38286)$. *Additionally, the Jacobian matrix evaluated at* $(0.285714, 3.38286)$ *is*

$$\begin{bmatrix} 1-0.671429\beta & -0.0571429\beta \\ 11.84\beta & 1 \end{bmatrix} \quad (19)$$

and the characteristic equation (19) is obtained as

$$\lambda^2 + (-2+0.671429\beta)\lambda + 1 - 0.671429\beta + 0.676571\beta^2 = 0. \quad (20)$$

From the Jury condition, we conclude that if $0 < \beta < 0.9923991$, *then the roots of (20) lie in a unit open disk. Therefore, the Neimark-Sacker bifurcation is fully controlled for values* β *in the obtained range.*

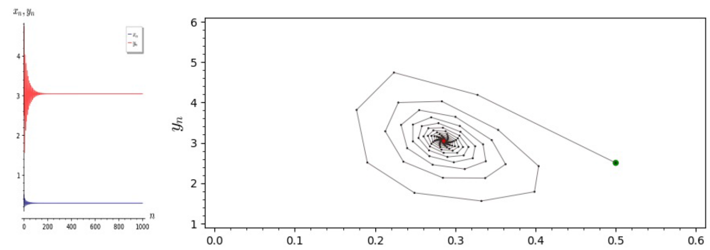

(a) **(b)**

Figure 4 **(a)** *The trajectories of the controlled system (18) for* $b = 0.2$, $d = 3.5$, *h=0.002*, $a = 2.35$, *and* $\beta = 0.9$. **(b)** *The phase portrait of the controlled system (18) for* $b = 0.2$, $d = 3.5$, *h=0.002*, $a = 2.35$, *and* $\beta = 0.9$.

CONCLUSION

Harvesting in a natural population is one of the most important concerns in population ecology. In this study, the dynamics of system (1) are investigated depending on the harvest effect applied to the prey population. We determine that system (1) has a trivial (extinction) fixed point E_0, an exclusion fixed point E_1, and a coexistence fixed point E^*. The stability conditions of extinction and exclusion fixed points are investigated. The stability and bifurcation conditions of the coexistence fixed point of system (1) are also obtained. To examine the Neimark-Sacker bifurcation, the growth rate of the prey population a is taken as a bifurcation parameter. The stabilization of the unstable fixed point of system (1) is provided by the hybrid control method. The hybrid control strategy allows us to successfully control the chaotic behavior by suppressing the unstable fixed point. The dynamic properties of system (1) are presented by the trajectories, phase portraits, and bifurcation diagram belonging to system (1) by means of SageMath (see Kapçak (2018)). Furthermore, diagrams presenting the dynamic behaviour of system (1) with and without the harvesting effect are included in Figure 5 and Figure 6. A comparison is provided by giving the bifurcation value obtained without the harvesting effect. These dynamic behaviours are applied to understand the difference caused by the harvesting effect. In the examples given, the system behaviour is examined by choosing the initial point close to the fixed point.

Without the harvesting effect while system (1) undergoes a Neimark-Sacker bifurcation for $a = \frac{d}{d-2}$, with the harvesting effect, it undergoes a Neimark-Sacker bifurcation for $a = \frac{d(1+h)}{d-2}$. For $h = 0.025$, the bifurcation values are $a = 2.88864$ and $a = 2.81818$ with and without the harvesting effect, respectively. With this effect, the system will continue to remain stable for a certain period. If h is taken as 0.002, the bifurcation point is obtained as $a = 2.82382$. The smaller the effect value, the shorter the equilibrium time of the system. In other word, as the harvesting effect value increases, the bifurcation of the system will be delayed. We conclude that the harvesting effect on the prey population delays the Neimark-Sacker bifurcation (see (Danca *et al.* 2019)). Thus, the population will remain in equilibrium for a while.

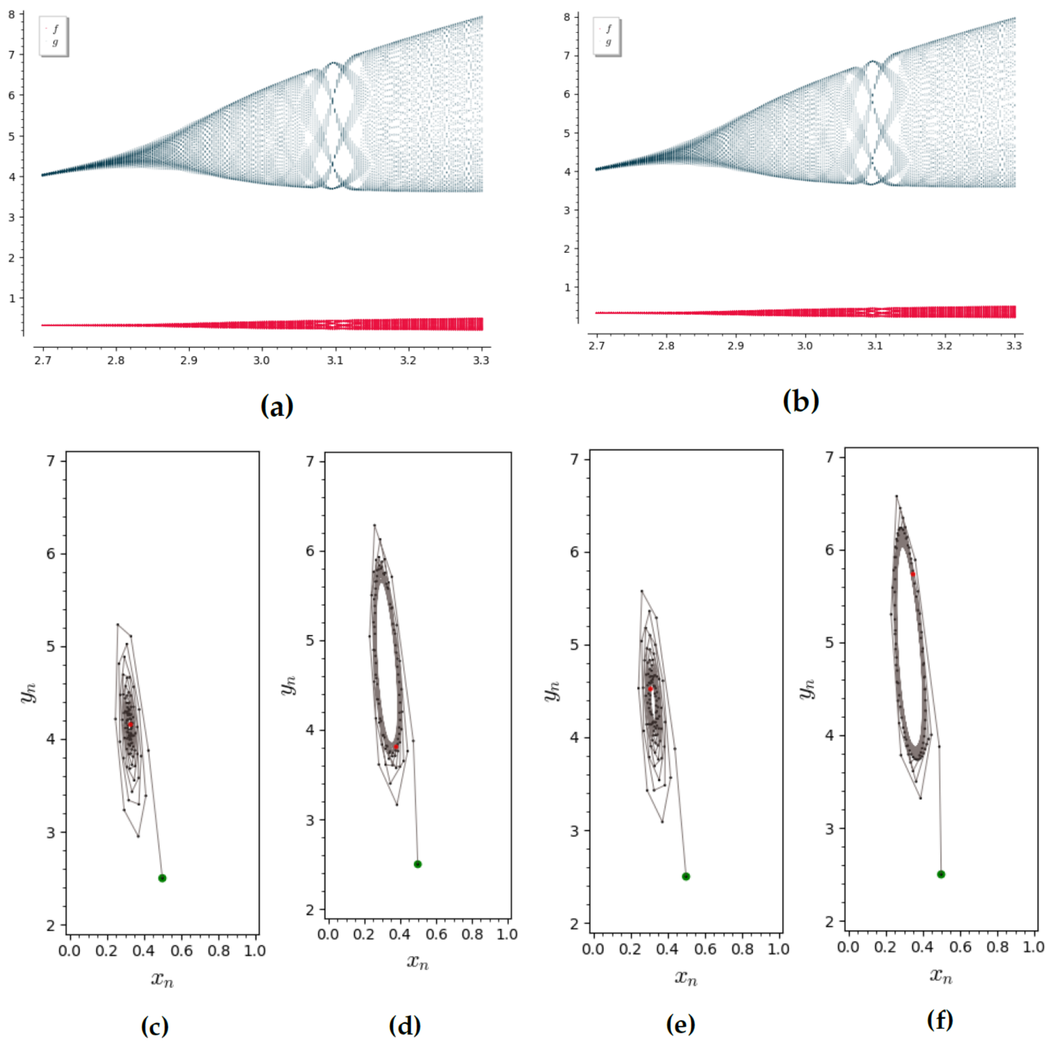

Figure 5
(a) *Bifurcation diagram of the prey-predator system (1) without the harvesting effect for the parameter values* $a \in (2.7, 3.3)$, $b = 0.2$, and $d = 3.1$. **(b)** *Bifurcation diagram of the prey-predator system (1) with the harvesting effect for* $a \in (2.7, 3.3)$, $b = 0.2$, $d = 3.1$ and $h = 0.020$. **(c)** *The phase portrait of system (1) without the harvesting effect for* $a = 2.7, b = 0.2$, and $d = 3.1$ **(d)** The phase portrait of system (1) without the harvesting effect for $a = 2.9, b = 0.2, d = 3.1$. **(e)** *The phase portrait of system (1) with the harvesting effect for* $a = 2.8, b = 0.2, d = 3.1$, and $h = 0.020$. **(f)** *The phase portrait of system (1) with the harvesting effect for* $a = 3, b = 0.2, d = 3.1$, and $h = 0.020$.

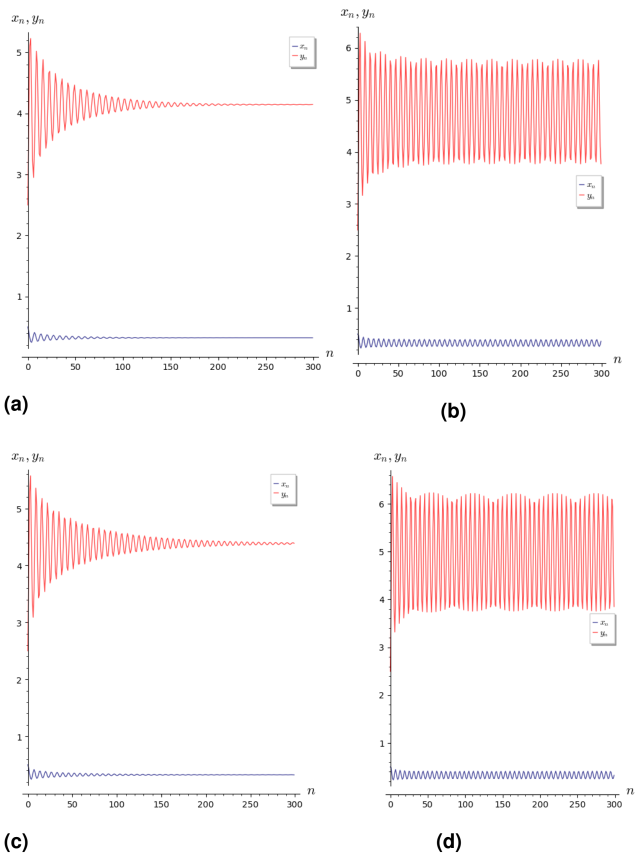

Figure 6
(a) *Time series diagram of system* (1) *without the harvesting effect for the parameter values* $a = 2.7$, $b = 0.2$, and $d = 3.1$. **(b)** Time series diagram of system (1) without the harvesting effect for the parameter values $a = 2.9$, $b = 0.2$, and $d = 3.1$. **(c)** Time series diagram of system (1) with the harvesting effect for the parameter values $a = 2.8$, $b = 0.2$, $d = 3.1$ and $h = 0.020$. **(d)** Time series diagram of system (1) with the harvesting effect for the parameter values $a = 3$, $b = 0.2$, $d = 3.1$and $h = 0.020$.

Conflicts of interest

The author declares that there is no conflict of interest regarding the publication of this paper.

Availability of data and material

Not applicable.

LITERATURE CITED

Ak Gümüş, Ö., 2014 Global and local stability analysis in a nonlinear discrete-time population model. Advances in Difference Equations **2014**: 1–9.

Clark, C., 1985 Bioeconomic modelling and fisheries management. wiley. New York .

Clark, C. and P. Clark, 1990 *Mathematical Bioeconomics: The Optimal Management of Renewable Resources*. Pure and Applied Mathematics: A Wiley Series of Texts, Monographs and Tracts, Wiley.

Danca, M.-F., M. Fečkan, N. Kuznetsov, and G. Chen, 2019 Rich dynamics and anticontrol of extinction in a prey–predator system. Nonlinear Dynamics **98**: 1421–1445.

Din, Q., 2013 Dynamics of a discrete lotka-volterra model. Advances in Difference Equations **2013**: 1–13.

Din, Q., Ö. A. Gümüş, and H. Khalil, 2017 Neimark-sacker bifurcation and chaotic behaviour of a modified host–parasitoid model. Zeitschrift für Naturforschung A **72**: 25–37.

Elaydi, S. N., 1996 An introduction to difference equations. Springer-Verlag, New York **10**: 978–1.

Elsadany, A.-E. A., H. El-Metwally, E. Elabbasy, and H. Agiza, 2012 Chaos and bifurcation of a nonlinear discrete prey-predator system. Computational Ecology and Software **2**: 169.

Gümüş, Ö. A., 2015 Dynamical conseqences and stability analysis of a new host parasitoid model. General Mathematics Notes **27**: 9–15.

Gümüş, Ö. A., 2020 Neimark-sacker bifurcation and stability of a prey-predator system. Miskolc Mathematical Notes **21**: 873–885.

Gümüş, Ö. A., Q. Cui, G. M. Selvam, and A. Vianny, 2022a Global stability and bifurcation analysis of a discrete time sir epidemic model. Miskolc Mathematical Notes **23**: 193–210.

Gümüş, Ö. A. and M. Feckan, 2021 Stability, neimark-sacker bifurcation and chaos control for a prey-predator system with harvesting effect on predator. Miskolc Mathematical Notes **22**: 663–679.

Gümüş, Ö. A. and F. Kangalgil, 2015 Allee effect and stability in discrete-time host-parasitoid model. Journal of Advanced Research in Applied Mathematics **7**: 94–99.

Gümüş, Ö. A. and H. Kose, 2012 Allee effect on a new delay population model and stability analysis. Journal of Pure and Applied Mathematics: Advances and Applications **7**: 21–31.

Gümüs, Ö. A., A. Maria Selvam, and R. Janagaraj, 2020 Stability of modified host-parasitoid model with allee effect. Applications and Applied Mathematics: An International Journal (AAM) **15**: 20.

Gümüş, Ö. A., A. G. Selvam, and R. Dhineshbabu, 2022b Bifurcation analysis and chaos control of the population model with harvest. International Journal of Nonlinear Analysis and Applications **13**: 115–125.

Gümüş, Ö. A., A. G. M. Selvam, and D. A. Vianny, 2019 Bifurcation and stability analysis of a discrete time sir epidemic model with vaccination. International Journal of Analysis and Applications **17**: 809–820.

Gümüş, Ö. A., A. G. M. Selvam, and D. Vignesh, 2022c The effect of allee factor on a nonlinear delayed population model with harvesting. Journal of Science and Arts **22**: 159–176.

Kapçak, S., 2018 Discrete dynamical systems with sagemath. Electronic Journal of Mathematics & Technology **12**.

Kuznetsov, Y. A., I. A. Kuznetsov, and Y. Kuznetsov, 1998 *Elements of applied bifurcation theory*, volume 112. Springer.

Liu, C., Q. Zhang, Y. Zhang, and X. Duan, 2008 Bifurcation and control in a differential-algebraic harvested prey-predator model with stage structure for predator. International Journal of Bifurcation and Chaos **18**: 3159–3168.

Liu, X. and D. Xiao, 2007 Complex dynamic behaviors of a discrete-time predator–prey system. Chaos, Solitons & Fractals **32**: 80–94.

Lotka, A. J., 1925 *Elements of physical biology*. Williams & Wilkins.

Madhusudanan, V., A. K, S. Vijaya, and M. Gunasekaran, 2014 Complex effects in discrete time prey-predator model with harvesting on prey. The International Journal of Engineering and Science **3**: 01–05.

Merdan, H. and Ö. A. Gümüş, 2012 Stability analysis of a general discrete-time population model involving delay and allee effects. Applied Mathematics and Computation **219**: 1821–1832.

Merdan, H., O. A. Gumus, and G. Karahisarli, 2018 Global stability analysis of a general scalar difference equation. Discontinuity, Nonlinearity, and Complexity **7**: 225–232.

Murray, J. D., 2002 *Mathematical biology: I. An introduction*. Springer.
Paul, P., T. Kar, and E. Das, 2021 Reactivity in prey–predator models at equilibrium under selective harvesting efforts. The European Physical Journal Plus **136**: 1–30.
Peng, G., Y. Jiang, and C. Li, 2009 Bifurcations of a holling-type ii predator–prey system with constant rate harvesting. International Journal of Bifurcation and Chaos **19**: 2499–2514.
Rana, S. S., 2015 Bifurcation and complex dynamics of a discrete-time predator-prey system. Computational Ecology and software **5**: 187.
Robinson, C., 1998 *Dynamical systems: stability, symbolic dynamics, and chaos*. CRC press.
Selvam, A. G. M., R. Dhineshbabu, and O. A. Gumus, 2020 Stability and neimark-sacker bifurcation for a discrete system of one-scroll chaotic attractor with fractional order. In *Journal of Physics: Conference Series*, volume 1597, p. 012009, IOP Publishing.
Singh, A., A. A. Elsadany, and A. Elsonbaty, 2019 Complex dynamics of a discrete fractional-order leslie-gower predator-prey model. Mathematical Methods in the Applied Sciences **42**: 3992–4007.
Volterra, V., 1978 Variations and fluctuations in the numbers of coexisting animal species. In *The golden age of theoretical ecology: 1923–1940*, pp. 65–236, Springer.
Wiggins, S., 2003 *Introduction to Applied Nonlinear Dynamical Systems and Chaos*. Texts in Applied Mathematics, Springer New York.
Yuan, L.-G. and Q.-G. Yang, 2015 Bifurcation, invariant curve and hybrid control in a discrete-time predator–prey system. Applied Mathematical Modelling **39**: 2345–2362.

How to cite this article: Gümüş, Ö. A. Dynamics of a Prey-Predator System with Harvesting Effect on Prey. *Chaos Theory and Applications*, 4(3), 144-151, 2022.

CHAOS Theory and Applications in Applied Sciences and Engineering

e-ISSN: 2687-4539
RESEARCH ARTICLE
Vol.4 / No.3 / 2022 / pp.152-156
https://doi.org/10.51537/chaos.1168824

Numerical Analysis of Semiconductor Ring Lasers with Backscattering Coefficients Mismatch

Nasr Saeed [*,1], **Alain Francis Talla** [α,2], **Alhadji Abba Oumate** [β,3] and **Sifeu Takougang Kingni** [α,4]

[*]Department of Physics, College of Education, Nyala University, P.O. Box: 155, Nyala, Sudan, [α]Department of Mechanical Petroleum and Gas Engineering, National advanced school of Mines and Petroleum Industries, University of Maroua, P.O. Box 46, Maroua, Cameroon, [β]Department of Physics, Faculty of Science, University of Maroua, P.O. Box 814, Maroua, Cameroon.

ABSTRACT The numerical analysis of a semiconductor ring laser (SRL) by using the basic two-mode model and a parameter mismatch in the backscattering coefficients is presented in this paper to account for the asymmetry along the ring. The operation of SRL is discovered to be affected by changing the conservative backscattering parameter for a fixed value of the dissipative backscattering parameter, and the bidirectional regime with alternating oscillation can be suppressed. The numerical results of this paper and the experimental results of the literature depicts a good correspondence.

KEYWORDS
Semiconductor ring laser
Parameter Mismatch
Backscattering parameter
Oscillations

INTRODUCTION

Semiconductor ring lasers are particularly well suited for monolithic integration because, unlike integrated lasers of the Fabry-Perot type, they do not require cleaved facets or gratings to provide the essential optical feedback (M. Sorel and Donati 2002; M. Sorel and Laybourn 2002; T. Krauss and Roberts 1990). Key elements of photonic integrated circuits are SRLs. Due to the active cavity's circular design, a SRL can function in either the clockwise (CW) or counterclockwise (CCW) directions (CCW). For applications such as wavelength filtering, multiplexing-demultiplexing, electrical and all-optical switching, and bistable optical memory, SRLs are potential possibilities (J. J. Liang and Ballantyne 1997). For the investigation of generalized rings and two-mode laser systems, many theoretical models with an emphasis on the interaction between two counter-propagating modes and their interaction with the active medium have been developed. The He-Ne ring laser (Menegozzi and Lamb 1973) and the CO2 laser (H. Zeghlache and Mello 1988) are the systems that have received the most attention, as they were able to take advantage of the rotation-induced asymmetry between the two counter-propagating modes.

In the case of two-mode semiconductor lasers, Etrich et al. (C. Etrich and Zeghlache 1992) have proposed a model based on the time evolution of the electric fields. They discussed how the two counter-propagating modes' interference caused a slowly fluctuating carrier-induced grating that had an impact on how the device operated. In other studies, the formation of intensity oscillations brought on by mode-to-mode phase-coupling is highlighted (R. C. Neelen and Woerdman 1992; P. Mandel and Otsuka 1993; P. A. Khandokhin and Mande 1995). A particular treatment was devised for the SRL by Sargent et al. (Sargent 1993) who derived a simple model for the intensities of the two modes starting from first principles, enlightening the importance of the self- and cross-gain saturation parameters. Later, Sorel et al. (M. Sorel and Donati 2002) proposed a model which takes into account self- and cross-gain saturation effects as in the work of Sargent (Sargent 1993) and includes backscattering contributions originating at the coupling to an output waveguide.

An oscillating bidirectional regime in SRLs was experimentally observed, and this model, which is based on two mean-field equations for the counter-propagating modes and a third rate equation for the carriers, has been successful in explaining this finding. By studying optical switching has been found to be helpful as well (T. Perez and Mirasso 2007) However, as shown by the experimental data, it has not been able to explain the discrepancy in the intensities of the two counter-propagating modes observed in the bidirectional continuous wave (bi-cw) and bidirectional with alternate oscillations (bi-AO) regimes (M. Sorel and Donati 2002; M. Sorel and Donat 2003).

Manuscript received: 31 August 2022,
Revised: 14 October 2022,
Accepted: 15 October 2022.

[1] nasrsaeed19@yahoo.com
[2] alainfrancis.aft@gmail.com (**Corresponding Author**)
[3] oumatealhadji.ao@gmail.com
[4] stkingni@gmail.com

In addition some of the experiments made in SRLs (M. Sorel and Laybourn 2002) showed that applying a current bias on the output waveguide contacts affects the laser operation and unidirectional mode can be achieved. To the best of our knowledge, there is not yet a numerical explanation of the above mentioned experimental results. This paper shows that parameter mismatch in the backscattering coefficients explains the experimental results. The remainder of the paper is as follows. Section 2 presents the rate equations of SRLs and the results obtained during the numerical investigation of SRLs under the backscattering coefficients mismatch .Section 3 concludes the paper.

RATE EQUATIONS OF SRLS AND RESULTS

Due to the fact that the two-mode model has represented SRLs as gyroscopes (Numa 2000) and accounted for the noticed alternating oscillation regime in the light-intensity (L-I) characteristics of the SRL (M. Sorel and Donati 2002). So the model used in this paper is built on the fundamental two-mode model but has a mismatched parameter in the dissipative $k_d{}'$ and conservative $k_c{}'$ backscattering coefficients. The ideal symmetry along the ring is actually never achieved in a real system for a variety of reasons, including flaws in the waveguide, output coupler, and scattering centers [1]. The sum of the two counter-propagating waves can be used to represent the overall electric field inside the ring cavity in the single longitudinal mode operation: $E'(x,t) = E_1{}' \mathrm{e}^{-\mathrm{i}(!_0 \mathrm{t} - \mathrm{kx})} + E_2{}' \mathrm{e}^{-\mathrm{i}(!_0 \mathrm{t} - \mathrm{kx})} + \mathrm{cc}$ where $E_1{}'$ and $E_2{}'$ are the mean-field slowly varying complex amplitudes of the electric field associated with the two propagation directions, i.e., mode 1 is CCW and mode 2 is CW; x is the longitudinal spatial coordinate along the ring circumference, assumed positive in the CCW direction and ω_0 is the optical frequency of the selected longitudinal mode. The rate equations are given by (M. Sorel and Donati 2002; M. Sorel and Donat 2003; L. Gelens and Danckaer 2009; S. T. Kingni and Danckaert 2012; S. T. Kingni and Orou 2020).

$$
\begin{aligned}
\frac{dE_1{}'}{dt'} &= (1+i\alpha)[G_n(N-N_0)(1-\varepsilon_s)|E_1{}'|^2 - \varepsilon_c|E_2{}'|^2 - \frac{1}{\tau_p}]E'_1 \\
&- k'_1 E'_1 \qquad (1a) \\
\frac{dE_2{}'}{dt'} &= (1+i\alpha)[G_n(N-N_0)(1-\varepsilon_s)|E_2{}'|^2 - \varepsilon_c|E_1{}'|^2 - \frac{1}{\tau_p}]E'_2 \\
&- k'_1 E'_2 \qquad (1b) \\
\frac{dN}{dt'} &= \frac{J}{el} - \frac{N}{\tau_s} - G_n(N-N_0)(1-\varepsilon_s|E_1{}'|^2 - \varepsilon_c|E_2{}'|^2) \\
&- G_n(N-N_0)(1-\varepsilon_s|E_2{}'|^2 - \varepsilon_c|E_1{}'|^2)\,. \qquad (1c)
\end{aligned}
$$

where $E_{1,2}$ the fields, $N(t)$ the carrier density, α denotes the linewidth enhancement factor accounting for phase-amplitude coupling in the semiconductor medium, G_n the modal gain factor for the two modes, which depending on the semiconductor gain factor, N_0 the carrier density at transparency, ε_s and ε_c are self-and cross-gain saturation coefficients, respectively and τ_p the photon lifetime in the ring cavity. The parameters $k'_{1,2} = k'_{d_1,d_2} + ik'_{c_1,c_2}$ are the complex backscattering coefficient where k'_{d_1,d_2} the parameters and k'_{c_1,c_2} represent the dissipative and conservative components of backscattering respectively. The parameter J, e, l, τ_s represent the injected ring current density, the electron charge, the active layer thickness and the carrier lifetime, respectively. A suitable normalization of equations (1a) to (1c) leads to the following dimensionless form (M. Sorel and Donati 2002):

$$
\begin{aligned}
\frac{dE_1}{dt} &= (1+i\alpha)\left[n\left(1-s|E_1|^2 - c|E_2|^2\right) - 1\right]E_1 \\
&- (k_{d1} + ik_{c1})\,E_2 \qquad (2a) \\
\frac{dE_2}{dt} &= (1+i\alpha)\left[n\left(1-s|E_2|^2 - c|E_1|^2\right) - 1\right]E_2 \\
&- (k_{d2} + ik_{c2})\,E_1 \qquad (2b) \\
\frac{dn}{dt} &= \gamma(\mu - n\left(1-s|E_1|^2 - c|E_2|^2\right)|E_1|^2 \\
&- n\left(1-s|E_2|^2 - c|E_1|^2\right)|E_2|^2)\,. \qquad (2c)
\end{aligned}
$$

with the following rescalings:

$$
\begin{aligned}
& t = \tfrac{t'}{\tau_p};\;\; E_1 = (G_n\tau_p)^{\frac{1}{2}} E'_{1,2};\;\; n = G_n(N-N_0)\,\tau_p; \\
& s = \tfrac{\varepsilon_s}{G_n\tau_s};\;\; c = \tfrac{\varepsilon_c}{G_n\tau_s};\;\; \gamma = \tfrac{\tau_p}{\tau_s} \qquad (3) \\
& k_{d1,2} = \tau_p k'_{d1,2};\;\; k_{c1,2} = \tau_p k'_{c1,2}; \\
& J_0 = \tfrac{el}{\tau_s}N_0;\;\; J_{th} = \tfrac{el}{\tau_s}\left(N_0 + \tfrac{1}{G_n\tau_p}\right);\;\; \mu = \tfrac{J-J_0}{J_{th}-J_0}\,.
\end{aligned}
$$

SRL is numerically analyzed by integrating the set of equations (2a) to (2c) with similar values of parameters to those of (M. Sorel and Donati 2002), but assuming that the backscattering coefficients are varied following the general rule: $k_{c_1,d_1} = k_{c_2,d_2} + \sigma_{c,d}$ or $k_{c_2,d_2} = k_{c_1,d_1} + \sigma_{c,d}$ where the values of the backscattering parameters coincide with those used in (M. Sorel and Donati 2002) and $\sigma_{c,d}$ are the mismatch parameters k_{c_2,d_2} or k_{c_1,d_1} in the conservative and dissipative backscattering coefficients, respectively. The authors of (Kenmogne *et al.* 2022, 2021) present the bifurcation diagrams which depict the local maxima of the trajectories of the systems under investigation. While, Figures 1,2,4,5 and 6 are the amplitude curves which present the global maxima of the trajectories of the sets equations (2a) to (2c). Figure 1 illustrates the L-I curves of both modes by using numerical simulation of sets equations (2a) to (2c) obtained for $k_{d_1} = k_{d_2} = 3.27 \times 10^{-4}$; $k_{c_2} = 4.4 \times 10^{-2}$; $\sigma_c = 10^{-3}$ and $k_{c_1} = k_{c_2} + \sigma_c$.

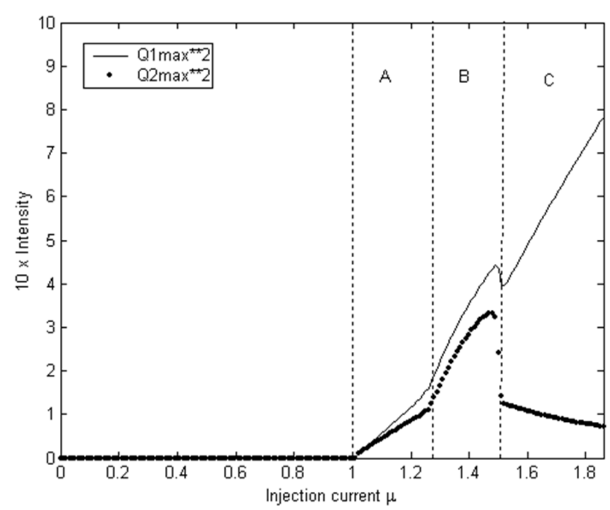

Figure 1 L–I curve for $\alpha = 3.5$, $s = 5 \times 10^{-3}$, $c = 10^{-2}$, $\gamma = 2 \times 10^{-3}$, $k_{d_1} = k_{d_2} = 3.27 \times 10^{-4}$, $k_{c_2} = 4.4 \times 10^{-2}$, $\sigma_c = 10^{-3}$ and $k_{c_1} = k_{c_2} + \sigma$.

When the injection currentμ is increased, Figure 1 exhibits bi-cw (regime A), bi-A0 (regime B) and unidirectional (regime C). Figure 1 shows that $|E_1|^2$ is a bit larger than $|E_2|^2$ in bi-cw and bi-AO regimes as the revealed experimental results of Figure 2.a of (M. Sorel and Donati 2002) whereas in Fig. 2.b of (M. Sorel and Donati 2002) without taking into account the parameter mismatch in the backscattering coefficients, the two modes have the same intensities in regimes A and B. The threshold current in Fig. 2.b of (M. Sorel and Donati 2002) ($\mu_{th} = 1.0$) is equal to the one of Fig. 1 This means that parameter mismatch in the conservative backscattering coefficient does not affect the threshold current in the model. So, one can note that Fig. 1 is more close to the experimental results (see Fig. 2.a of (M. Sorel and Donati 2002)) than Fig. 2.b of (M. Sorel and Donati 2002). Therefore, the mathematical model with parameters mismatch used here is the most indicated way to explain the SRL behaviour. Assuming now $k_{c_2} = k_{c_1} + \sigma$ and $\sigma_c = 10^{-3}$ Figure 2 presents three distinct operating regimes and the same threshold current ($\mu_{th} = 1.0$) as in Fig. 1 but the intensity of CW mode is a bit larger than the intensity of CCW mode.

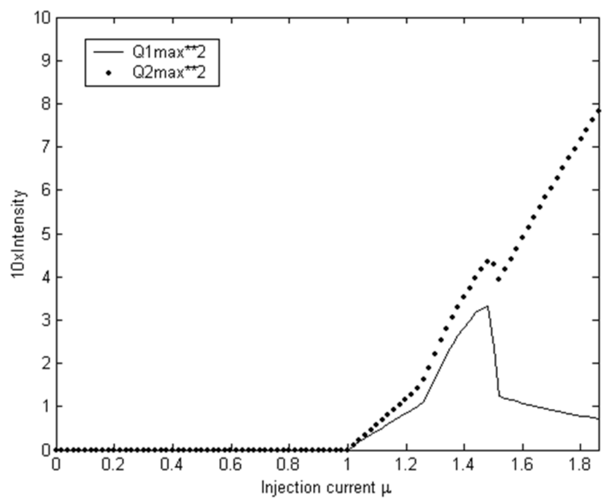

Figure 2 L–I curve for $\alpha = 3.5, s = 5 \times 10^{-3}, c = 10^{-2}, \gamma = 2 \times 10^{-3}, k_{d_1} = k_{d_2} = 3.27 \times 10^{-4}, k_{c_2} = 4.4 \times 10^{-2}, \sigma_c = 10^{-3}$ and $k_{c_2} = k_{c_1} + \sigma_c$.

From Figure 2, one can remark a selection between the two modes according to whether the corresponding mode of is larger or not. The implications of the ring lasing direction when the output waveguide contacts are forward biased, as seen in Figure 3 , are discussed in (M. Sorel and Laybourn 2002), which clarifies this behavior.

According to (M. Sorel and Laybourn 2002) applying bias current I_{W_1} on port 1 larger than 30 mA, the CCW mode is completely suppressed by the increased power sent back into the ring, which also directs the unidirectional laser output to port 2, i.e., on CW mode. This can be seen in Figure 5 of (M. Sorel and Laybourn 2002) , which reports CW power for increasing ring current and for two different bias current values I_{W_1}. Figure 4 presents the L-I curves of both modesobtained for $k_{c_2} = k_{c_1} + \sigma_c$ in order to have the CW mode as a dominating mode.

The numerical findings of this paper and the experimental results of (M. Sorel and Laybourn 2002) are in good accord in Figure 4. To complete this comparison, the L- I curves of both modes are plotted by using the same parameters values as in Fig. 4.

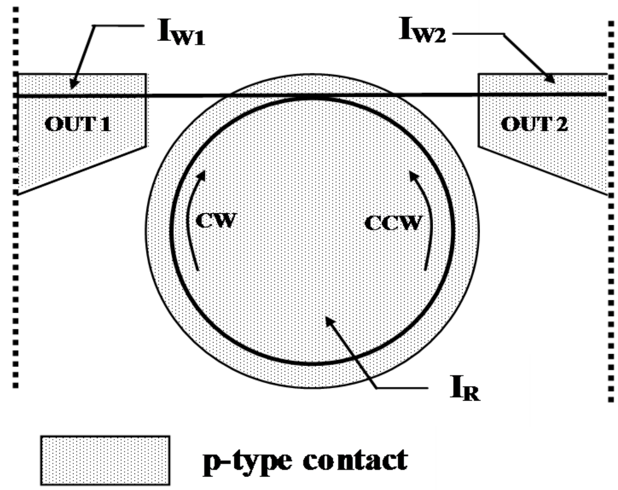

Figure 3 Geometry of ring laser illustrating the layout contact: I_R, I_{W_1}, I_{W_2} indicate the current biases applied to the ring and to the two output waveguide contacts, respectively .

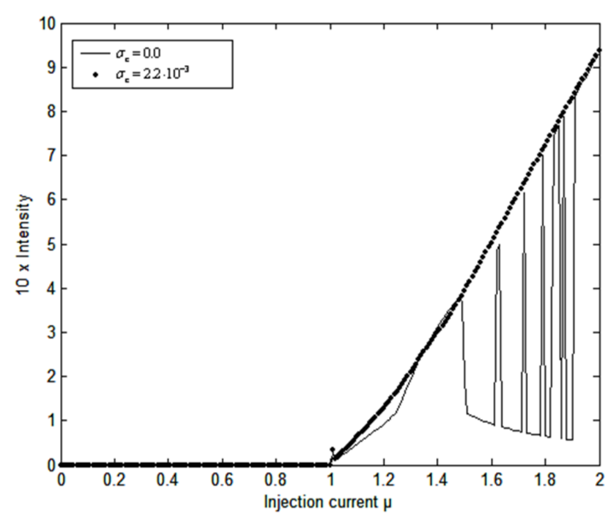

Figure 4 L- I curve of CW mode for $\alpha = 3.5, s = 5 \times 10^{-3}$, $c = 10^{-2}, \gamma = 2 \times 10^{-3}, k_{d_1} = k_{d_2} = 3.27 \times 10^{-4}, k_{c_2} = 4.4 \times 10^{-2}$, and $k_{c_2} = k_{c_1} + \sigma_c$. $\sigma_c = 0$ (solid line) and $\sigma_c = 2.2 \times 10^{-3}$ (dashed line).

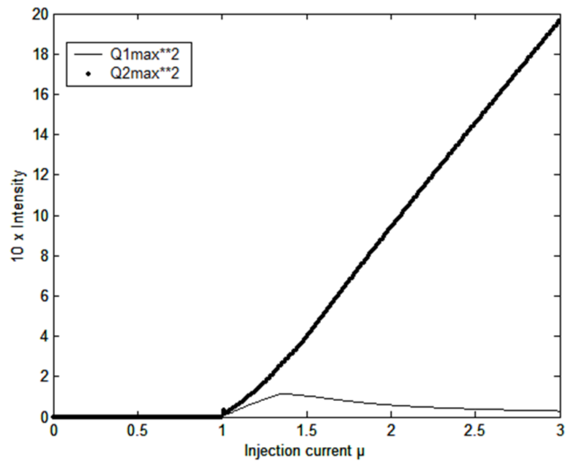

Figure 5 L- I curve of both modes. Parameters values of Figure 4 are conserved.

Figure 5 reveals that for high shift between the two conservative backscattering coefficients, the laser operates only in unidirectional regime. The existing mode is the one having the higher value of conservative backscattering parameters. Fig. 5 also illustrates a good correspondence with the experimental results of Sorel et al. (M. Sorel and Laybourn 2002). Therefore we can note that the experimental correspondence of conservative backscattering parameters $(k_{c_{1,c_2}})$ can be the current biases applied to the two output waveguide contacts (I_{W_1,W_2}). The higher value of conservative backscattering coefficient of a mode corresponds to lower current bias applied to one of the two output waveguides. The disappearance (or death) of switching observed in Figs. 4 and 5 is sufficient to assert that $(k_{c_{1,c_2}})$ can be a control parameter for switching phenomenon.

For a fixed value of dissipative backscattering parameter $k_{d_1} = k_{d_2} = 3.27 \times 10^{-4}$, and when varying the conservative backscattering parameter according to $\sigma_c(k_{c_2} = 4.4 \times 10^{-2}$ and $k_{c_1} = k_{c_2} + \sigma$) it is found that the gap between ${Q_1}^2 = |E_1|^2$ and ${Q_2}^2 = |E_2|^2$ modes seen in bi-cw and bi-A0 regimes widens when σ_c is increased. We have also noted by increasing σ_c how the SRL acts to suppress the bi-A0 regime as shown Fig. 6.

In Figure 6, when σ_c is increased, the ${Q_{1,2}}^2 = |E_{1,2}|^2$ in bi-A0 regime narrows progressively. This reduction is due to the decrease of maximum values and the increase of minimum values of each mode simultaneously. In addition, the pump current (μ) interval for the bi-A0 shrinks (see Fig. 6.a to Fig. 6.c) when σ_c is increased and can definitely disappear (see Fig.6.d). Then, we have noted that by increasing σ_c the switching between the two modes is not suppressed, but it is observed just for high value of (μ). Now as the mismatch in the dissipative backscattering is concerned, we have found that using $(k_{c_1} = k_{c_2})$ and $k_{c_1} = k_{c_2} + \sigma$ there is no significant change in the SRL behaviour.

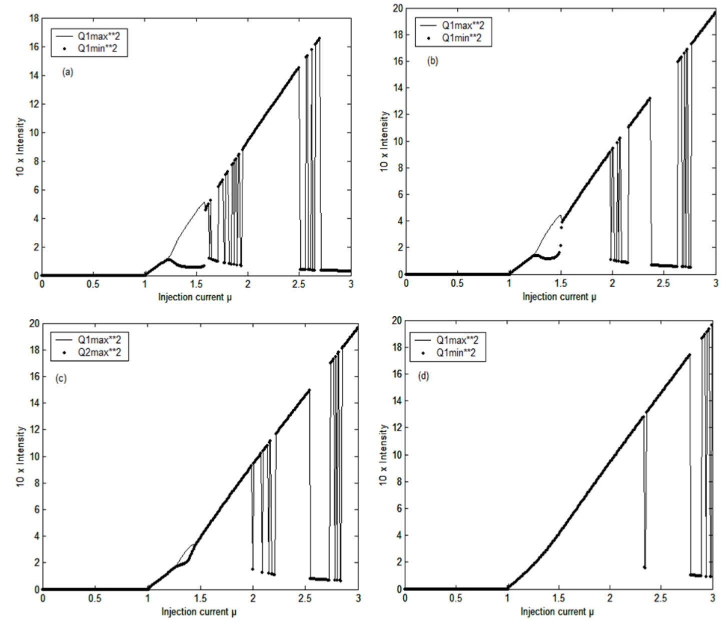

Figure 6 L- I curve of mode 1 displaying the effect of increasing σ_c on the bi-AO regime for $\alpha = 3.5$, $s = 5 \times 10^{-3}$, $c = 10^{-2}$, $\gamma = 10^{-3}$, $k_{d_1} = k_{d_2} = 3.27 \times 10^{-4}$, $k_{c_2} = 4.4 \times 10^{-2}$, $k_{c_2} = k_{c_1} + \sigma$. a) $\sigma_c = 0$; b) $\sigma_c = 10^{-3}$; c) $\sigma_c = 1.7 \times 10^{-3}$ and d) $\sigma_c = 3 \times 10^{-3}$

CONCLUSION

This paper was devoted to the numerical investigation of semiconductor ring laser based on the basic two-modes model with inclusion of a parameter mismatch in the dissipative and conservative backscattering parameters. By varying the conservative backscattering parameter, it was demonstrated that the pump interval for the bidirectional with alternate oscillationsregime shrinks and finally disappears for a given value of the dissipative backscattering parameter. While the difference between the intensities of the two counter-propagating modes were observed in the bidirectional continuous wave and bidirectional with alternate oscillations regimes grows. The mismatch in dissipative backscattering coefficient has no effect on the SRL behaviour. A good correspondence between our numerical resultsof this paper and the experimental results of Sorel et al. (M. Sorel and Donati 2002; M. Sorel and Laybourn 2002) is revealed.

Acknowledgments

S.T.K. is grateful to Professor Paul Woafo (University of Yaounde I, Cameroon) and Doctor Jimmy Hervé Talla Mbe (University of Dschang, Cameroon) for valuable discussions.

Conflicts of interest

The authors declare that there is no conflict of interest regarding the publication of this paper.

Availability of data and material

Not applicable.

LITERATURE CITED

C. Etrich, N. B. A., P. Mandel and H. Zeghlache, 1992 Dynamics of a two-mode semiconductor laser. IEEE J. Quantum Electron **28**: 811–821.

H. Zeghlache, N. B. A. L. M. H. G. L. L., P. Mandel and T. Mello, 1988 Bidirectional ring laser: Stability analysis and time-dependent solutions. Phys. Rev. A **37**: 470–497.

J. J. Liang, M. H. L., S. T. Lau and J. M. Ballantyne, 1997 Unidirectional operation of waveguide diode ring lasers. Appl. Phys. Lett. **70**: 1997–1997.

Kenmogne, F., S. Noubissie, G. B. Ndombou, E. T. Tebue, A. V. Sonna, *et al.*, 2021 Dynamics of two models of driven extended jerk oscillators: Chaotic pulse generations and application in engineering. Chaos, Solitons & Fractals **152**: 111291.

Kenmogne, F., M. L. Wokwenmendam, H. Simo, A. D. Adile, P. M. A. Noah, *et al.*, 2022 Effects of damping on the dynamics of an electromechanical system consisting of mechanical network of discontinuous coupled system oscillators with irrational nonlinearities: Application to sand sieves. Chaos, Solitons & Fractals **156**: 111805.

L. Gelens, S. B., G. Van Der Sande and J. Danckaer, 2009 Phase-space approach to directional switching in semiconductor ring lasers. Phys. Rev. E **79**: 016213.

M. Sorel, A. S. R. M. J. P. R. L., G. Giuliani and S. Donat, 2003 Operating regimes of GaAs-AlGaAs semiconductor ring lasers: experiment and model. IEEE J. Quantum Electron. **39**: 1187–1195.

M. Sorel, A. S. S. B. G. G. R. M., P. J. R. Laybourn and S. Donati, 2002 Alternate oscillations in semiconductor ring lasers. Opt. Lett. **27**: 1992–1994.

M. Sorel, S. D., G. Giuliani and P. J. R. Laybourn, 2002 Unidirectional bistability in semiconductor waveguide ring lasers. Appl. Phys. Lett. **80**: 3051–3053.

Menegozzi, L. N. and W. E. Lamb, 1973 Theory of a Ring Laser. Phys. Rev. A **8**: 2103–2125.

Numa, T., 2000 Analysis of signal voltage in a semiconductor ring laser gyro. IEEE J. Quantum Electron. **36**: 1161–1167.

P. A. Khandokhin, I. K., I. V. Koryukin and P. Mande, 1995 Influence of carrier diffusion on the dynamics of a two-mode laser. IEEE J. Quantum Electron. **31**: 647–652.

P. Mandel, C. E. and K. Otsuka, 1993 Laser rate equations with phase sensitive interactions. IEEE J. Quantum Electron. **29**: 836–843.

R. C. Neelen, D. B., M. P. Van Exter and J. P. Woerdman, 1992 Mode competition in a semiconductor ring laser. J. Mod. Opt. **39**: 1623–821.

S. T. Kingni, L. G. T. E., G. Van der Sande and J. Danckaert, 2012 Direct modulation of semiconductor ring lasers: numerical and asymptotic analysis. JOSA B **29**: 1983–1992.

S. T. Kingni, V. V. T., C. Ainamon and B. C. Orou, 2020 Directly modulated semiconductor ring lasers: Chaos synchronization and applications to cryptography communications. Chaos Theory and Applications **2**: 31–39.

Sargent, M., 1993 Theory of a multimode quasi-equilibrium semiconductor laser. Phys. Rev. A **48**: 717–726.

T. Krauss, P. J. R. L. and J. S. Roberts, 1990 CW operation of semiconductor ring lasers Electron. Appl. Phys. Lett. **26**: 2095–2097.

T. Perez, G. V. d. S. P. C., A. Sciré and C. R. Mirasso, 2007 Bistability and all-optical switching in semiconductor ring lasers. Opt. Express **15**: 12941–12948.

How to cite this article: Saeed, N., Talla, A. F., Oumate, A. A., and Kingni, S. T. Numerical Analysis of Semiconductor Ring Lasers with Backscattering Coefficients Mismatch. *Chaos Theory and Applications*, 4(3), 152-156, 2022.

e-ISSN: 2687-4539
RESEARCH ARTICLE
Vol.4 / No.3 / 2022 / pp.157-168
https://doi.org/10.51537/chaos.1199241

Blockchain-based Cryptocurrency Price Prediction with Chaos Theory, Onchain Analysis, Sentiment Analysis and Fundamental-Technical Analysis

Akif Akgul[*,1], **Eyyüp Ensari Şahin**[β,2] **and Fatma Yıldız Şenol**[β,3]
[*]Department of Computer Engineering, Faculty of Engineering, Hitit University, 19030, Çorum, Türkiye, [β]Department of Banking and Finance, Faculty of Economics and Administrative Sciences, Hitit University, Çorum, Türkiye.

ABSTRACT Crypto assets succeeded in making their name known to large masses with Bitcoin, which emerged as a result of the creation of the first genesis block in 2008. Until 2010, the aforementioned recognition showed itself mostly in areas such as games, but over time it managed to enter the portfolios of individual investors. Especially as of end of 2017, the rapid increases in monetary value quickly attracted the attention of corporate companies and then the (Central Banks). These assets have created different alternatives (also know as altcoins) by working and have managed to become one of the important financial instruments today. This study has examined in detail the techniques (Chaos theory, Onchain analysis and Sentiment analysis) developed on the price predictions of crypto assets, which are very important in terms of the number and quality of investors. In the study, findings were obtained that new techniques such as onchain and sentiment are more prominent in estimating crypto asset prices compared to traditional asset price estimation methods of crypto assets and that these techniques can make consistent estimations.

KEYWORDS
Blockchain
Cryptocurrency
Chaos theory
Onchain analysis
Sentiment analysis

INTRODUCTION

Blockchain is a revolutionary technology that allows transactions to be conducted without the need for intermediaries in peer-to-peer transfer. First mentioned in Satoshi Nakamoto's (2008) article "Bitcoin: A Peer-to-Peer Electronic Cash System", this system has the ability to perform financial/non-financial transactions on a decentralized infrastructure. The basic premise of the system initiated from Stuart Haber and W. Scott Stornetta's idea of presenting digital documents with a time stamp, which prevents these documents from being changed, while allowing for a computationally useful solution (AJ and Vanstone 1990). It has become known for its structure that can reliably organize different processes without a systems tool and without the need for a central authority, as well as through Bitcoin, a cryptocurrency that has affected the whole world. The production of Bitcoin started with the creation of the first block and currently has reached a weight that can be considered important in the portfolio of investors with its alternatives approaching 18000.

Cryptocurrencies are new currencies and are also among the popular investment tools. There are many questions about this type of money, which is newly included in the financial system, as they are decentralized and are separated from the conventional monetary system by their nature. Since cryptocurrencies are freely shaped according to supply and demand in the market, one of the most curious subjects in literature has been their value; what will they be and how they will be shaped. There are many studies and methods for determining the future price of a security in traditional financial markets. However after a brief introduction to the research topic in the first part, the second part includes a literature review, followed by a basic and technical analysis, the studies on chaos theory, onchain analysis, and sentiment analysis.

Hacinliyan and Kandiran (2015) investigated the possible fractal behaviors in the Istanbul Stock Exchange indices within the scope of chaos theory. To observe whether there were any chaotic and fractal behaviors, Higuchi and Katz methods were used to analyze the monofractal behavior of the selected indices while the Transformed Width (R/S) and Adjusted Fluctuation (DFA) ana-

Manuscript received: 4 November 2022,
Revised: 27 November 2022,
Accepted: 29 November 2022.

[1] akifakgul@hitit.edu.tr
[2] eyupensarisahin@hitit.edu.tr (**Corresponding Author**)
[3] fatmayildizsenol@gmail.com

lyzes were used to examine the chaotic behavior. As a result, it was concluded that there is chaotic behavior in the relevant indices.

Alpar and Özge (2016) used the data between 1988-2004 in order to prove the existence of chaos theory in the stock market. Using the Lyapunov exponential model, the result was found to be 18. The time series analysis showed that the stock market is chaotic the direction of price movements can be predicted as the 2 days before and 4 days after repeated each other. Biswas *et al.* (2018) has defined the chaos theory for the sciences and gave information about the detection and management of chaos for the related sciences. In these areas, the boundaries of chaos theory were drawn and relevant literature studies were included.

Abraham *et al.* (2018) collected Twitter and Google trend data to analyse the Etherum and Bitcoin price changes. Sentiment analysis of VADER (Valence Aware Dictionary For Sentiment Reasoning) was used to analyze the collected data. This method was chosen in the study because VADER analysis provided several benefits, including not only classifying text as positive, negative, or neutral, but also measuring the density of words used. The sentiment of tweets was not included as it was said not to be a reliable indicator when crypto currency prices were falling. Tweet volume was taken into account. Both Google Trends and tweet volumes were found to be highly correlated with price. In addition, the correlation held during periods of increasing and decreasing prices shows that the relationship is robust against periods with high variance and non-linearity. Direct one-to-one comparisons were made using a linear model, as the input variables followed the same nonlinear trends as the response. As a result, it was shown that it is partly due to work done at a time when cryptocurrency prices were always rising. Additionally, Twitter sentiment regarding cryptocurrencies tended to be positive regardless of the future price changes. A positive correlation was also observed by the author between Google searches and the value of cryptocurrencies, and the price changes in the relevant cryptocurrencies were followed, and it was concluded that it was indeed compatible with the model created.

In order to comprehend the temporal link between variables, Cortez *et al.* (2018) concentrated on the pricing of mineral commodities and used econometric techniques, machine learning, and chaos theory-based techniques. They concluded that while Gaussian and stochastic algorithms did not perform well enough, chaotic behavior may be seen when using machine learning techniques and methodologies based on chaos theory.

The study by Lahmiri and Bekiros (2018) focused on multiple fractalism and chaos theory in the Bitcoin market, where they investigated whether the prices followed the random law repetitively between the years 2010-2017. The Lyapunov exponent, Shannon entropy and generalized Hurst exponent models were applied and chaos, randomness and multi fractal stylized features of price and returns in the Bitcoin market were examined. As a result of the study, it was concluded that, contrary to returns, prices included and exhibited chaotic dynamics, but the prices did not repeat in a predictable way. It focused on three digital currencies namely Bitcoin, Digital Cash and Ripple. The analysis showed that all three tools have fractal dynamics, long memory and self-similarity.

By trying to predict Bitcoin and Litecoin prices two hours in advance, based on the sentiment expressed in the current Tweets, Jain *et al.* (2018) aimed to explore whether social factors can predict of cryptocurrency prices. Therefore, they used the Multiple Linear Regression (MLR) model to estimate a two-hour average price from the number of positive, neutral, and negative Tweets accumulated every two hours between March 1-11, 2018.

Bouri *et al.* (2019) examined the effect of herd behavior in the cryptocurrency market. As a result, strong evidence was found to support the existence of herd behavior in this market. The results of the logistic regression analysis, showed that the increase in uncertainty, the herd tendency also provides evidence for this.

To understand the relationship between Bitcoin and Etherum news and the price prediction, Vo *et al.* (2019) conducted an analysis based on the assumption that there is a relationship between the mood of the public and the cryptocurrency market, like traditional financial markets. Data were obtained using daily time series data from July 30, 2017 to October 5, 2018. For the sensitivity analysis, the news of the last 7 days were collected. An algorithm was created with a dictionary-based approach, with the thought of distinguishing the effect of the news about cryptocurrencies on the price movement, and with the thought that it can provide investors with a buying and selling advantage. They created a model that can directly predict the price direction by specifying whether to buy, sell or hold, and they concluded that the model they created correctly predicts the price movement in two cryptocurrencies.

Holiachenko *et al.* (2022) aimed to explain cryptocurrencies using fundamental and technical analysis. A technical analysis method was developed with different currencies in the same stock market in order to achieve maximum gain. In the conclusion part of the study, where many scenarios and graphics related to arbitrage were created, it was stated that the developed methodwas resistant to fluctuations in oil and gold prices.

Hudson and Urquhart (2021) conducted atechnical analysis of Bitcoin, Ethereum, Bitstamp and Litecoin in their study and although predictability continues in other cryptocurrency markets, it has been concluded that there is no predictability for Bitcoin in the out-of-sample period.

In order to test the validity of the efficient market hypothesis in the crypto money market, Kang *et al.* (2019) investigated the random walk theory. They concluded that among crypto exchanges established before November 2017, large exchanges are more likely to satisfy weak and semi-strong forms of market efficiency.

Pietrych *et al.* (2021) investigated the existence of chaos theory in cryptocurrencies. The nonlinearity and chaos in cryptocurrencies (Bitcoin, Ethereum, Ripple and Litecoin) were tested and concluded that these time series show strong evidence supporting the hypothesis that these time series come from an unknown production process that behaves nonlinearly and chaotically.

The effect of crypto money on the economy was analyzed by Yue *et al.* (2021) using a bibliometric analysis. Literature studies related to the subject were extensively covered. Bibliometric analysis aims to reveal previously unknown patterns by collecting a large number of relevant information in a specific area or a specific area of the subject. In this context, starting from the keywords in the literature, using the CiteSpace 5.7. the research outline of the economic effects of the study was created. Data obtained from the literature studies were clustered according to events that could affect the value of Bitcoin and its effects on the economy, and made available for analysis. the results obtained for direct economic effects are as follows:

1) While the impact of speculative trading on cryptocurrency differs in different studies, bitcoin price fluctuations will affect macroeconomic policy to some extent.

2) The hedging and safe-haven characteristics of cryptocurrencies continue to change over different periods of research. Some research finds that Bitcoin can act as a speculative asset.

3) External events such as the Covid pandemic can increase price fluctuations and improve the hedge effectiveness of cryp-

tocurrencies.

Another valuable result of the study is as follows: While computer science literature and interdisciplinary fields are concerned with the economic phenomenon caused by technologies, it has been concluded that previous researches are more concerned with economic results in economic fields.

Gözde (2021) examined sentiment analysis of Tweets posted as "Bitcoin" on Twitter. Orange Data Mining program was used for this. As a result; It has been observed that there is a predominant sense of joy about Bitcoin and investors feel happy when they buy Bitcoin.

Gurrib and Kamalov (2021) tried fluctuations in the crypto money market to be predicted by using sentiment analysis. It was determined that tweets about crypto money in a 3-week period were directly related to the market value of coins, and the model used in this study was determined to be critical. It is emphasized that it is a good model for predicting the value of pto money.

Jagannath *et al.* (2021) conducted an onchain analysis study in order not to predict Ethereum prices. It was chosen because it is Etherum, which is the most popular currency after Bitcoin, and because it uses an open network structure. In this paper, data has been collected from the public Ethereum blockchain and application programming interfaces (APIs) of online resources. In this study, the linear effect of each important Ethereum on-chain metric on price is examined using Pearson's and Spearman correlation coefficients. In addition, there is a model study for calculating the estimated price using machine learning models. The author's working comment on the result obtained is: An LSTM model was developed that uses three different self-adaptive methods to determine the best hyperparameter values to predict Ethereum price. Each self-adaptive technique was compared with each other and with a traditional LSTM model. In contrast, self-adaptive algorithm-based LSTM models provide a faster and more accurate price prediction for Ethereum.

Gu *et al.* (2022) tried to detect abnormal transaction amount in cryptocurrency exchanges with On-Chain analysis. In order to obtain the most important factors affecting the trading volume of different exchanges, a correlation analysis was performed and a model was developed to predict the effect of various factors on the trading volume. A case study of the detection results revealed that some abnormal transaction amounts were related to policy changes and industry events, while others were legal. He calculated the deviation between the estimated transaction amount and the actual transaction amount based on deep learning to provide a basis for the abnormal transaction amount detection.

El Montasser *et al.* (2022) calculated the closing prices of different cryptocurrencies in his study. The results of the authors who made balloon studies in terms of market size were interpreted by comparing them with the Covid 19 period. As a result of the study, a high correlation was found between the Covid 19 period and the crypto market. This indicates that the market activity behavior of major traded cryptocurrencies has changed strongly following the COVID-19 pandemic announcement.

We examine the efficiency of cryptocurrency markets by exploring how cryptocurrency bubbles and the COVID-19 pandemic affect market efficiency that changes over time. Our results show that the market activity behavior of major traded cryptocurrencies has changed strongly following the COVID-19 pandemic announcement. However, the results identified three cryptocurrency bubbles; End of 2017, beginning of 2018 and throughout July 2020. It is concluded that these decentralized finance bubbles have a lower impact on cryptocurrency market efficiency. The purpose of the study is mainly the effectiveness of cryptocurrencies and the existence of price bubbles.

Nie (2022) used a network method to identify critical events in the correlation dynamics of cryptocurrencies, taking networks around January 6, 2021 as an example to illustrate local and drastic changes in the correlation structure, helping to analyze the dynamics of the emerging market, the correlation structure in the cryptocurrency market. analyze its stability and fragility. The basic analysis in the network method used is: Using the influence power of the relevant cryptocurrency network (IS). The empirical analysis concluded that the market index showed large fluctuations near the critical event and that there was a correlation between the dynamics of the correlation matrix and the market conditions. In addition, he found a synchronization between changes in correlation and changes in network structure, and a positive correlation is observed

Wasiuzzaman *et al.* (2022) examined the performance of Islamic gold-backed cryptocurrencies during the 2020 bear market. Price data was collected for three Islamic gold-backed cryptocurrencies, OneGram, HelloGold and X8X, and traditional gold-backed cryptocurrency PaxGold. Bitcoin, the traditional fiat-backed cryptocurrency from December 2019 to November 2020. Analysis through ARMA-EGARCH models shows that returns for all cryptocurrencies were lower during the bear market, but only with the Islamic gold-backed cryptocurrency. It was concluded that volatility is higher for all five cryptocurrencies, but the impact of the bear market on volatility is significant only for traditional cryptocurrencies.

BLOCKCHAIN TECHNOLOGY

Blockchain is the infrastructure technology that forms the basis of the relevant subject for the trading of cryptocurrencies and the execution of smart contracts. This system, which was first mentioned in Satoshi Nakamoto's article named "Bitcoin: A Peer-to-Peer Electronic Cash System", has found a wide application area not only in cryptocurrencies, but also in the traditional financial system, allowing new application areas to be opened. Since Blockchain is known for Bitcoin, negative attitudes towards Bitcoin were initially considered within the Blockchain, but over time, this technology brought by Bitcoin began to receive the attention it deserved. However, the emergence of Blockchain dates back to the early 1990s, when Stuart Haber and W. Scott Stornetta first applied cryptographic techniques as an alternative way of storing digital documents and protecting against cyber attack. Blockchain brought; transparency, decentralization, verifiable and strong structure and started to be the center of attention and multifaceted academic reviews were realized. After examining its definition, functions and potential in general terms, the following definition emerged: Blockchain Technology not only processes monetary transactions, but can also enable transactions to comply with programmable rules in the form of "smart contracts" (Tschorsch and Scheuermann 2016). Thus, the ability of the parties to carry out their transactions freely without any trust problems played a leading role in the interest in digital systems.

Although blockchain is anonymous, decentralized, what makes it unique is that it cannot be hacked. Data is stored in a network on the blockchain. Computers working connected to a network called miner, bring together the processed data, archive it in accordance with encryption standards, and turn it into blocks. Transactions turn into a Hash algorithm as a summary function, and either a thousand-page text or a one-line 64-character cryptography information is encrypted with the encryption system for the relevant network (for example, Hash-256 in Bitcoin). That is, as input, the desired length of file data and etc. are. entered, but its output is called Hash or Digital Digest The information about the network participants, called "Node" is verified and added to the network.

Since each node is connected with the previous node, a change made in the related node causes a change in all other nodes. Since the core of the system is based on a decentralized and intermediary system, a ledger is required, for example for crypto money transfer or trading registration. In this system, the name of this notebook is "Ledger", which is responsible for keeping the necessary records transparently. It acts as an exceptionally secure intermediary between the sender and the receiver. Thanks to the e-signature, it assumes the function of confirming the amount sent by the sender to the recipient. In the digital world, transfer and registration transactions are more reliable thanks to this technology, compared to the type of fraud and insecurity, such as forged signature etc in real life. It is a database that is included and synchronized in the decentralized network (Sarmah 2018). Some of the areas where Blockchain is used are: Finance, Health, Logistics, Creation and storage of valuable documents and official documents, E-commerce, Tokens and cryptocurrencies, Insurance, Supply Chain. While many fields such as Games, Media, Real Estate and art collecting use it, research shows that Blockchain is used in the production and industry sector applications.

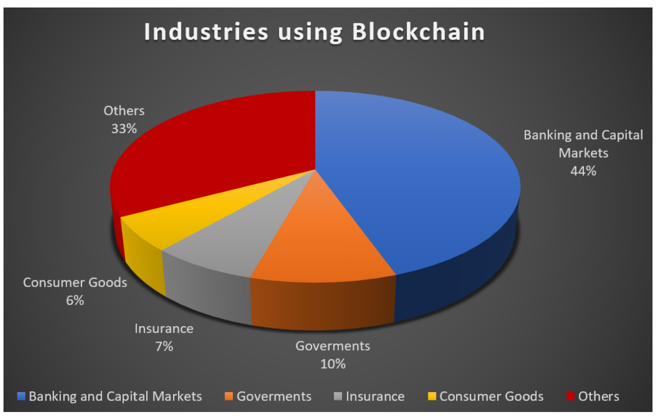

Figure 1 Blockchain usage area (Sarmah 2018)

Considering that the idea of decentralized digital money has just emerged with all this technology, when viewed chronologically, many steps are encountered in the way of creating digital money and the use of blockchain. In the first place, studies were made mostly on encryption and privacy, and with these encryption techniques that developed over time, the financial system and currency continued to develop with cryptographic and digitalization. The information obtained from the studies carried out are listed chronologically as follows:

In 1976, Diffie and Hellman published a paper and presented a method based on a secure exchange in an environment where there is no sense of trust by using private keys and cryptographic encryption techniques (Diffie and Hellman 2022).

An algorithm called RSA was proposed by Shamir, Rivest and Adleman in 1977. In this way, the RSA algorithm was developed in accordance with asymmetric encryption algorithms and e-signature, and authentication processes were developed. A system was developed to be used in secure key sharing operations (Yerlikaya 2006).

In 1980-1990, David Chaum developed a cryptographic encryption. In fact, there is quite a lot of work in this field. Although he first worked on encryption, the encryption system was not in demand because it was not sufficient in terms of mutual trust and confidentiality. He has also developed E-Cash, that is, electronic payment systems, and made innovations such as saving money or investing in the digital environment through the bank.

In 1995, DigiCash company created the first digital currency with e-Cash. In 1996, it introduced e-gold into the system. This system has received a lot of attention, because it allowed system users to open a gold account and then be able transfer this gold (Simsek *et al.* 2020). Then, he laid the foundations of the idea of creating an institution that can make money payments without an intermediary institution, called B-Money. Chaum, who is considered the inventor of digital money. It is known for his contribution to the system on privacy and cryptography. It was the first known proposal of a blockchain protocol. Dr. Chaum continued to develop the first digital currency, eCash, and made numerous contributions to secure voting systems in the 1990s. Today, Dr. Chaum Co-founded Elixxir and Praxxis networks, which combines decades of research and contributions in cryptography and privacy to deliver cutting-edge blockchain solutions.

- In 1999, the Napster program, which allows online and peer-to-peer file sharing, took its place on the market.
- In 2003, the Second Life game became one of the first stages of the transition to virtual currency and digital economy.
- In 2008, Satoshi Nakomato made a creative destruction in this process with his article describing the blockchain-based crypto currency that include all these systems announcing the creation of a decentralized and anonymous crypto currency without the need for a financial intermediary security-based transparent system has been outlined (Nakamoto 2008).

There is no government or banks in the system. A peer-to-peer transfer system has been created in a 24/7 open digital environment. Cryptocurrencies are created with a value whose rate is determined according to the supply and demand in the current system. The Prof of Work(POW) cryptography at the base of the system has solved two basic problems:

1) Problem with keeping records among network participants,
2) Resistance to cyber attack.

Before the emergence of Bitcoin, the function of transferring and preserving money could not be imagined without an intermediary institution, but after the emergence of Bitcoin, it was an important step to overcome the intermediary institution costs or transaction costs that were most criticized in the current financial system.

In this process starting from 2008, many different cryptocurrencies have emerged. There are cryptocurrencies, called Altcoin (Alternative Coin), that have the same production method as Bitcoin and exist on a completely different Blockchain network. These cryptocurrencies, whose number is about 2700, are based on smart contracts due to their organizational structure, and also include many corporate companies in its ecosystem (Şahin 2020). Although the system was created in 2008, it started to attract attention after 2015. At first it consisted of a crypto money given to the miners who contributed to the functioning of the system. Miners perform the most important task of the Blockchain system, for example, they approve the transfer process in a transfer transaction. The operations performed by the miners, who perform tasks such as adding a new Bitcoin to the system, solving the double-spending problem and posting unconfirmed Bitcoins, are as follows:

1) Announcing a new transaction to the entire network,
2) Collecting the node transaction to the relevant block,
3) Issuing a new block after each transaction,
4) Confirming the transactions made.

With each completed task, a new Bitcoin or cryptocurrency appears. According to the data of CoinMarketCap for 2022, there are over 12,954 cryptocurrencies, mainly Bitcoin, Ethereum, XRP, and Bitcoin Cash. According to literature, the ten most popular cryptocurrencies are Bitcoin, in particular, Etherum, Tether, Biancecoin, USDC, Binancecoin, USD, XRP, Cardano, Solana, Dogecoin.

Bitcoin is the most known and most invested in the world of crypto money. However, there are also Altcoins in the crypto money ecosystem. Altcoins were created right after Bitcoin became popular and its formation is clear. Altcoins that can be converted as alternative coins are essentially the name given to cryptocurrencies other than Bitcoin. The first Altcoin created was "Namecoin". The emergence of altcoins is used to eliminate the problems experienced during the formation of Bitcoin, for example, there is an intense energy consumption during the mining phase for the formation of Bitcoin and it is time-consuming. On the other hand, the "Proof of stake" system is used instead of the POW system. This system provides comparative advantage and speed. Although technically crypto investors often refer to low-value cryptocurrencies as Altcoins, which are easy to use and turn into cash faster, they are relatively more affordable than Bitcoin in mining equipment. The disadvantage is that they are very open to speculation. The most popular altcoins are Ethereum, XRP, Tether, Cardano, Polkadot, Stellar, Dogecoin, Chainlink, Uniswap.

METHODS USED FOR PRICE PREDICTION OF CRYPTO ASSETS

Fundamental-Technical Analysis

The analysis that investors basically use in their financial investments is fundamental and technical analysis. While fundamental analysis considers the macroeconomic trend, technical analysis is an analysis that helps predict future price movements of financial assets based on past price movements. The most widely used type of analysis is technical analysis, but whether it is possible to repeat past price movements in the future is a controversial issue. Both types of analysis contradict the Efficient Markets Hypothesis (EPH). The reason for this is the principle that no investor gets abnormal returns since all information is reflected in the prices (Malkiel 2003). With technical analysis, based on past price movements, current prices do not reflect the market.

Fundamental Analysis Various macroeconomic factors are brought together to try to predict the price of the security. The main goal is that the investor's security is overvalued? Is it low value? to seek answers to questions such as Fundamental analysis is examined in 3 groups as firm, sector and economic analysis. In economic analysis, the investor makes a general assessment of the current macroeconomic situation, examines the profitability of the firm during the expansion or contraction periods in the cyclical fluctuation of the economy and tries to predict the direction of the movement of the stock price. After the economic analysis, issues such as sector analysis, the competitive situation of the relevant company in the sector, how much the firm's sector will/will be affected during economic contraction and expansion periods are taken into consideration. After the economic and sector analysis, a firm analysis is made and the return of the stock of the relevant firm is calculated and expected.

The application of this analysis to the cryptocurrency market is to decide whether the price of an asset is higher or lower than its value, depending on how the intrinsic value of the asset is viewed. Fundamental analysis is done by looking at more objective indicators of the estimated value of the relevant crypto-asset, such as the usage density of the network, the activity status of the relevant network, or the business model and the roadmap (Lyashenko *et al.* 2021). Generally, the news and comments about crypto money are evaluated, and then if there are any, speculation or manipulation movements are tried to be detected. All information about the relevant crypto currency is tried to be collected. In order to calculate the returns of alternative investment instruments, domestic macroeconomic variables and investment instruments are also followed. However, using social media for this analysis will not generate correct results because of the possibility of fake accounts and manipulation. Therefore, fundamental analysis of cryptocurrency looks at 3 metrics: on-chain metrics, project metrics, and financial metrics.

To put it briefly:

- On-Chain Metrics, involves obtaining and looking at blockchain data. The node for the desired network is run and viewed by accessing the relevant information. However, since it is a time-consuming method, websites designed for this process are used for more practically. The network transaction count is also a good guide.
- Project Metric, where on-chain metrics relate to observable blockchain data, it includes a qualitative approach that looks at factors such as project metrics, team performance (if applicable), whitepaper, and upcoming roadmap.
- Financial Metrics are concerned with the value of the crypto asset in the relevant period, the price of which it was traded before. Interests can be useful in fundamental analysis. However, other metrics that might fall into this category include gathering information about the economics and incentives of the crypto-asset protocol. The importance of fundamental analysis in terms of cryptocurrencies helps us to determine the suspected values correctly, or to put it more clearly, to conduct a long-term value analysis for cryptocurrencies where there is doubt about buying and selling, or if there is investment hesitation.

Technical Analysis In technical analysis, the investor makes an investment decision with the price and volume information of the asset he wants to invest. Technical analysis defines it as the study of any market that uses price and volume information solely to predict future price movements and trends (Stevens 2002). The most widely used analysis tool for technical analysis is charts. Information is collected by using the graphics of the relevant financial asset. Trends and support and resistance points are also analyzed with the moving average method and various indicators. It is tried to make predictions about the future based on the price movements in the past. Dow theory forms the basis of technical analysis. To summarize this theory, the market consists of a cycle and all prices continue on a continuum. This event is like a tide event.Technical analysis is extremely helpful when reading charts in Cryptocurrencies. Some of these benefits are:

- A single graph reading gives information about an entire process.
- Even just reading charts on trading volume and prices can provide an understanding of the overall picture.
- It is tried to predict the direction of the market with the help of technical analysis.

- With Bitcoin technical analysis, the past and future of crypto money are followed.In general, movements in crypto currency exchanges occur downward, upward and horizontally.To summarize the usefulness of technical analysis in terms of cryptocurrencies, it helps about short-term price movements.

Chaos Theory

Chaos theory has been used in various branches of science to describe order within disorder. Its application in the field of economics was used by G.D.Cole while investigating the causes of the crisis, as well as of the Great Depression of 1929, with the view that nonlinear relations could be explained in the market under certainty conditions.

The most important contribution to chaos theory was by Lorenz during the preparation of the weather forecast report. Chaos theory is a sub-title of nonlinear systems. In the 19th and 20th centuries, it was called the 'butterfly effect' because the Lorenz Diagram is shaped like a Butterfly that popularizes this theory.

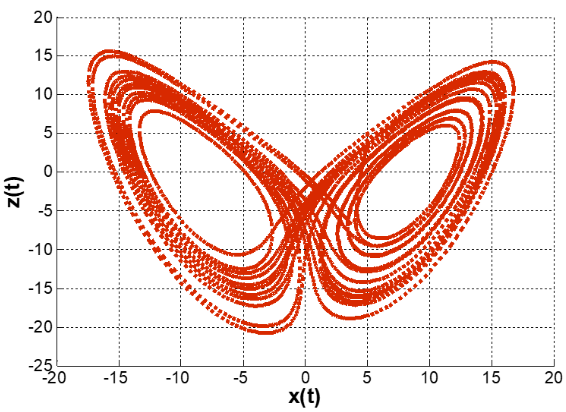

Figure 2 Lorenz chaotic system (x-z)

With the use of chaos theory in the economic sense, studies on, investor and decision-maker behaviors in stock markets and foreign exchange markets, foreign trade problems, crisis period cause-effect relations, hyperinflation periods and banks are the areas where nonlinear equations have also started. The financial application of nonlinear equations is the result of knowledge economy and some models have been developed within the scope of chaos theory. These models are: Logistics equation, One-dimensional discrete maps, High-order discrete maps, and continuous Time Models (Tosun 2006).

Chaos theory is not an induction or a mathematical method. In essence, it explains the tendency of the parts that make up the whole to form that whole separately. The reason for the interest in Chaos theory in economics stems from the fact that this theory can also offer a new perspective on system control strategies, which has some particularly interesting insights for economic policies (Faggini and Parziale 2012).

Chaotic behavior is used in a wide variety of scientific disciplines, including astronomy, biology, chemistry, ecology, engineering, and physics. In economic models, the chaotic existence and cause of the variable, which is tightly connected to the initial cause, is tried to be determined tightly, but it may be difficult to distinguish between random economic shocks and internal fluctuations. For this reason, some analyzes are made to investigate the compatibility with Chaos theory: Correlation, Lyapunov Test, and BDS Test (Klioutchnikov *et al.* 2017).

In order to investigate the chaos, randomness and multi-scale temporal correlation structure for the crypto money market, it is a suitable theory to measure the chaos in prices, the uncertainty in the returns during the high price period, or the change in the returns in the time period when the value decreases. However, when performing a chaos analysis for an econometric series, the basic question is if the fluctuation in the current variable from a stochastic system or if it comes from a deterministic, i.e. chaotic system. One of the most common approaches to answer these question is time series analysis The basic techniques used to measure chaotic systems in general are:

1) Lyapunov Exponent: It is the name given to the instruction that a signal follows along the phase space. It is a measure of the amount of separation between neighboring orbitals. It can measure the stability and instability of the chaotic system (Lv *et al.* 2022).

2) Dimensions (Fractal Dimension): The trend from unidentified disorder to identifiable order is proved with the help of fractal curves. Fractal structures can provide important information about the long-term and repetitive process of market behavior, since the parts are completely similar (Ural and Demireli 2009).

3) Unpredictability: Chaos theory sees the world not as a predictable mechanism, but as an open and flexible system. argues that we are never capable of reaching the initial conditions of necessary certainty related to the functioning of the physical world (Trigg and Yerci 1996).

4) Mixing and Feedback: The order formed in the chaos process shows commitment in a very short time and this is a kind of feedback.

5) Butterfly Effect (Dependence on Initial State): This concept emerged with Lorenz, and when considered for economics, it can be interpreted as that it is sensitive to the initial values for time series and subtle changes will affect the final shape and state of the whole structure (Su 2021).

The efficient market hypothesis, which is the most important theory in financial terms, states that the fluctuations in prices follow the normal distribution within the scope of the random walk feature and that a fair or efficient price will be formed in the market. However, in reality, the fluctuations in prices do not show a random walk feature and do not follow the normal distribution. As an explanation for this situation, the "Fractal Market Hypothesis" was developed. It highlights that the fractal feature can be seen in financial markets. Here, two important points are emphasized that are not included in the efficient market hypothesis: market liquidity and information (Erdoğan 2017).

Market liquidity consists of different opinions on the value of a security based on the trading transactions of investors with each other. In other words, one thinks that the value of the relevant security will increase, while the other thinks that the value of the related security will decrease. Because of the information they do not provide to each other, one party can gain because they reach the information before the other. The second factor, information, is that different values are attributed to the available information in different periods, since the periods in which the investors invest are different. Therefore, prices may consist of a short-term technical and long-term heuristic dimension. To express this differently, there is randomness in the short term and global determinism in the long term, which is related to the fractal dimension.

Fractalism has 3 basic dimensions: Power law, Self-similarity, and fixed scale. An object is fractal if it is similar to its smaller sized parts and is directly related to fractals. The fractal size of the object indicates the degree of similarity to itself. Fractal models are statistical and the standard deviation of the part is proportional to the standard deviation of the whole, giving meaningful results. In addition to being statistical, it is similar to itself, that is, to be expressed mathematically as the similarity seen in printing an image vertically and horizontally.

In the literature, Chaos theory is generally applied for time series to show whether the time series move randomly. Instead of "Efficient Market Hypothesis" and "Random Walk Model", which are basically the bedside theories of finance science, "chaos theorem" has begun to be accepted. Because with globalization, fluctuations in financial markets have started to be seen much more. In financial markets, the chaos theorem is against the efficient market hypothesis, and each investor and system has taken on a very chaotic structure. As can be seen in the studies in the literature review section, chaotic behaviors have been observed in the crypto money market, especially after 2010.

Onchain Analysis

Onchain analysis is the study of data stored in a blockchain network. In essence, it can be called a blockchain analysis. It is possible to see the entire data as all transactions are recorded on the Blockchain and cannot be changed. In this way, the thoughts and investment direction of all system users can be predicted. To a bitcoin Merchant, it gives another idea of where the price might go depending on the transaction patterns, the type of Bitcoin owner making the transaction, and where the coins might move. This analysis is similar to technical analysis but is more fundamental. The data used to make the relevant analysis can be broadly classified into three different categories:

1) Transaction Data (sending and receiving address, amount transferred, remaining value for a given address),

2) Block Data (time stamps, miner fees, rewards),

3) Smart contract code (i.e. business logic encoded on a blockchain).

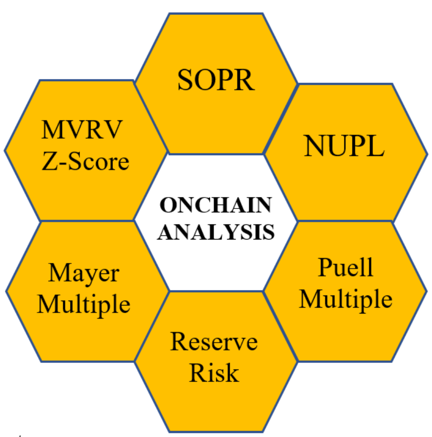

Figure 3 Onchain analysis indicators

Looking at its history, it dates back to 2011. By comparing the value of the network with the transaction volume recorded on the blockchain, it is possible to determine when a cryptocurrency is overvalued. For this, various ratios and indicators have been developed. In this way, market sentiment analysis is made, and the amount of traded /untraded crypto money or token can be determined because whales (people or organizations who own large amounts of crypto currency) sometimes pose a great danger for the crypto money world. Popularized by CoinMetrics, Chris Burniske and Jack Tatar developed the Network Value-to-Transaction (NVT) ratio in the summer of 2017 to measure the utility value of a cryptocurrency, specifically its transactional utility. It was one of the commonly used measures for cryptocurrencies. According to the NTV ratio if the network value is high, the NTV ratio decreases. Conversely, as the value of the network decreases, the NTV ratio increases. The explanation for this is that, if the network value is extremely low, it may indicate that a more substantial price is warranted given the trading volume.

The so-called UTXO (unspent transaction outputs) is a very important concept. It represents the amount of crypto money left over from each transaction. By using this, it is possible to see how long these funds are kept in the wallet. Based on the UTXO data, HODL waves are drawn. Using UTXO, the amount of unused crypto money in the wallets are determined and for how long they are kept.

Holder with an increasing number of investments means that the circulating supply is lower, that is, they do not decrease the sale and the circulating supply can said to be less. This indicator also reflects the investor psychology, allowing us to observe whether people want to sell coins or not. For example, considering investors who have started to sell the coins they have kept in their wallets for more than 1 year, Holder decreases, which means that the investor is selling his crypto asset because they are making a profit. With this indicator, investments can be made by looking at the buying/selling times. Warm colors, such as red, orange, yellow, represent Bitcoin that has been used within 1 year, while cold colors represent Bitcoin that has not been used for more than 1 year.

Another indicator used in onchain analysis is MVRV Z-SCORE. This indicator shows the period when Bitcoin is overvalued and undervalued. Certain values in the past are taken into account and the formula is as follows:

$$MVRVZ - Score : \frac{MarketCap_{USD} - RealizedCap_{USD}}{StdDev\,(orMarketCap_{USD})} \quad (1)$$

The MVRV Z-score is a function obtained by dividing the difference between the total market value and the realized market value by the standard deviation of the market value. This shows how many standard deviations the market value differs from the realized value. Market value indicates a peak if it is significantly higher than realized value, but a bottom vice versa. In other words, it shows whether the realized value with the market value is over or undervalued than the Bitcoin price. The ultimate goal is 7. The probability of a Balloon asset above 7 is high.

The Z-Score is a number used to measure the relationship of a value with the group average of that value. It is measured with a standard deviation, and for example, Z-Score 0 means the value is the same as the group mean, and if the Z-Score is 1, that value is 1 standard deviation from the group mean. It is more important in determining extraordinary movements. If the Z-Score -Red Line-enters the pink box, it means that there is an excessive increase beyond the true value. The probability of the price falling increases.

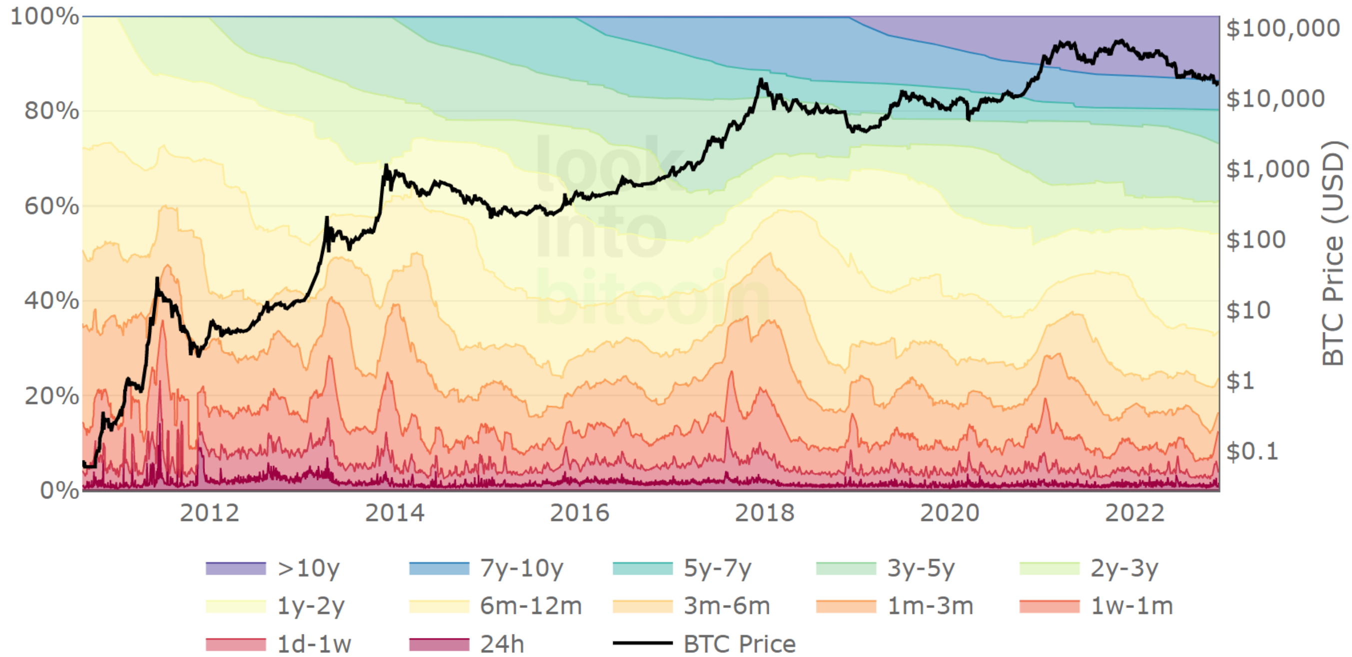

Figure 4 HODL Wave Graph (Lookintobitcoin 2022 (accessed November 7, 2022)

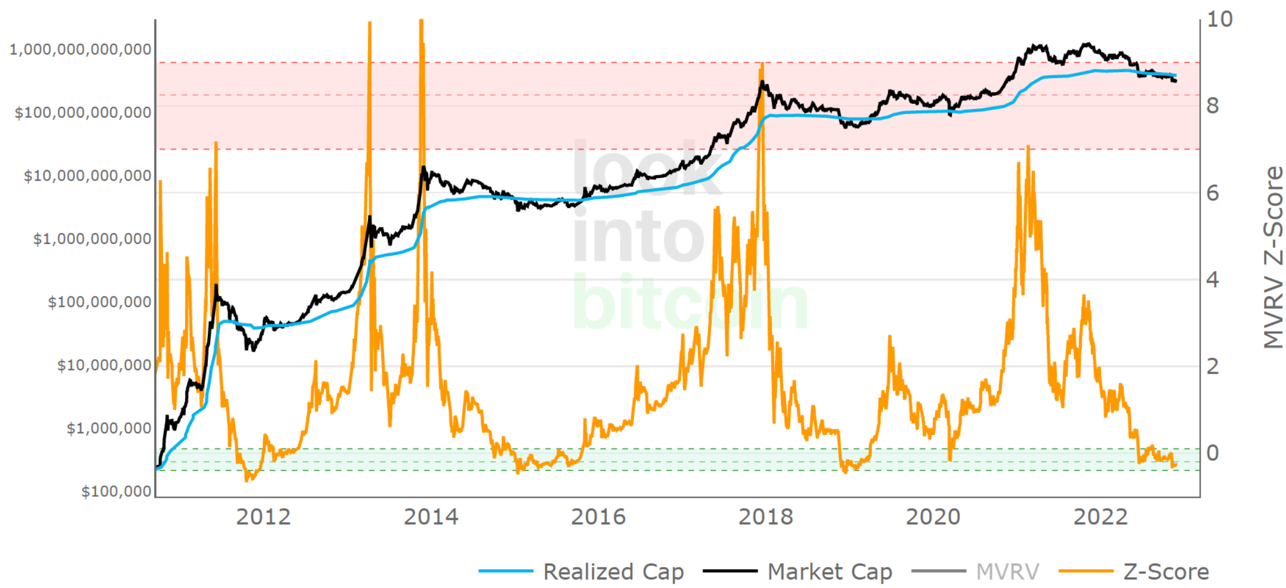

Figure 5 MVRV Z-Score (Lookintobitcoin 2022 (accessed November 7, 2022)

Another indicator is NUPL. NUPL is derived from both the market value and realizable value. Market Cap is the current price of Bitcoin multiplied by the number of coins in circulation. Actual Value is the price of Bitcoin at the time it was last transferred, that is, the last time it was transferred from one wallet to another. All these individual prices are then summed up and averaged, then multiplie with the total number of coins in circulation. It is the difference between the market value and the realized value. Formula NUPL value it is:

$$NUPL = \frac{MarketCap - RealizedCap}{MarketCap} \tag{2}$$

Net Unrealized Profit/Loss (NUPL) can use market participant data to help predict when Bitcoin price hits highs or lows. It is a convenient tool to show potential market participant sentiment at a given moment, which can be useful for predicting the Bitcoin price and where it may move over time. How this tool should be interpreted in its graph is shown in the Fig 6.

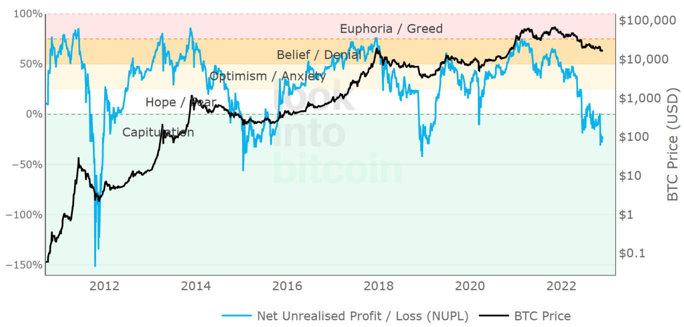

Figure 6 NUPL Graph (Lookintobitcoin 2022 (accessed November 7, 2022)

To generate this indicator, the difference between unrealized losses and unrealized gains is calculated, so that when it acquires a value greater than zero it indicates that at that moment the network is in profit, while values less than zero indicate a state of loss. The indicator is shown on a graph as a curve that oscillates between positive and negative values, and in general, the further the NUPL curve moves away from zero, the closer the prices are to the market highs or lows.

Puell Multiple metric focuses on the revenue of bitcoin miners. In this environment where prices are volatile, miners can affect prices in order to meet fixed costs. The daily issuance value of Bitcoins is calculated by averaging the 365-day issuance value. If the values are higher than the annual average it indicate the current miner profitability. Low values indicate that current miner profitability is lower than the annual average.

The Mayer Multiple shows the time period when it is overvalued and undervalued above the 200-day moving average. If this value falls below 1, it is a buying opportunity. In the short term, this value is desired to exceed 1. Falling below 1 is not a good indicator for the investor. It is calculated using the formula:

$$MayerMultiple = \frac{BTC_{USD}}{MA_{200}(BTC_{USD})} \tag{3}$$

Reserve Risk is a cyclical indicator that monitors the risk-reward balance based on the confidence and belief of long-term holders. It is an indicator that models the ratio between the current price (sell incentive) and long-term investors' opinion (opportunity cost of not selling). This indicator is compatible with bull and bear markets. If confidence is high and the price is low, the Reserve Risk is low, making it attractive to invest. If the confidence is low, the reserve risk is high, and this may mean a price peak. In other words, low reserve risk can mean low value and high reserve risk can mean overvaluation.

There are some free websites that provide on-chain analysis for cryptocurrencies : Glassnode offers simple on-chain metrics at zero cost, plus advanced metrics and high-frequency time series data for a fee. CoinMetrics offers free data for around 37 crypto assets. This includes on-chain metrics and correlations.

IntoTheBlock is also a platform that provides a wide range of analytical tools. It covers sentiment analysis, order book data, and on-chain analysis for various crypto assets.

Other sites include Santiment/Sanbase and CQ.Live. There can be various difficulties in performing Onchain analysis. Not all blockchains are evenly distributed. For example, the Bitcoin network has the motivation to make digital money, while the Etherum network has a wider range of services. Measurements may differ due to inequality in the blockchain. When comparing Bitcoin to other new Altcoins, Bitcoin has more than ten years of data to support historical analysis, while new altcoins have less data, as well as longer term analysis. It may not give the right buy-sell signal in the short term.

Sentiment Analysis

It is the formation of thoughts on the subject through the evaluation of the feelings and thoughts of a community. The idea is to obtain efficient and usable findings from these evaluations. Its other name is "Idea mining". Sentiment Analysis is used in many fields such as finance, medicine, stockbroking, media, politics. It is a widely used technique in product reviews to measure a consumers satisfaction with a product. The data related to the subject in question can be defined as positive, negative, or neutral. In terms of Sentiment Analysis research levels are examined under three main headings; document level, sentence level (sentence level) and view level (aspect level).

Sentiment analysis at the document level: In this method, without going into too much detail, the entire document is considered as a single idea and classified according to whether it expresses positive or negative emotions. However, this method cannot be used in cases where there is more than one variable, since it gives a single result.

Sentence Level Sentiment: After checking whether each sentence is subjective or objective, if the sentence is subjective, classification is made according to whether the sentence expresses positive or negative emotions (Medhat *et al.* 2014).

At The Level of View, Sentiment: Makes it possible to deal with all aspects of existence. In the classifications at the document and sentence levels, the comments do not have to be detailed, but at this view level, the comments are detailed because it is aimed to determine the direction of emotion regarding certain features of a certain entity (Medhat *et al.* 2014).

Sentiment Analysis Methods are divided into 3 as Machine Learning, Hybrid Model and Dictionary Based Approach.

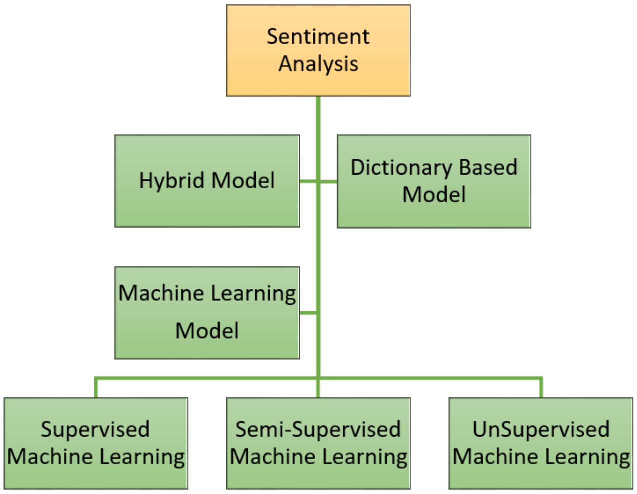

Figure 7 Types of sentiment analysis

Dictionary Based Approach Using natural language processing method and the tools of this method, methods based on emotional analysis of sentences are used. Here, sentences related to the relevant subject are analyzed and it is desired to reach a conclusion about these sentences. Three methods are used when applying this method are:

a) Conditional Random Fields: Based on the words in the sentence, the purpose of the chosen word is determined.

b) Dependency Tree: Elements are created in the sentence and the dependencies of the created elements are investigated. A sentiment analysis is performed by analyzing the relationships between the nodes in the created loyalty tree.

c) Rule Based Approach: Rules based on different natural language processing features, especially word types and word type patterns, are determined, and semantic inferences are made by analyzing sentence structures that comply with these rules.

Hybrid Approach They are approaches in which machine learning algorithms and dictionary-based approaches are used together. Sentiment analysis in crypto money is generally related to social media etc. about crypto money. It started to be implemented based on the findings that opinions affect the value of crypto money. If emotion is expressed in financial terms, they are an opinion expressed about the state of a market. Crypto market sentiment defines the general emotional views and attitudes of investors towards the asset. In essence, Sentiment analysis for cryptocurrencies can yield several notable statistics that can be used to analyze cryptocurrency market sentiment: funding rates, sentiment indices, social media and community analytics, and tracking of cryptocurrency whales, trajectory and movements of crypto assets.

The basis of this analysis is based on Sentiment analysis methods. It can answer many questions for the investor who has invested in the crypto money market for at least a year, such as coin transactions. For example, if a coin, which is stated to have given a "buy" order on social media, has been purchased and sufferes a loss in the future, this victimization of the investor may affect the view of the entire crypto money investment. Here, the concepts of "FOMO" and "FUD" come to the fore. These concepts are from everyday language, but are also used in literature to reflect the psychological state of the user.

Fear of missing out (FOMO) is the fear of people of not knowing or missing out on the news, developments and information in daily life. It is the concern that a crypto-related opportunity will be missed. Fud (fear, uncertainty and doubt) expresses the uneasiness that there will be a loss which will decrease the prices in the market.

The emotions expressed here may belong to the individual or the community. In the existing studies in the literature, for example Husband 2021, a Sentiment Analysis study with Twitter Data on Bitcoin was carried out. A predominant feeling of joy was observed. Another study in the literature included the relationship between news about Bitcoin and ether and price prediction. Sentiment Analysis related to the relevant crypto money can be made.

Machine Learning Approach Present data using mathematical and statistical methods is a sub-branch of artificial intelligence consisting of modeling and algorithms that make inferences from the future and make predictions about the unknown with these inferences. It is divided into three as supervised machine learning, unsupervised machine learning and semi-supervised machine learning.

a) Supervised Machine Learning: The target values corresponding to an existing group of input values are given, and it is aimed to produce the outputs closest to the target values by learning the dependency between the input and the target of the created model (Ciftci and Apaydin 2018). We can use supervised machine learning to learn a model for the relationship between example: x and y. It reason it is called supervised machine learning is because requires human oversight. The majority of the data that is currently available is unlabeled. For data to be adequately labeled and ready for supervised learning, human input is typically necessary. Supervised learning is used in financial applications for credit scoring, algorithmic trading, and bond classification. Supervised learning problems can be further grouped into regression and classification problems.

b) Semi-Supervised Machine Learning: Labeled and unlabeled data are separated in order to form the appropriate model. If unlabeled data is less, semi-supervised machine learning is preferred. It is a relatively more flexible model.

c) Unsupervised Machine Learning: It finds similar samples within the group and aims to model the underlying structure or distribution in the data to learn more. It is desired to make a meaning out of meaningless data. It is applied on raw data. It is used quite often to determine the trends, likes, etc. of the datasets we have.

The requirement for labeled training data distinguishes supervised learning from unsupervised learning. Unsupervised machine learning processes unlabeled or raw data, whereas supervised machine learning uses labelled input and output training data. The Possibilistic Fuzzy C-Means (PFCM) and Fuzzy C-Means (FCM) algorithms are frequently utilized techniques (Wang *et al.* 2020).

Deep learning techniques have been used recently in research projects to forecast bitcoin prices. compared cutting-edge deep neural networks for predicting Bitcoin price, including Long Short-Term Memory (LSTM), Deep Neural Networks (DNNs), deep residual network, and their combinations.

Cryptocurrencies give very successful results in terms of price prediction thanks to their own features. When the studies in the literature are examined, successful results are obtained (Chen *et al.* 2020). There is consensus in the literature that machine learning provides robust techniques for exploring the predictability of cryptocurrencies even in adverse market conditions and developing profitable trading strategies in these markets (Sebastião and Godinho 2021). The combination of these trust frameworks, which hold the frontiers of machine-work analytics and blockchain, enables smarter decisions, increased trust, more automation, and decentralized intelligence.

As a result, a machine computer and blockchain duo sustain the positive effects of the workload and its financial performance. It creates a system for storing and sharing big data with the help of smart contracts in blockchain networks. Machine learning is the basis of system behaviors necessary to optimize blockchain mechanisms. Trade forecasting is known for its great forecasting capabilities and efficient data analysis methods. Also, ML models can be used to improve data validation procedures and detect malicious attacks or fraudulent transactions on the blockchain. Machine learning and blockchain build a mutually beneficial relationship that is all about data. However, if you use machine learning for blockchain management, you have a chance to gain unprecedented data security. But at the same time, machine learning can take advantage of the decentralized nature of blockchain to build better models and handle large volumes of data.

CONCLUSION

Cryptocurrency is a new unit that is used and there are many questions about it. One of these questions is what its value will be in the future. When we look at the studies in the literature, the value of this crypto money using onchain and sentiment analysis, which are couple of the chaotic behaviors and new analysis types, as well as fundamental and technical analyses. It is possible to monitor the correct predictions and crypto money behavior. Sentiment analysis is used in cryptocurrency forecasting, just as it is used in traditional finance, and produces successful analyzes about the investor's thoughts about the relevant currency. When viewed from the framework of chaotic behavior, it is highly dependent on initial conditions because it is not centralized. In most startups, this currency behaves chaotically and that small effects make big changes.

Fundamental and technical analysis in the Crypto market refers to the evaluation of the market environment and other important factors that can affect the market trend. It includes the analysis of numbers and statistics that can determine the price movements and trading volume of digital assets. Investors identify past market trends and price movements to determine whether digital assets are worth investing in. It seems to be a commonly used method. Technical analysts use a variety of indicators to identify market trends based on charts and historical price movements. One of the key premise of technical analysis is that market prices already reflect all fundamental factors. However, unlike the approach of technical analysis, which focuses heavily on historical price data, fundamental analysis adopts a broader research strategy with a greater emphasis on qualitative factors. For this reason, many investors seem to use a combination of both methods to get the most accurate insight.

Onchain analysis, on the other hand, needs to be able to look at various metrics for the analysis of Bitcoin and other cryptocurrencies. Traders and investors often pair On-Chain analysis with technical analysis to identify suitable short-term entry and exit points for crypto assets. In other words, it is not based on speculation, it will help to make more accurate short or long targeting by making an interpretation as a result of these metrics and analyzes that are shared regularly and consistently. It is mostly like technical analysis, but on-chain analysis is achieved by interpreting all transactions that have taken place completely on the blockchain. Just like in technical analysis, there are indicators used in on-chain analysis. On-chain analysis gives us ideas about where we are now and what may happen in the future. On-chain sentiment analysis means the interpretation of crypto money transfers that take place on-chain. These two new analyzes can contain the most reliable price predictions as they reflect the nature of crypto money. In short, on-chain analysis offers cryptographers a fascinating tool to explore real-time insights into a blockchain network. This gives them the opportunity to take advantage of a more abundant and transparent data encryption market.

In this study, analysis methods and explanations of these methods are included in order to make price estimation. The wide definition of sentiment analysis and onchain analysis, which are two new types of analysis, makes the study valuable. Besides all these, the discovery of the chaotic behavior of the decentralized currency will help us understand the nature of cryptocurrencies.

Conflicts of interest

The authors declare that there is no conflict of interest regarding the publication of this paper.

Availability of data and material

Not applicable.

LITERATURE CITED

Abraham, J., D. Higdon, J. Nelson, and J. Ibarra, 2018 Cryptocurrency price prediction using tweet volumes and sentiment analysis. SMU Data Science Review **1**: 1.

AJ, H. S. S. W. M. and S. Vanstone, 1990 How to time-stamp a digital document. In *Advances in Cryptology-CRYPT0*, volume 1991.

Alpar, O. and E. Özge, 2016 Imkb100 endeks değişim değerlerinde lyapunov üsteli metoduyla kaosun incelenmesi. İstanbul Aydın Üniversitesi Dergisi **8**: 151–174.

Biswas, H. R., M. M. Hasan, and S. K. Bala, 2018 Chaos theory and its applications in our real life. Barishal University Journal Part **1**: 123–140.

Bouri, E., R. Gupta, and D. Roubaud, 2019 Herding behaviour in cryptocurrencies. Finance Research Letters **29**: 216–221.

Chen, Z., C. Li, and W. Sun, 2020 Bitcoin price prediction using machine learning: An approach to sample dimension engineering. Journal of Computational and Applied Mathematics **365**: 112395.

Ciftci, B. and M. S. Apaydin, 2018 A deep learning approach to sentiment analysis in turkish. In *2018 International Conference on Artificial Intelligence and Data Processing (IDAP)*, pp. 1–5, IEEE.

Cortez, C. T., S. Saydam, J. Coulton, and C. Sammut, 2018 Alternative techniques for forecasting mineral commodity prices. International Journal of Mining Science and Technology **28**: 309–322.

Diffie, W. and M. E. Hellman, 2022 New directions in cryptography. In *Democratizing Cryptography: The Work of Whitfield Diffie and Martin Hellman*, pp. 365–390.

El Montasser, G., L. Charfeddine, and A. Benhamed, 2022 Covid-19, cryptocurrencies bubbles and digital market efficiency: sensitivity and similarity analysis. Finance Research Letters **46**: 102362.

Erdoğan, N. K., 2017 Finansal zaman serilerinin fraktal analizi. Aksaray üniversitesi iktisadi ve idari bilimler fakültesi dergisi **9**: 49–54.

Faggini, M. and A. Parziale, 2012 The failure of economic theory. lessons from chaos theory .

Gözde, K., 2021 Bitcoin üzerine twitter verileri ile duygu analizi. Anadolu Üniversitesi İktisadi ve İdari Bilimler Fakültesi Dergisi **22**: 19–30.

Gu, Z., D. Lin, and J. Wu, 2022 On-chain analysis-based detection of abnormal transaction amount on cryptocurrency exchanges. Physica A: Statistical Mechanics and its Applications **604**: 127799.

Gurrib, I. and F. Kamalov, 2021 Predicting bitcoin price movements using sentiment analysis: a machine learning approach. Studies in Economics and Finance .

Hacinliyan, A. and E. Kandiran, 2015 Türkiye'deki borsa endekslerinin fraktal analizi. AJIT-e: Bilişim Teknolojileri Online Dergisi **6**: 7–19.

Holiachenko, A., L. Lyushenko, and O. Strutsynsky, 2022 Modified method of cryptocurrency exchange rate forecasting based on arima class models with data verification. In *The International Conference on Artificial Intelligence and Logistics Engineering*, pp. 123–136, Springer.

Hudson, R. and A. Urquhart, 2021 Technical trading and cryptocurrencies. Annals of Operations Research **297**: 191–220.

Jagannath, N., T. Barbulescu, K. M. Sallam, I. Elgendi, B. McGrath, *et al.*, 2021 An on-chain analysis-based approach to predict ethereum prices. IEEE Access **9**: 167972–167989.

Jain, A., S. Tripathi, H. D. Dwivedi, and P. Saxena, 2018 Forecasting price of cryptocurrencies using tweets sentiment analysis. In *2018 eleventh international conference on contemporary computing (IC3)*, pp. 1–7, IEEE.

Kang, K., E. Abdelfatah, and M. Pournik, 2019 Nanoparticles transport in heterogeneous porous media using continuous time random walk approach. Journal of Petroleum Science and Engineering **177**: 544–557.

Klioutchnikov, I., M. Sigova, and N. Beizerov, 2017 Chaos theory in finance. Procedia computer science **119**: 368–375.

Lahmiri, S. and S. Bekiros, 2018 Chaos, randomness and multifractality in bitcoin market. Chaos, solitons & fractals **106**: 28–34.

Lookintobitcoin, 2022 (accessed November 7, 2022)a Hodl-wave. https://www.lookintobitcoin.com/charts/hodl-waves/.

Lookintobitcoin, 2022 (accessed November 7, 2022)b Mvrv z-score. https://www.lookintobitcoin.com/charts/mvrv-zscore/.

Lookintobitcoin, 2022 (accessed November 7, 2022)c Nupl graph. https://www.lookintobitcoin.com/charts/relative-unrealized-profit--loss/.

Lv, Z., F. Sun, and C. Cai, 2022 A new spatiotemporal chaotic system based on two-dimensional discrete system. Nonlinear Dynamics **109**: 3133–3144.

Lyashenko, V., M. Bril, and O. Shapran, 2021 Dynamics of world indices as a reflection of the development world financial market .

Malkiel, B. G., 2003 The efficient market hypothesis and its critics. Journal of economic perspectives **17**: 59–82.

Medhat, W., A. Hassan, and H. Korashy, 2014 Sentiment analysis algorithms and applications: A survey. Ain Shams engineering journal **5**: 1093–1113.

Nakamoto, S., 2008 Bitcoin: A peer-to-peer electronic cash system. Decentralized Business Review p. 21260.

Nie, C.-X., 2022 Analysis of critical events in the correlation dynamics of cryptocurrency market. Physica A: Statistical Mechanics and its Applications **586**: 126462.

Pietrych, L., J. E. Sandubete, and L. Escot, 2021 Solving the chaos model-data paradox in the cryptocurrency market. Communications in Nonlinear Science and Numerical Simulation **102**: 105901.

Şahin, E. E., 2020 Kripto para fiyatlarında balon varlığının tespiti: Bitcoin, iota ve ripple örneği. Selçuk Üniversitesi Sosyal Bilimler Enstitüsü Dergisi pp. 62–69.

Sarmah, S. S., 2018 Understanding blockchain technology. Computer Science and Engineering **8**: 23–29.

Sebastião, H. and P. Godinho, 2021 Forecasting and trading cryptocurrencies with machine learning under changing market conditions. Financial Innovation **7**: 1–30.

Simsek, M., M. Samar, A. Oweida, A. F. Hersh, A. Alkış, *et al.*, 2020 Necmettin erbakan üniversitesi yayınları: 47 islami finans ve finansal teknolojiler (fintech) blokzincir-akıllı sözleşmeler-kripto paralar editörler .

Stevens, L., 2002 *Essential technical analysis: tools and techniques to spot market trends*, volume 162. John Wiley & Sons.

Su, F., 2021 The chaos theory and its application. In *Journal of Physics: Conference Series*, volume 2012, p. 012118, IOP Publishing.

Tosun, T., 2006 *Türev Araçlar, Kaos Teorisi ve Fraktal Yapıların Vadeli İşlem Zaman Serilerinde Uygulanması*. Ph.D. thesis, Marmara Universitesi (Turkey).

Trigg, R. and K. Yerci, 1996 *Akılcılık ve bilim: bilim her şeyi açıklayabilir mi?*. Sarmal Yayınevi.

Tschorsch, F. and B. Scheuermann, 2016 Bitcoin and beyond: A technical survey on decentralized digital currencies. IEEE Communications Surveys & Tutorials **18**: 2084–2123.

Ural, M. and E. Demireli, 2009 Hurst üstel katsayisi araciliğiyla fraktal yapi analizi ve imkb'de bir uygulama. Atatürk üniversitesi iktisadi ve idari bilimler dergisi **23**: 243–255.

Vo, A.-D., Q.-P. Nguyen, and C.-Y. Ock, 2019 Sentiment analysis of news for effective cryptocurrency price prediction. International Journal of Knowledge Engineering **5**: 47–52.

Wang, S., W. Chen, S. M. Xie, G. Azzari, and D. B. Lobell, 2020 Weakly supervised deep learning for segmentation of remote sensing imagery. Remote Sensing **12**: 207.

Wasiuzzaman, S., A. N. M. Azwan, and A. N. H. Nordin, 2022 Analysis of the performance of the islamic gold-backed cryptocurrency during the bear market of 2020. Emerging Markets Review p. 100920.

Yerlikaya, T., 2006 Yeni şifreleme algoritmalarının analizi. trakya üniversitesi. Fen Bilimleri Enstitüsü, Bilgisayar Mühendisliği Anabilim Dalı, Doktora Tezi .

Yue, Y., X. Li, D. Zhang, and S. Wang, 2021 How cryptocurrency affects economy? a network analysis using bibliometric methods. International Review of Financial Analysis **77**: 101869.

How to cite this article: Akgul, A., Sahin, E. E., and Senol F. Y. Blockchain-based Cryptocurrency Price Prediction with Chaos Theory, Onchain Analysis, Sentiment Analysis and Fundamental-Technical Analysis. *Chaos Theory and Applications*, 4(3), 157-168, 2022.

CHAOS Theory and Applications in Applied Sciences and Engineering

e-ISSN: 2687-4539
RESEARCH ARTICLE
Vol.4 / **No.**3 / 2022 / **pp.**169-178
https://doi.org/10.51537/chaos.1202558

Bibliometric Analysis of Publications on Chaos Theory and Applications during 1987 - 2021

Omer Faruk Akmese *,1
*Department of Computer Engineering, Faculty of Engineering, Hitit University, 19030, Çorum, Türkiye.

ABSTRACT

The number of studies based on chaos theory is quite high. Therefore, it is important to analyze chaos theory's development over the years deeply. However, there is no study in the literature examining the research status of this field. The article presents the bibliometric analysis of the studies on the keywords "Chaos Theory" and "Applications" indexed in Scopus between 1987 and 2021. This study aims to quantitatively evaluate the academic output in chaos theory research, make sense of the data, reveal the state of scientific knowledge in the field, and provide scientists with a general perspective on the subject. Bibliometrix and Microsoft Excel programs were used for bibliometric analysis. Nine thousand one hundred different authors identified a total of 5088 studies. Of these studies, 60.3% were research articles, and 32.9% were conference papers. Chaos Solitons and Fractals was the most published journal, with 206 articles. Only China and the USA contributed 39.7% to the studies. Vaidyanathan, S. was the most prolific author with 72 articles. Vel Tech Rangarajan Dr. Sagunthala R&D Institute of Science and Technology was the most productive institution with 74 studies. The most cited article was the econometrics of financial markets.

KEYWORDS
Chaos Theory
Bibliometric analysis
Citation analysis
Network analysis
Scopus

INTRODUCTION

Chaos, characterized by the high sensitivity of its initial values, is significant in science. Chaos theory continues to pique people's interest because it describes nonlinear and unpredictable behavior. Chaos theory examines the dependence of motion-expressing systems (physical, economic, mathematical, biological, etc.) on initial conditions, unpredictable phase spaces of time series, and non-periodic system behavior. Scientifically, "chaos" refers to a combination that allows us to understand the cause of seemingly complex and random events.

Chaos is a branch of science aimed at understanding the movements of all kinds of events and structures that occur in the universe, from the most microstate to the most macro-state (Leutcho *et al.* 2020). Their most crucial characteristic is that chaotic systems depend on the initial condition. These systems consistently display unpredictable behavior and non-periodic traits (Thompson *et al.* 1990; Wei *et al.* 2019). Chaos studies have been observed in many branches of science, such as biology, medicine, ecology, electronics, economics, encryption, etc. (Wang *et al.* 2016; Liu *et al.* 2009; Sun *et al.* 2020; Pandey *et al.* 2016; Rajagopal *et al.* 2019). Bibliometric analysis is a common technique for researching and analyzing vast scientific data. The latest status in a field related to the available scientific knowledge can be mapped using bibliometrics. Bibliometric analysis has gained immense popularity in recent years as the availability and accessibility of software such as Gephi, Leximancer, VOSviewer, and Bibliometrix and scientific databases such as Scopus and Web of Science have increased (Donthu *et al.* 2021; Sengupta 1992).

Bibliometric analysis is a helpful tool for mapping the literature pertinent to a specific research area (Falagas *et al.* 2006). Bibliometric analysis is employed for several purposes, including examining the performance of articles and journals, patterns of collaboration, new developments in research components, and the intellectual composition of a specific field in the body of literature (Donthu *et al.* 2021; Verma and Gustafsson 2020). While bibliometrics facilitates retrospective research, it can also aid in the quantitative and objective exploration of research points and development trends in disciplines. The results of bibliometric analysis contribute to advancement in a specific field of research in various ways. The

Manuscript received: 10 November 2022,
Revised: 27 November 2022,
Accepted: 30 November 2022.

[1] ofarukakmese@hitit.edu.tr (**Corresponding Author**)

bibliometric analysis assesses progress, identifies the most reliable and popular sources of scientific publication, recognizes key scientific actors such as authors and institutions, establishes the academic foundation for evaluating new developments, identifies emerging research interests, and forecasts future research success. It also assists researchers in identifying potential research topics, appropriate research institutions with which to collaborate, and potential academic collaborators (Song *et al.* 2019; Martínez *et al.* 2015; Mazloumian 2012; Geng *et al.* 2017).

This study, which covers top journals, institutions, keyword features, citation network analysis, and a review of the most significant articles, offers the potential to track historical and geographic trends at a global level using proper bibliometric analysis techniques. This work aims to reveal the state of scientific knowledge in the field by making sense of large volumes of data on "Chaos theory" and "Applications" and to present a general viewpoint to scientists on the subject.

In addition, it is aimed to evaluate the academic outputs of chaos theory research quantitatively. This study can make various contributions to the research field. First, it can provide field experts with a comprehensive overview of the research situation. Additionally, it can help researchers identify authors, institutions, journals, and countries/regions with the most significant potential. It can also increase researchers' awareness when deciding on topic selection. Finally, it can explain how the subject has evolved over time.

MATERIAL AND METHODS

The bibliometric methodology covers the application of quantitative methods to bibliometric data. Early discussions on bibliometrics, which began in the 1950s, show that bibliometric methodology is not new (Donthu *et al.* 2021; Broadus 1987; Wallin 2005; Pritchard 1969). Scopus was preferred for the collection of bibliometric information. It has been determined that Scopus offers a more comprehensive journal profile to the user than WoS and brings faster results from more articles in citation analysis.

All publications indexed in Scopus (accessed 21.10.2022) on Chaos Theory between 1987-2021 were analyzed using bibliometric methods. "Chaos Theory" and "Applications" were used as search keywords. Documents were searched in article title, abstract, and keywords. Scopus codes used in our search are as follows; ("Chaos Theory" AND "Applications") AND (EXCLUDE (PUBYEAR, 2023) OR EXCLUDE (PUBYEAR, 2022)).

With this search method, all articles published between 1987-2021 containing the words "Chaos Theory" and "Applications" in the title, abstract, and keywords of the studies were found in the Scopus database. Microsoft Excel and Bibliometrix (Aria and Cuccurullo 2017) were used for bibliometric network visualizations.

BIBLIOMETRIC ANALYSIS OF PUBLICATIONS ON CHAOS THEORY AND APPLICATIONS

Literature Distribution

From 1987 to 2021, 5088 publications of different types appeared: articles (3068, 60.3%), conference papers (1674, 32.9%), reviews (117, 2.3%), book chapters (78, 1.5%), conference reviews (77, 1.5%), book (52, 1%) and others (15, 0.29%). As shown in Figure 1, articles on Chaos Theory; "Engineering" (2815, 33%), "Computer Science" (2291, 21%), "Mathematics" (1625, 19%), "Physics and Astronomy" (1355, 16%), "Materials Science" (499, 6%) and "Multidisciplinary and others" (453, 5%). Since a study can be matched into different categories, the total number of studies is more than 5088.

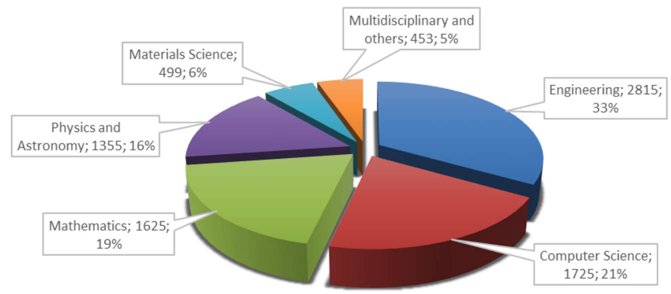

Figure 1 The distribution of subject areas

Development of Publications

Figure 2 shows the annual scientific production graphic. Despite some fluctuations, the number of publications generally increased until 2004. It is seen that the number of studies decreased from 2004 to 2008. Although there was a slight increase in the number of publications in the following years, it generally remained stable.

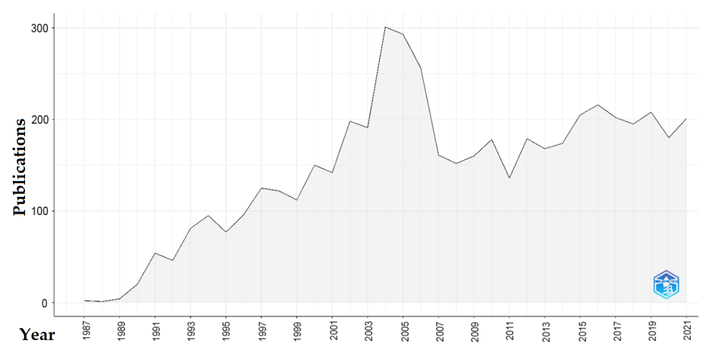

Figure 2 Annual scientific production

Active Authors

A total of 5088 publications were produced by 9100 authors. Of these, 3068 authors published articles, and 1674 authors published conference papers. The top five authors producing the highest number of publications were Vaidyanathan S. (72, 1.4%), Zhang Y. (54, 1%), Wang X. (48, 0.94%), Chen G. (39, 0.76%) and Wang Y. (36, 0.7%). These authors were significant research pioneers in "Chaos Theory" and "Applications" related fields. Table 1 shows the top 25 authors with the highest *h_index* for "Chaos Theory" and "Applications".

Figure 3 shows the collaboration network of the top 25 authors. The larger the circle, the greater the cooperation. Clusters are separated by colors. The strength of collaboration between authors is expressed in the thickness of the lines.

Table 1 Top 25 authors with h_index (TC: Total Citation, NP: Number of Publication, PY_start: Start of Publication Year).

No	Author	h_index	g_index	m_index	TC	NP	PY_start
1	VAIDYANATHAN S.	26	55 Sec.	2.6	3048	72	2013
2	CHEN G.	19	39	0.633	2890	39	1993
3	WANG X.	16	28	0.667	834	48	1999
4	LIAO X.	15	16	0.75	1197	16	2003
5	ZHANG Y.	14	34	0.56	1207	54	1998
6	AIHARA K.	13	19	0.406	753	19	1991
7	WANG L.	13	32	0.52	1379	32	1998
8	LEUNG H.	11	20	0.344	636	20	1991
9	LI C.	11	21	0.55	960	21	2003
10	LIU L.	11	16	0.524	709	16	2002
11	PEHLIVAN I.	11	14	0.917	952	14	2011
12	SAVI MA.	11	16	0.579	313	16	2004
13	ROVATTI R.	10	15	0.385	742	15	1997
14	SETTI G.	10	17	0.385	748	17	1997
15	WANG Y.	10	16	0.4	278	36	1998
16	BANERJEE S.	9	11	0.375	610	11	1999
17	JAFARI S.	9	9	0.6	413	9	2008
18	KURTHS J.	9	10	0.31	1274	10	1994
19	LIU X.	9	20	0.45	559	20	2003
20	PHAM VT.	9	14	1.125	700	14	2015
21	ZHANG X.	9	13	0.391	207	29	2000
22	AKGUL A.	8	9	1.143	569	9	2016
23	CHEN Z.	8	15	0.333	397	15	1999
24	LI H.	8	13	0.364	196	19	2001
25	LIU J.	8	14	0.308	212	20	1997

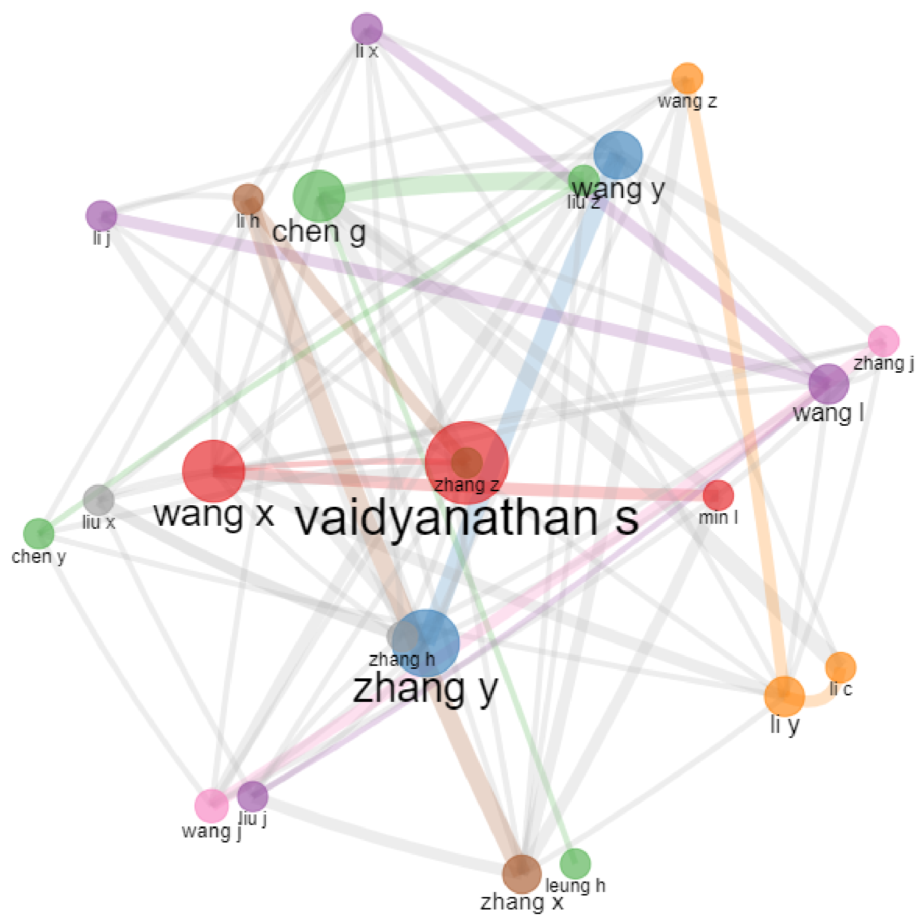

Figure 3 Authors collaboration network

Active Institutions

The top 7 organizations that contributed the most to the literature were: Vel Tech Rangarajan Dr.Sagunthala R&D Institute of Science and Technology (74, 1.4%), City University of Hong Kong (57, 1.1%), Zhejiang University (45, 0.88%), Ministry of Education China (42, 0.82%), and Shanghai Jiao Tong University (41, 0.8%). Figure 4 shows the number of publications published by institutions over the 1987-2021 period, with an increasing trend with slight fluctuations.

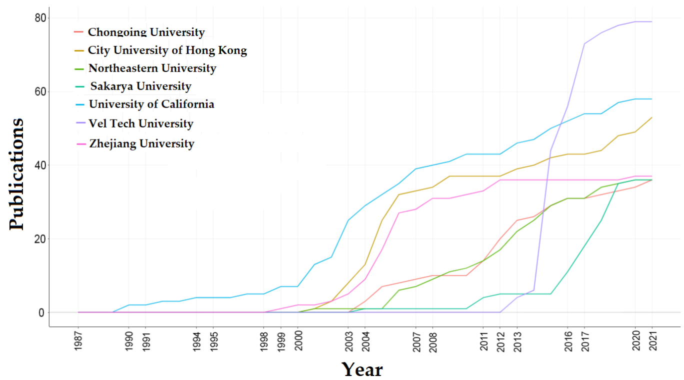

Figure 4 Affiliation production over time

Figure 5 shows the cooperation network of the top 25 institutions. The larger the circle, the greater the cooperation. Clusters are separated by colors. The strength of collaboration between institutions is expressed in the thickness of the lines.

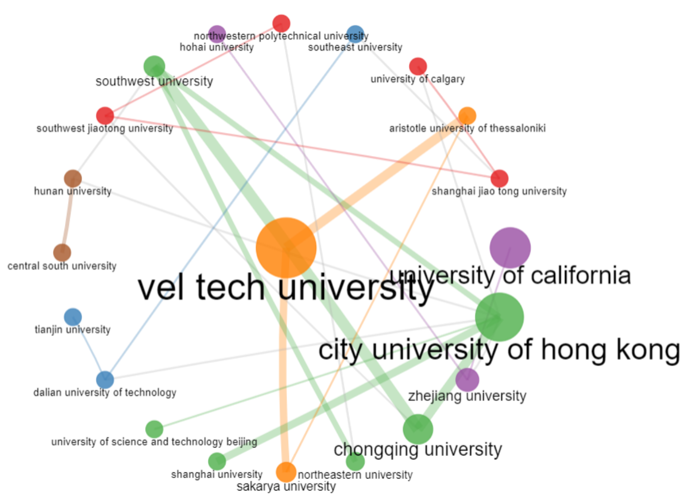

Figure 5 Instutions collaboration network

Active Journals

In total, 5088 articles were published in 659 journals. Table 2 shows the top 25 journals with the highest *h_index* on "Chaos Theory" and "Applications". Chaos, Solitons, and Fractals by chart IEEE Transactions on Circuits and Systems I: Fundamental Theory and Applications, Nonlinear Dynamics, Physical Review E - Statistical, Nonlinear, and Soft Matter Physics, International Journal of Bifurcation and Chaos are the most productive journals. More than 22% of 5088 articles are from these 25 sources.

The citation visualization map between these journals is given in Figure 6. Figure 6 shows the common citation network of the top 25 journals. The larger the circle, the greater the number of citations. Clusters are separated by colors. The strength of collaboration between magazines is expressed in the thickness of the lines.

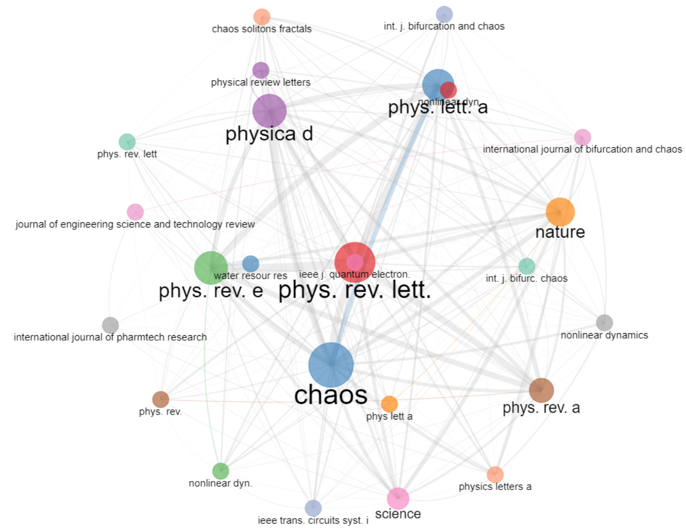

Figure 6 Sources co-citation network

In Figure 7, there is a graph of the increase in the number of publications according to the topics that are the research subject for the first six journals in terms of the number of publications between 1987-2021.

Active Countries

The analyses showed that the articles covered 91 different countries (or regions). The publication numbers of the first 25 countries are shown in Figure 8. a, and the collaboration network is shown in Figure 8. b. As for the number of publications, China ranked first with 1415 (27.8%) studies. The USA was in second place with 852 (16.7%) studies. India and Japan ranked third and fourth with 287 (5.6%) studies. The United Kingdom was ranked 5th with 276 (5.4%).

The geographical distribution of country collaboration for the overall study period is shown in Figure 9. Figure 10 shows the growth trends of publications for the six most productive countries from 1987 to 2021. Compared to the other five countries, the upward trend in the number of publications in China increased more rapidly after 2003. It is observed that the number of publications originating in the USA has decreased in the growth trend since 2006. It is seen that the number of publications in India has been on increasing trend since 2013. The growth trends of the number of publications in Japan, Italy, and the United Kingdom seem to have had a low rate of increase in the last fifteen years.

Table 2 Top 25 journals with h_index (TC: Total Citation, NP: Number of Publication, PY_start: Start of Publication Year).

No	Journals	h_index	g_index	m_index	TC	NP	PY_start
1	Chaos, Solitons and Fractals	46	84	1.484	8133	206	1992
2	IEEE Transactions on Circuits and Systems I: Fundamental Theory and Applications	35	58	1.129	5574	58	1992
3	Nonlinear Dynamics	34	54	1.172	3261	92	1994
4	Physical Review E - Statistical, Nonlinear, and Soft Matter Physics	27	42	1.227	1928	67	2001
5	International Journal of Bifurcation and Chaos	24	42	1.333	2164	107	2005
6	Physical Review Letters	20	24	0.769	2187	24	1997
7	Physica D: Nonlinear Phenomena	19	46	0.704	2392	46	1996
8	Physical Review E - Statistical Physics, Plasmas, Fluids, and Related Interdisciplinary Topics	18	27	0.692	1911	27	1997
9	Communications in Nonlinear Science and Numerical Simulation	17	29	0.895	1352	29	2004
10	International Journal of Chemtech Research	17	19	2.125	942	19	2015
11	Journal of Sound and Vibration	17	25	0.515	776	25	1990
12	IEEE Access	16	30	2.286	926	39	2016
13	International Journal of Bifurcation and Chaos in Applied Sciences and Engineering	16	42	0.762	1844	50	2002
14	Physica A: Statistical Mechanics and Its Applications	16	33	0.593	1145	44	1996
15	Optik	13	20	1.083	704	20	2011
16	Physics Letters, Section A: General, Atomic, and Solid State Physics	13	28	0.481	791	29	1996
17	IEEE Journal of Quantum Electronics	12	16	0.414	1238	16	1994
18	Multimedia Tools and Applications	12	23	1.5	564	23	2015
19	Neurocomputing	12	16	0.444	819	16	1996
20	IEEE Transactions on Circuits and Systems I: Regular Papers	11	14	0.579	628	14	2004
21	Neural Networks	11	14	0.344	460	14	1991
22	Proceedings - IEEE International Symposium on Circuits and Systems	11	18	0.344	446	60	1991
23	Signal Processing	11	14	0.379	1524	14	1994
24	Lecture Notes in Computer Science (Including Subseries Lecture Notes in Artificial Intelligence and Lecture Notes in Bioinformatics)	10	13	0.357	302	64	1995
25	Nonlinear Dynamics, Psychology, and Life Sciences	10	18	0.556	327	23	2005

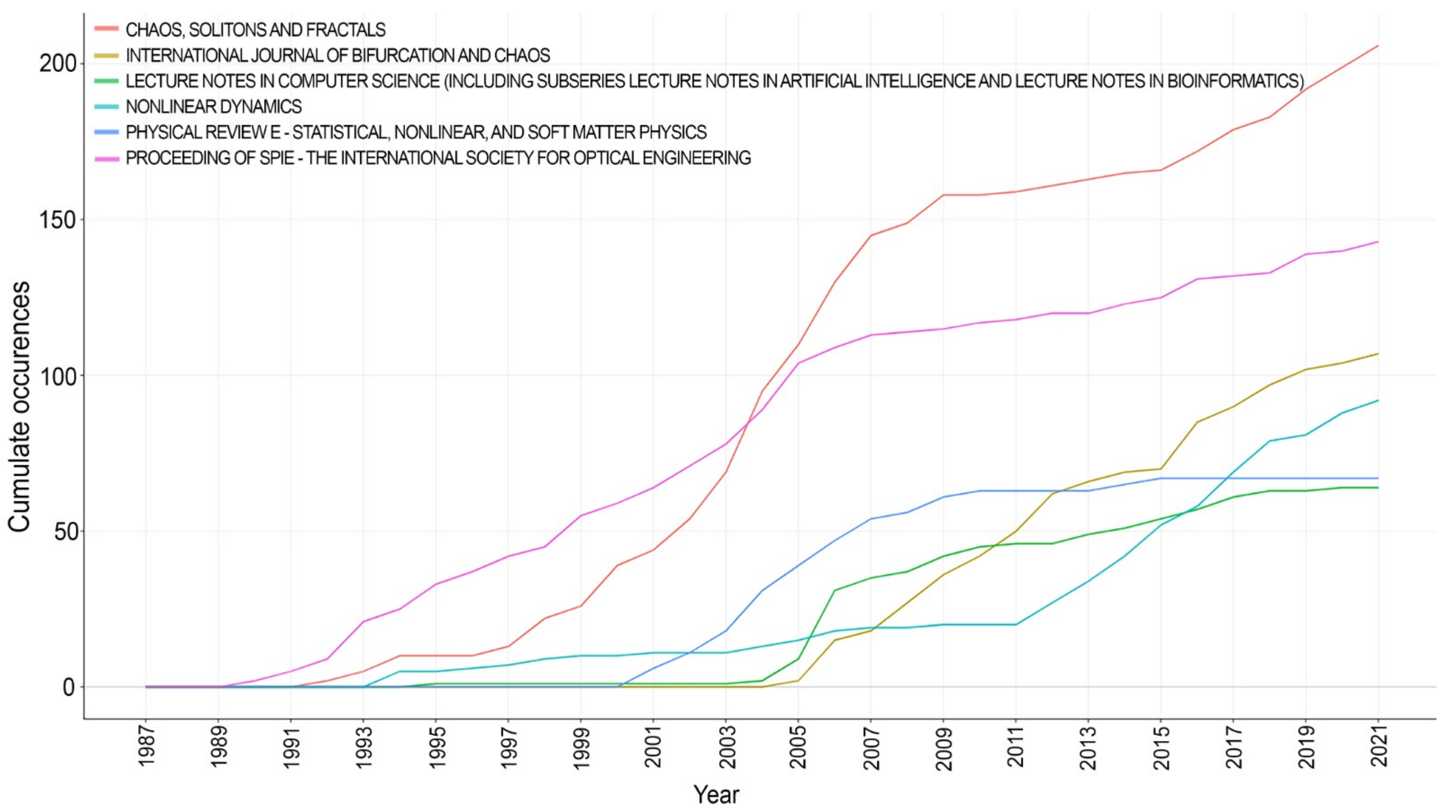

Figure 7 Top 6 journals with the highest number of articles

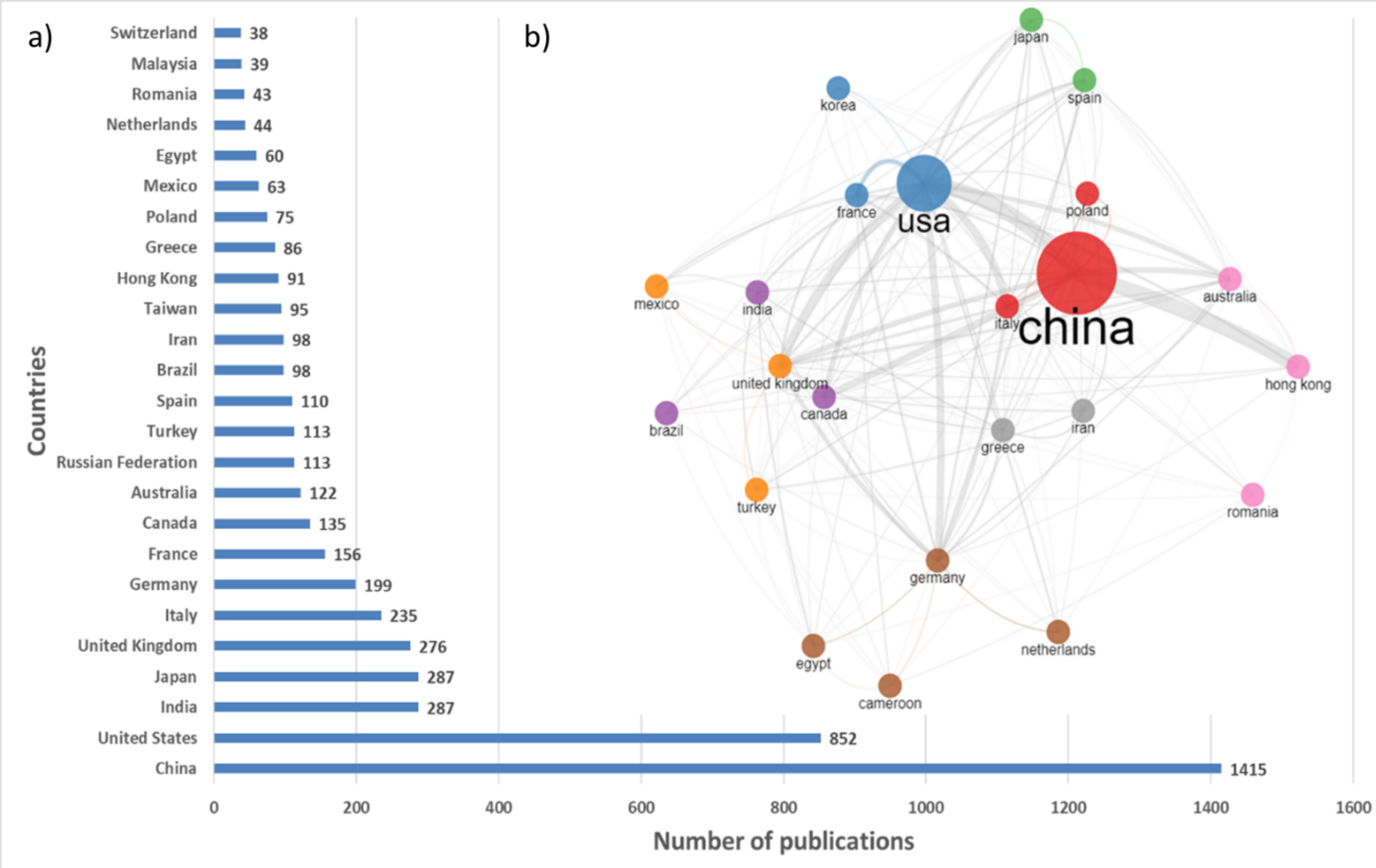

Figure 8 a) Bar chart showing the 25 most productive countries in the world. b) Network visualization map for international collaboration of countries on "Chaos Theory" and "Applications". Footnote: As the size of the circle increases, the number of publications also increases. Clusters are separated by colors. The thickness of the lines expresses the strength of cooperation between countries.

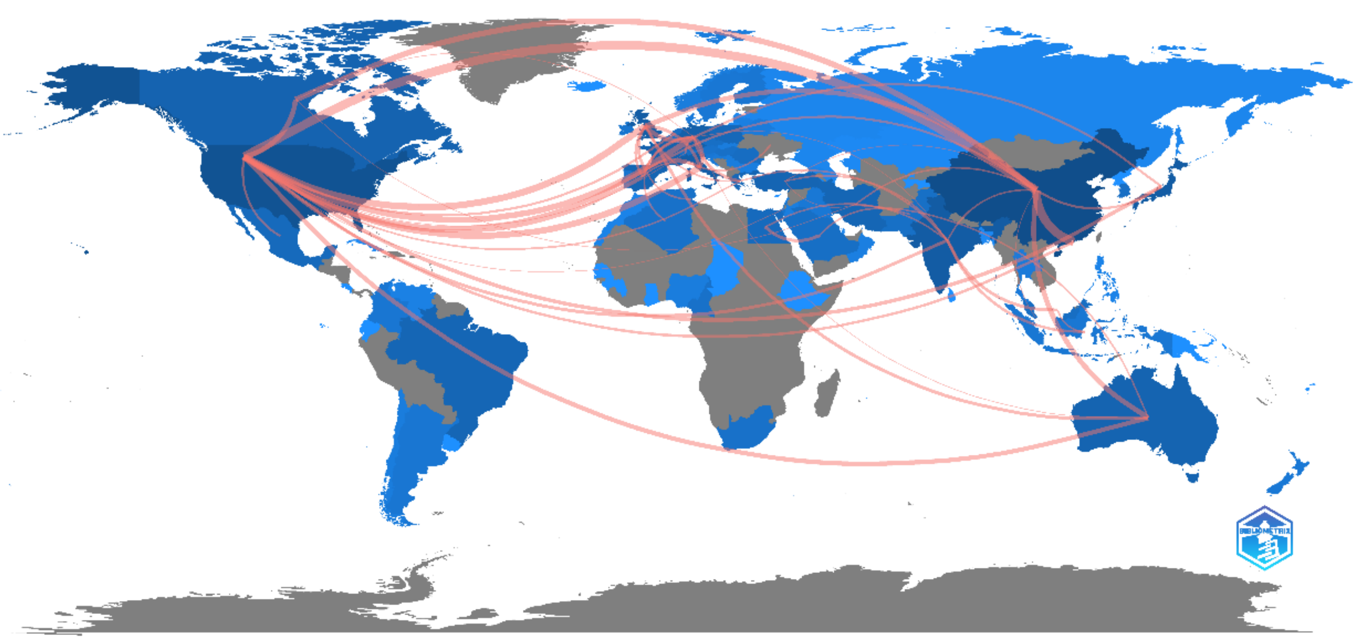

Figure 9 Country collaboration map.

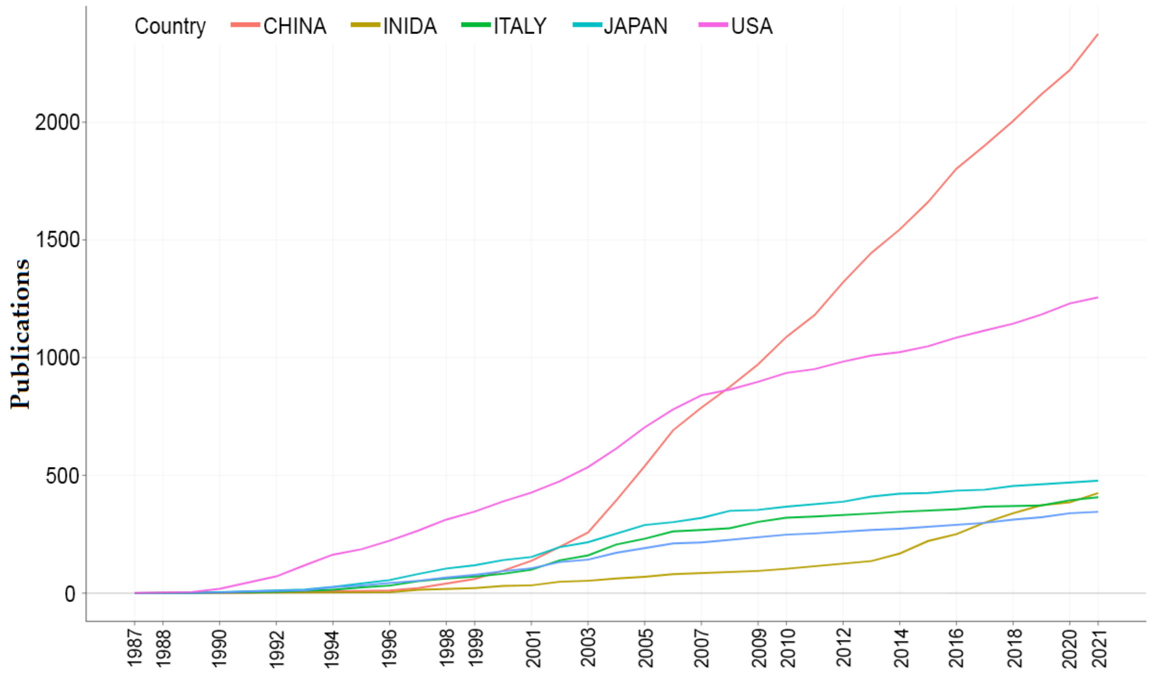

Figure 10 Country production over time

Citations

Citations are shown in Table 1 according to authors, Table 2 according to journals, and Table 3 according to publications. Figure 11 shows the co-citation network of the top 25 authors. As the size of the circle increases, the number of citations also increases. Clusters are separated by colors. The amount of citations between authors is expressed in line thickness.

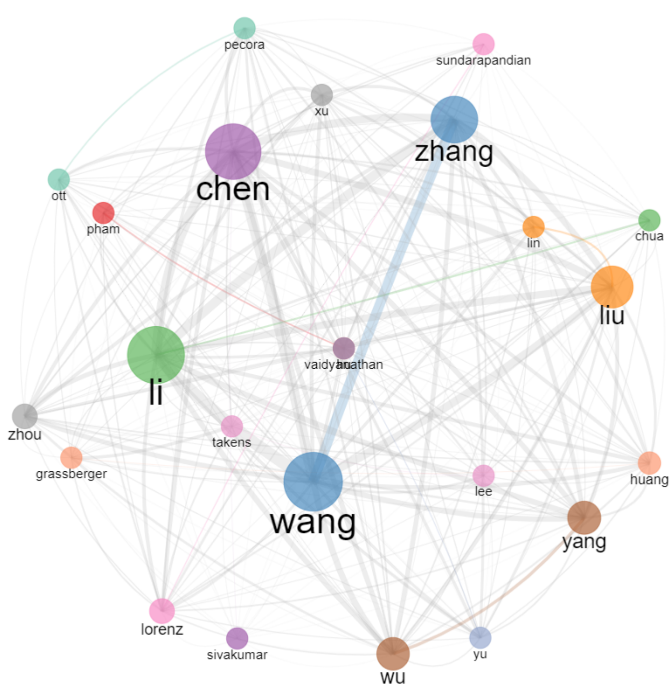

Figure 11 Author co-citation network

Price's Law

Price's Law is the most commonly used indicator when the aim is to analyze productivity in a specific discipline or a given country; it reflects an essential fact of scientific production, which is its exponential growth. According to Price's Law, the total number of citations for the first authors, obtained by taking the square root of the number of authors in our study, should be half the total number of citations. The total number of citations is 21783. When the square root of the number of 25 authors is taken, the number of citations of the first five authors with the highest number of scientific publications was found to be 9738. To assess whether the growth of scientific production in citations follows Price's Law of exponential growth, we made a linear adjustment of the data obtained, according to the equation y = 80.096x - 169.93, and another adjustment to an exponential curve, according to the equation $y = 196.94e^{0.0947}$ (Fig. 12).

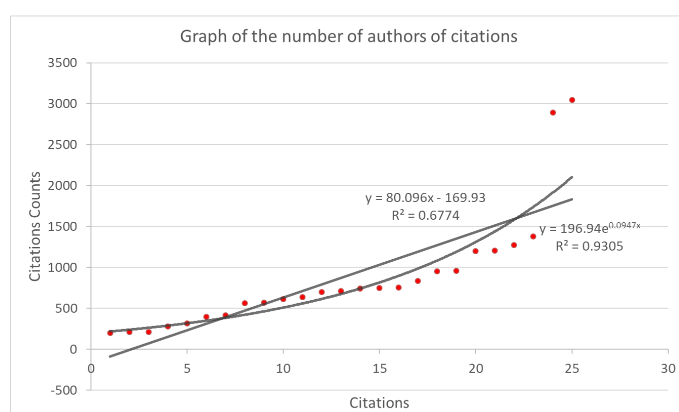

Figure 12 Price's Law

Table 3 Top 25 publications by the number of citations (TC: Total Citations).

No	Paper	Total Citations	TC per Year	Normalized TC
1	CAMPBELL JY, 2012, THE ECONOMETRICS OF FINANC MARK	2933	266.64	86.41
2	JAEGER H, 2004, SCIENCE	2150	113.16	56.15
3	SUDRET B, 2008, RELIAB ENG SYST SAF	1496	99.73	61.88
4	TULINO AM, 2004, FOUND TRENDS COMMUN INF THEORY	1086	57.16	28.36
5	CUOMO KM, 1993, IEEE TRANS CIRCUITS SYST II ANALOG DIGITAL SIGNAL PROCESS	968	32.27	31.39
6	MORMANN F, 2000, PHYS D NONLINEAR PHENOM	961	41.78	21.79
7	LIPSITZ LA, 1992, JAMA	909	29.32	19.79
8	LIU B, 2005, CHAOS SOLITONS FRACTALS	843	46.83	33.70
9	NOWAK MA, 2004, SCIENCE	792	41.68	20.68
10	BOCCALETTI S, 2000, PHYS REP	763	33.17	17.30
11	MARWAN N, 2002, PHYS REV E	740	35.24	24.58
12	YANG T, 1997, IEEE TRANS CIRCUITS SYST I FUNDAM THEOR APPL	699	26.88	33.58
13	ZHANG J, 2006, PHYS REV LETT	611	35.94	23.57
14	VINGA S, 2003, BIOINFORMATICS	598	29.90	27.44
15	NAJM HN, 2009, ANN REV FLUID MECH	567	40.50	28.50
16	MAO Y, 2004, INT J BIFURCATION CHAOS APPL SCI ENG	501	26.37	13.08
17	EL NASCHIE MS, 2004, CHAOS SOLITONS FRACTALS-a	490	25.79	12.80
18	LÜ. J, 2006, INT J BIFURCATION CHAOS	478	28.12	18.44
19	LIAO TL, 2000, CHAOS SOLITONS FRACTALS	475	20.65	10.77
20	KUREMOTO T, 2014, NEUROCOMPUTING	409	45.44	26.62
21	AREF H, 2002, PHYS FLUIDS	385	18.33	12.79
22	PAK C, 2017, SIGNAL PROCESS	384	64.00	22.46
23	GENESIO R, 1992, AUTOMATICA	375	12.10	8.16
24	GUAN ZH, 2005, IEEE TRANS AUTOM CONTROL	369	20.50	14.75
25	STOJANOVSKI T, 2001, IEEE TRANS CIRCUITS SYST I FUNDAM THEOR APPL-a	369	16.77	17.06

Keyword Analysis

The 25 most used keywords in 5088 articles were visualized. The network visualization map for the trend keywords obtained according to the actuality of the publications is shown in Figure 13. As the size of the circle increases, the number of uses of the keyword also increases. Clusters are separated by colors. The thickness of the lines expresses the link strength between keywords. Chaos theory, chaotic systems, Lyapunov methods, synchronization, bifurcation (mathematics), dynamical systems, differential equations, random processes, numerical methods, and Lyapunov exponent were the most frequently used keywords in the articles.

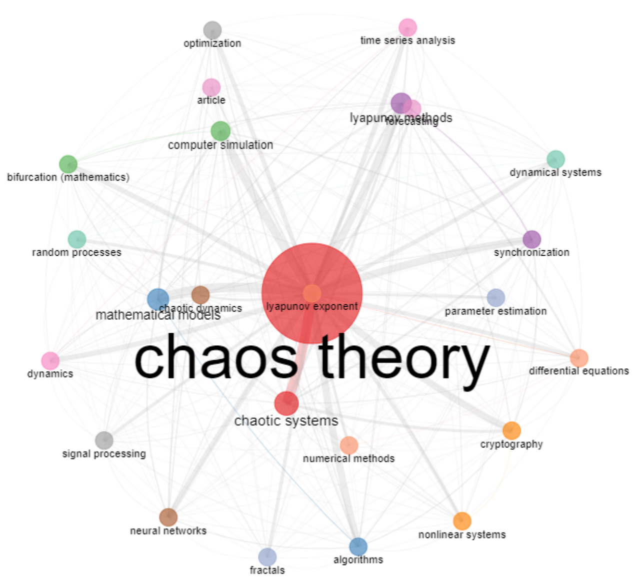

Figure 13 Keyword analysis

Thematic Evolution

The analysis of the evolution of the keywords in the research is shown in Figure 14. Figure 14 shows the most common keywords and their transformation over the years. The cut-off year was determined as 2008.

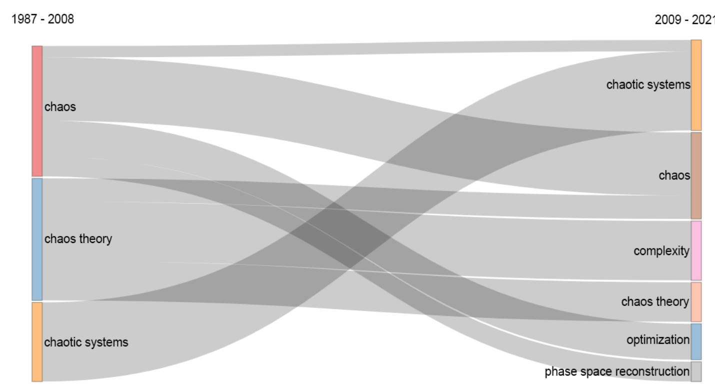

Figure 14 Thematic evolution by author's keywords

DISCUSSION

Despite the fluctuations in the distribution of the number of publications by years from 1987 to 2021, it is seen that the number of publications in general increased until 2004, and the number of publications decreased from 2004 to 2008. Although there has been a slight increase in the number of publications since 2008, it has been observed that it has not changed much in recent years. The subjects of the studies were engineering, computer science, mathematics, physics, and material science, respectively. Authors with the highest *h_index* on the subject: Vaidyanathan S., Chen G., Wang X., Liao X. and Zhang Y. Journals with the highest *h_index* on the subject: Chaos, Solitons and Fractals, IEEE Transactions on Circuits and Systems I: Fundamental Theory and Applications, Nonlinear Dynamics, Physical Review E - Statistical, Nonlinear, and Soft Matter Physics and International Journal of Bifurcation and Chaos. Institutions with the highest h_index on the subject: Vel Tech Rangarajan Dr.Sagunthala R&D Institute of Science and Technology, City University of Hong Kong, Zhejiang University, Ministry of Education China, and Shanghai Jiao Tong University.

When evaluating international cooperation, it is commonly assumed that regional geographical location has an impact on cooperation. When the number of publications in a particular country is evaluated, it is seen that countries with large populations or high economic power, such as China, the USA, India, Japan, and the United Kingdom, publish the most studies on chaos theory. This is in line with the literature showing that academic productivity has a significant relationship with economic power (Demir 2019; Yildirim and Demir 2019; Doğan and Kayır 2020).

From the Price's Law and curve-fitting analyses, we can conclude that the analyzed database is compatible with a more exponential fit than a linear one and that the Price law assumptions are met. López-Muoz et al. used Price's Law as a bibliometric indicator of production in their studies (López-Muñoz *et al.* 2016, 2014). The Price Law was calculated in my study, and similar results were obtained in these studies. The most cited article (Campbell et al. 1998) was published in Macroeconomic Dynamics with the title "The econometrics of financial markets" (Campbell *et al.* 1998). The next most cited article (Jaeger and Haas 2004) was published in the journal Science with the title "Harnessing nonlinearity: Predicting chaotic systems and saving energy in wireless communication" (Jaeger and Haas 2004). The next most cited article (Sudret 2008) is "Global sensitivity analysis using polynomial chaos expansions" (Sudret 2008).

The most frequently used keywords in the articles were chaos theory, chaotic systems, Lyapunov methods, synchronization, bifurcation (mathematics), dynamical systems, differential equations, random processes, numerical methods, and Lyapunov exponent. The limitations of the study, although the Scopus database is advantageous compared to other databases in terms of the number of publications, not all publications were included in the study.

CONCLUSION

This study presents a holistic review of articles on chaos theory and its applications from 1987-2021. According to the findings, there has been a decrease in the annual number of studies produced after 2003. It was seen that the author with the highest *h_index* on the subject was Vaidyanathan S., the journal with the highest *h_index* was Chaos, Solitons, and Fractals, and the institution with the highest *h_index* was Vel Tech Rangarajan Dr.Sagunthala R&D Institute of Science and Technology. The most cited article (Campbell et al. 1998) was published in Macroeconomic Dynamics with the title "The econometrics of financial markets." The most productive countries in publications on the subject are developed or overpopulated countries. It can assist researchers in developing or underdeveloped countries in conducting more research on this topic by planning multinational studies rather than regional studies.

Conflicts of interest

The author declares that there is no conflict of interest regarding the publication of this paper.

Availability of data and material

Not applicable.

LITERATURE CITED

Aria, M. and C. Cuccurullo, 2017 bibliometrix: An r-tool for comprehensive science mapping analysis. Journal of informetrics **11**: 959–975.

Broadus, R. N., 1987 Toward a definition of "bibliometrics". Scientometrics **12**: 373–379.

Campbell, J. Y., A. W. Lo, A. C. MacKinlay, and R. F. Whitelaw, 1998 The econometrics of financial markets. Macroeconomic Dynamics **2**: 559–562.

Demir, E., 2019 The evolution of spirituality, religion and health publications: yesterday, today and tomorrow. Journal of religion and health **58**: 1–13.

Doğan, G. and S. Kayır, 2020 Global scientific outputs of brain death publications and evaluation according to the religions of countries. Journal of religion and health **59**: 96–112.

Donthu, N., S. Kumar, D. Mukherjee, N. Pandey, and W. M. Lim, 2021 How to conduct a bibliometric analysis: An overview and guidelines. Journal of Business Research **133**: 285–296.

Falagas, M. E., A. I. Karavasiou, and I. A. Bliziotis, 2006 A bibliometric analysis of global trends of research productivity in tropical medicine. Acta tropica **99**: 155–159.

Geng, Y., W. Chen, Z. Liu, A. S. Chiu, W. Han, *et al.*, 2017 A bibliometric review: Energy consumption and greenhouse gas emissions in the residential sector. Journal of cleaner production **159**: 301–316.

Jaeger, H. and H. Haas, 2004 Harnessing nonlinearity: Predicting chaotic systems and saving energy in wireless communication. science **304**: 78–80.

Leutcho, G. D., J. Kengne, L. K. Kengne, A. Akgul, V.-T. Pham, *et al.*, 2020 A novel chaotic hyperjerk circuit with bubbles of bifurcation: mixed-mode bursting oscillations, multistability, and circuit realization. Physica Scripta **95**: 075216.

Liu, Z., J. Bian, Y. Wang, Y. Zhao, D. Yan, *et al.*, 2009 Construction and identification of lentiviral rna interference vector of rat leptin receptor gene. Frontiers of Medicine in China **3**: 57–60.

López-Muñoz, F., F. J. Povedano, and C. Álamo, 2016 Bibliometric study of scientific research on melatonin during the last 25 years. In *Melatonin, neuroprotective agents and antidepressant therapy*, pp. 25–42, Springer.

López-Muñoz, F., W. W. Shen, N. Shinfuku, C.-U. Pae, D. J. Castle, *et al.*, 2014 A bibliometric study on second-generation antipsychotic drugs in the asia–pacific region. Journal of Experimental & Clinical Medicine **6**: 111–117.

Martínez, M. A., M. J. Cobo, M. Herrera, and E. Herrera-Viedma, 2015 Analyzing the scientific evolution of social work using science mapping. Research on social work practice **25**: 257–277.

Mazloumian, A., 2012 Predicting scholars' scientific impact. PloS one **7**: e49246.

Pandey, R., A. K. Singh, B. Kumar, and A. Mohan, 2016 Iris based secure nroi multiple eye image watermarking for teleophthalmology. Multimedia Tools and Applications **75**: 14381–14397.

Pritchard, A., 1969 Statistical bibliography or bibliometrics. Journal of documentation **25**: 348.

Rajagopal, K., M. Tuna, A. Karthikeyan, İ. Koyuncu, P. Duraisamy, *et al.*, 2019 Dynamical analysis, sliding mode synchronization of a fractional-order memristor hopfield neural network with parameter uncertainties and its non-fractional-order fpga implementation. The European Physical Journal Special Topics **228**: 2065–2080.

Sengupta, I. N., 1992 Bibliometrics, informetrics, scientometrics and librametrics: an overview .

Song, Y., X. Chen, T. Hao, Z. Liu, and Z. Lan, 2019 Exploring two decades of research on classroom dialogue by using bibliometric analysis. Computers & Education **137**: 12–31.

Sudret, B., 2008 Global sensitivity analysis using polynomial chaos expansions. Reliability engineering & system safety **93**: 964–979.

Sun, J., C. Li, T. Lu, A. Akgul, and F. Min, 2020 A memristive chaotic system with hypermultistability and its application in image encryption. IEEE Access **8**: 139289–139298.

Thompson, J. M. T., H. B. Stewart, and R. Turner, 1990 Nonlinear dynamics and chaos. Computers in Physics **4**: 562–563.

Verma, S. and A. Gustafsson, 2020 Investigating the emerging covid-19 research trends in the field of business and management: A bibliometric analysis approach. Journal of Business Research **118**: 253–261.

Wallin, J. A., 2005 Bibliometric methods: pitfalls and possibilities. Basic & clinical pharmacology & toxicology **97**: 261–275.

Wang, M., J. J. Carver, V. V. Phelan, L. M. Sanchez, N. Garg, *et al.*, 2016 Sharing and community curation of mass spectrometry data with global natural products social molecular networking. Nature biotechnology **34**: 828–837.

Wei, Z., Y. Li, B. Sang, Y. Liu, and W. Zhang, 2019 Complex dynamical behaviors in a 3d simple chaotic flow with 3d stable or 3d unstable manifolds of a single equilibrium. International Journal of Bifurcation and Chaos **29**: 1950095.

Yildirim, E. and E. Demir, 2019 Comparative bibliometric analysis of fertility preservation .

How to cite this article: Akmese, O. F. Bibliometric Analysis of Publications on Chaos Theory and Applications during 1987 - 2021. *Chaos Theory and Applications*, 4(3), 169-178, 2022.